

Aquifer Storage & Recovery (ASR) system improvement in northern Ghana

by

Frank J. van den Toorn

to obtain the degree of Master of Science
at the Delft University of Technology,
to be defended publicly on .. August .., 2018 at AM.

Student number:	4179404
Project duration:	September 18, 2017 – August .., 2018
Thesis committee:	Prof. dr. ir. M. Bakker, TU Delft (Chair)
	Prof. dr. ir. N.C. van de Giesen, TU Delft
	Dr. ir. J.S. Timmermans, TU Delft
	Ir. D.A. Brakenhoff, Witteveen+Bos

An electronic version of this thesis is available at <http://repository.tudelft.nl/>.



Preface

This thesis accommodates the final product in becoming a Master of Science in Watermanagement at the Delft University of Technology - faculty of Civil Engineering and Geosciences. I would like to acknowledge all the people who contributed to my graduation. Some deserve special emphasis. First of all, I would like to thank the entire committee for assessing my thesis. Subsequently, I would like to give a word of gratitude to Witteveen+Bos - Herman Mondeel & Davíd Brakenhoff - for the research facilities and daily supervision. And, last but not least, I owe Conservation Alliance (CA) - Paa Kofi Osei-Owusu - a special gratitude. Without the cooperation of CA, the fieldwork data collection within the northern Ghana local communities would not have been possible.

*Frank J. van den Toorn
Delft, August 2018*



Summary

Work In Progress. Summary will follow.

Contents

List of Figures	ix
List of Tables	xiii
1 Introduction	1
2 Aquifer test	5
2.1 Research locations in northern Ghana	5
2.2 Methods - Set-up & analysis	6
2.2.1 Measurement set-up	6
2.2.2 Data analysis	8
2.3 Data processing	10
2.3.1 Location: Bingo	10
2.3.2 Location: Nungo	11
2.3.3 Location: Nyong Nayili	11
2.3.4 Location: Janga (1/2)	12
2.3.5 Location: Janga (2/2)	13
2.3.6 Location: Ziong (monitoring)	14
2.4 Results & conclusions	15
3 ASR system - Improvements & sensitivities	19
3.1 Methods - ASR system simulation.	19
3.1.1 Soil scenarios	19
3.1.2 ASR system - Synthetic base model definition (reference)	19
3.1.3 ASR system improvements.	22
3.1.4 ASR system sensitivities	22
3.1.5 Test criteria - sustainability	22
3.2 ASR system base model performance.	23
3.2.1 Wet season	23
3.2.2 Dry season	24
3.2.3 Recovery ratio $R\%$	25
3.3 ASR system improvements	25
3.3.1 Extension of daily pumping time	26
3.3.2 Enlargement of borehole cross-sectional dimension	27
3.3.3 Reduction of well skin resistance	27
3.4 ASR system sensitivity	28
3.4.1 Degradation of well depth by clogging	28
3.4.2 Shortening wet season inundation time-span	29
3.4.3 Reduction wet season inundation level	30
3.5 The dimensionless ASR system recharge factor	31
3.6 Results & Conclusions	32
4 ASR system - Business case	33
4.1 Methods - From water volume to financial considerations	33
4.1.1 Yield - crops of interest.	33
4.1.2 Costs - water withdrawal.	35
4.2 Financial yield	36
4.3 Pumping costs	37
4.4 Results & conclusions	38

5 Discussion	41
5.1 Farmer's guideline - ASR system implementation	41
5.2 Fieldwork analysis	41
5.3 ASR system - Improvements & sensitivities	41
5.4 ASR system - Financial magnitude	41
6 Conclusions & Recommendations	43
Bibliography	45
Appendices	47
A Original borehole log sheets	49
B Aquifer test - Data results (fact sheets)	55
C Aquifer test - Equipment	63
C.1 Pumping test	63
C.2 Water table monitoring	64
D Aquifer test - Data analysis overview	67
D.1 Example Python scripts	67
D.2 Data analysis overview.	68
D.2.1 Location: Bingo.	69
D.2.2 Location: Nungo	71
D.2.3 Location: Nyong Nayili.	72
D.2.4 Location: Janga (1/2)	74
D.2.5 Location: Janga (2/2)	76
D.2.6 Location: Ziong.	78
E MODFLOW - Model definition	81
E.1 Model design	81
E.1.1 MODFLOW-NWT.	81
E.1.2 MODFLOW - GHB	82
E.1.3 MODFLOW - MNW2	82
E.2 Leakage factor λ	83
F MODFLOW - Radial conversion	85
F.1 Test 1: Steady flow to a fully penetrating well in confined aquifer	88
F.2 Test 2: Steady flow to a fully penetrating well in unconfined aquifer	90
F.2.1 Constant head is 10 m	91
F.2.2 Constant head is 7 m	91
F.3 Test 3: Unsteady flow to a partially penetrating well in unconfined aquifer	93
G MODFLOW - Additional model results	95
G.1 ASR system base model performance.	95
G.2 ASR system sensitivity	96
H Product specifications - Pedrollo 4" submersible pump	99

List of Figures

1.1 Example on (a) flood near Weisi, Upper West Region and (b) drought near Nungo, Upper East Region	1
1.2 The year-round principal functions of an Aquifer Storage & Recovery (ASR) system	2
1.3 A simplified visualization of the desired results of ASR-system improvements	3
2.1 The northern Ghana research locations	5
2.2 Fieldwork (measurement) set-up (a) general, (b) simplistic	7
2.3 Schematic cross-sectional view of (a) generalized northern Ghana soil stratification and simplified representations: (b) a single layer system, (c) a double layer system, and (d) a system with two layers and partial penetration of the well	8
2.4 Bingo - Simplified models best fit	11
2.5 Nyong Nayili - Simplified models best fit	12
2.6 Janga first attempt - Simplified models best fit	13
2.7 Janga second attempt - Simplified models best fit	14
2.8 Ziong - Simplified models best fit	15
2.9 T & S bandwidth selection	17
3.1 Schematic base model & soil scenario definition	20
3.2 Base model soil scenario 3- Cross-sectional contour head after (a) five days and (b) 122 days of infiltration	23
3.3 Base model soil scenario 3 - Discharge performance for (a) the first five days and (b) the last five days of dry season	24
3.4 Base model soil scenario 3 - Cross-sectional contour head after four hours of pumping on (a) the first day (day 123) and (b) the last day (day 365) of dry season	25
3.5 Schematic extension daily pumping time	26
3.6 Results of yearly total volumes (in, out, ratio) by extension daily pumping time	26
3.7 Schematic enlargement borehole cross-sectional dimension	27
3.8 Results of yearly total volumes (in, out, ratio) by enlargement well cross-sectional dimension	27
3.9 Schematic reduction well skin resistance	28
3.10 Results of yearly total volumes (in, out, ratio) by reduction well skin resistance	28
3.11 Schematic degradation well depth by clogging	29
3.12 Results of yearly total volumes (in, out, ratio) by degradation well depth	29
3.13 Schematic shortening wet season inundation time-span	30
3.14 Results of yearly total volumes (in, out, ratio) while shortening wet season inundation time-span	30
3.15 Schematic reduction wet season inundation level	31
3.16 Results of yearly total volumes (in, out, ratio) by reduction of wet season inundation level	31
4.1 Crops of interest: (a) Tomatoes and (b) Groundnuts	33
4.2 Schematic of the ASR system operational pumping costs	35
4.3 Financial yield - Tomatoes (4 months) - three types of ASR system improvement	37
4.4 Financial yield - Groundnut (4 months) - three types of ASR system improvement	37
4.5 Pumping costs - dry season (8 months) - three types of ASR system improvement	37
4.6 Pumping costs - maximum pumping efficiency - dry season (8 months) - three types of ASR system improvement	38
4.7 Year-round net financial return - three types of ASR system improvement	38
4.8 Year-round net financial return - maximum pumping efficiency - three types of ASR system improvement	38

B.1	Fieldwork fact sheet: Bingo	56
B.2	Fieldwork fact sheet: Nungo	57
B.3	Fieldwork fact sheet: Nyong Nayili	58
B.4	Fieldwork fact sheet: Janga (attempt 1)	59
B.5	Fieldwork fact sheet: Jamga (attempt 2)	60
B.6	Fieldwork fact sheet: Ziong (location of monitoring)	61
C.1	Comparable example of the fieldwork submersible pump	63
C.2	Comparable example of the fieldwork generator	64
C.3	Actual fieldwork hose & bucket	64
C.4	Comparable examples of Van Essen TD- & Baro-Divers	65
C.5	Comparable examples of In-Situ TD- & Baro-Divers	65
C.6	Comparable example of the fieldwork water tape	66
D.1	Bingo single layer fieldwork data analysis by the optimization (a) fmin-RMSE method and (b) TTim calibration method	69
D.2	Bingo double layer fieldwork data analysis by the optimization (a) fmin-RMSE method and (b) TTim calibration method	69
D.3	Bingo partially penetrating double layer fieldwork data analysis by the optimization (a) fmin-RMSE method and (b) TTim calibration method	69
D.4	Bingo - overview determined (Fmin and Cal) optimal parameter values of (a) a single layer system, (b) a double layer system, and (c) a system with two layers and partial penetration of the well	70
D.5	Nyong Nayili single layer fieldwork data analysis by the optimization (a) fmin-RMSE method and (b) TTim calibration method	72
D.6	Nyong Nayili double layer fieldwork data analysis by the optimization (a) fmin-RMSE method and (b) TTim calibration method	72
D.7	Nyong Nayili partially penetrating double layer fieldwork data analysis by the optimization (a) fmin-RMSE method and (b) TTim calibration method	72
D.8	Nyong Nayili - overview determined (Fmin and Cal) optimal parameter values of (a) a single layer system, (b) a double layer system, and (c) a system with two layers and partial penetration of the well	73
D.9	Janga first attempt single layer fieldwork data analysis by the optimization (a) fmin-RMSE method and (b) TTim calibration method	74
D.10	Janga first attempt double layer fieldwork data analysis by the optimization (a) fmin-RMSE method and (b) TTim calibration method	74
D.11	Janga first attempt partially penetrating double layer fieldwork data analysis by the optimization (a) fmin-RMSE method and (b) TTim calibration method	74
D.12	Janga first attempt - overview determined (Fmin and Cal) optimal parameter values of (a) a single layer system, (b) a double layer system, and (c) a system with two layers and partial penetration of the well	75
D.13	Janga second attempt single layer fieldwork data analysis by the optimization (a) fmin-RMSE method and (b) TTim calibration method	76
D.14	Janga second attempt double layer fieldwork data analysis by the optimization (a) fmin-RMSE method and (b) TTim calibration method	76
D.15	Janga second attempt partially penetrating double layer fieldwork data analysis by the optimization (a) fmin-RMSE method and (b) TTim calibration method	76
D.16	Janga second attempt - overview determined (Fmin and Cal) optimal parameter values of (a) a single layer system, (b) a double layer system, and (c) a system with two layers and partial penetration of the well	77
D.17	Ziong single layer fieldwork data analysis by the optimization (a) fmin-RMSE method and (b) TTim calibration method	78
D.18	Ziong double layer fieldwork data analysis by the optimization (a) fmin-RMSE method and (b) TTim calibration method	78

D.19	Ziong partially penetrating double layer fieldwork data analysis by the optimization (a) fmin-RMSE method and (b) TTim calibration method	78
D.20	Ziong - overview determined (Fmin and Cal) optimal parameter values of (a) a single layer system, (b) a double layer system, and (c) a system with two layers and partial penetration of the well	79
F.1	Schematic of an axially symmetric model (Langevin, 2008)	85
F.2	Modflow topview schematisation of a: (a) Rectangular model, (b) Rectangular round model and (c) Single row model	87
F.3	Schematic test 1	88
F.4	Results test 1	89
F.5	Schematic test 2	90
F.6	Results test 2a	91
F.7	Results test 2b	92
F.8	Schematic test 3	93
F.9	Results test 3: Cross-section head contour after 1 day of pumping	93
F.10	Results test 3: Head after 1 day of pumping at 2.0m (relative to aquifer bottom)	94
G.1	Base model soil scenario 3 - Head in representative layers after (a) five days and (b) 122 days of infiltration	95
G.2	Base model soil scenario 3 - Head in representative layers after four hours of pumping on (a) the first day (day 123) and (b) the last day (day 365) of dry season	95
G.3	Degradation of well depth - Total recharge volume by layer - soil scenario 3	96
G.4	Shortening wet season inundation time-span - Recharge over time - soil scenario 3	96
G.5	Reduction wet season inundation levels - Recharge over time - soil scenario 3	97

List of Tables

2.1	Bingo - overview best fit parameters	11
2.2	Nyong Nayili - overview best fit parameters	12
2.3	Janga first attempt - overview best fit parameters	13
2.4	Janga second attempt - overview best fit parameters	14
2.5	Ziong - overview best fit parameters	15
3.1	Base model scenarios - Wet season recharge (m ³)	24
3.2	Base model scenarios - Dry season discharge (m ³)	25
3.3	Base model scenarios - Recovery ratio $R\%$	25
D.1	Overview - approaches in fieldwork data analysis	68
E.1	Lambda (m) overview per location	83
G.1	Degradation of well depth - soil scenario 3 - Screen average specific recharge and discharge volumes (m ³ /m)	96
G.2	Degradation of well depth - soil scenario 3 - Total recharge and discharge volumes specific reduction (m ³ /m)	96

Introduction

'End Hunger' is one of the Sustainable Development Goals stated by the United Nations (United Nations, 2018). Currently, 815 million people on earth suffer from hunger. In coherence with the prospects of the world population (growth up-to 10 billion people by the year 2050) hunger is likely to expand (United Nations, 2018). The UN Food and Agricultural Organisation (FAO) expects a needed doubling of the global food production (FAO, 2018d). Due to strong patterns of urbanization and changing diets the nutrition necessities are even higher in (among others) Sub-Saharan Africa (SSA). Local agricultural sectors within SSA can make a virtue of the inevitable rising food demands (Ministry of Foreign Affairs et al., 2018). The present gap between the actual and potential yield can be bridged by small-scale agricultural innovations. Small-holder farmers can increase productivities by the implementation of more resource-efficient techniques. This bottom-up development approach is for example supported by the government of the Netherlands (SBIR program) (Ministry of Foreign Affairs et al., 2018).

Water availability is of key interest in food production. 70 percent of the entire humanitarian fresh water-use serves agricultural purposes (United Nations, 2014). Within SSA, the northern Ghana region encounters favourable agricultural climatological conditions (semi-arid). The Ghana Meteorological Services Department (MSD) measured (1971-2007) annual average precipitation of 800-1250 mm/y (Canadian International Development Agency, 2011). In absolute terms, satisfying water quantities to become self-sufficient in food supply (Ministry of Foreign Affairs et al., 2018). However, precipitation is unevenly spread over the year. The utmost extent of annual precipitation is typically covered by four months of wet season (late May - October). As a consequence, northern Ghana is subjected to both seasonal flooding and long periods of drought (Figure 1.1).



(a)



(b)

Figure 1.1: Example on (a) flood near Weisi, Upper West Region (source: (Owusu et al., 2017) and (b) drought near Nungo, Upper East Region

Northern Ghana's food production is predominantly cultivated during the wet season. Dry season (irrigation based) agriculture takes place at small-scale. Only restricted quantities of groundwater are used in the irrigation process. Currently, local groundwater use is estimated to be approximately 5% of the annual recharge (2.5-10% of annual precipitation) (Martin, 2008). The amount of water withdrawn is marginal and the environment is self-reliant. However, climate change can potentially have a negative influence. Natural recharge can become lower, while governmental policies are more and more pointed at the intensification of dry season agriculture (Wood, 2013). In the near future, it is possible that discharge rates will exceed natural recharge and groundwater extraction is no longer sustainable. Managed Aquifer Recharge (MAR) can potentially contribute to the continued sustainable use of groundwater in northern Ghana.

Aquifer Storage & Recovery (ASR) systems

Water entering a catchment (e.g. precipitation, river or groundwater flow) partially and temporarily contributes to local recharge of groundwater (Fitts, 2012). The natural water cycle can be manipulated by human interventions. Temporarily available water can be added to the subsurface by the creation of preferential flow paths; Managed Aquifer Recharge (MAR) (Dillon et al., 2009). Different objectives can induce the implementation of MAR. One can think of underground water storage to reduce flooding or to counter groundwater shortages. Moreover, implementation can be beneficial for the local retention of water. MAR applications reduce water losses through evaporation and run-off.

MAR concepts exist in wide varieties, e.g. surface infiltration basins and sand dams (Dillon et al., 2009). A particular MAR type takes central stage in this research; Aquifer Storage and Recovery (ASR) systems. Besides the basic MAR principle, groundwater recharge, ASR systems are designed for groundwater withdrawal as well. The principle functions of an ASR system are visualized in Figure 1.2.

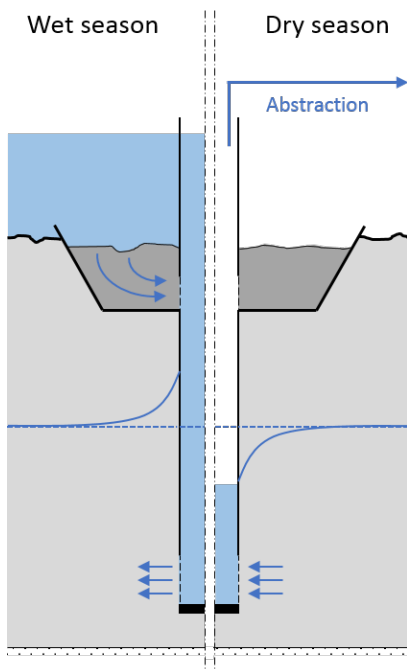


Figure 1.2: The year-round principal functions of an Aquifer Storage & Recovery (ASR) system

An ASR system offers a solution when natural surface infiltration characteristics are insufficient. Wet season water surpluses (e.g. flood and inundation) can be stored in the subsurface by the use of an ASR system. Flood water enters the system under gravity. An infiltration bed around the borehole serves as the preferential path of flow. For purification purposes the bed is designed with a specific soil arrangement (Owusu et al., 2017). Dependent on borehole screen depth the ASR system can be connected to shallow (unconfined) and/or deeper ground layers (unconfined/confined). Dry season water withdrawal takes place by the installation of a submergence pump.

Research questions

Northern Ghana based ASR systems make use of locally available natural resources. The system acts as a seasonal bridge, it converts flood water into irrigation water. In the northern Ghana context, the ASR system relation to absolute water volumes is undetermined (e.g. impact on local nature and agricultural benefits). From a sustainable point of view it is desirable to gain knowledge on year-round ratios between groundwater recharge (wet season) and discharge (dry season). Furthermore, northern Ghana smallholder farmers can potentially benefit from increased system efficiencies (Figure 1.3). A desired development in the process of becoming a (more) self-sufficient food region. However, the impacts of ASR system innovations are undiscovered. Objective of this research is to conduct a feasibility study on sustainable use of a synthetic ASR system in northern Ghana; taking present conditions and multiple system improvements into account. This research aims to answer the following research question:

How can Aquifer Storage and Recovery (ASR) systems be improved to increase the availability and sustainable use of groundwater in northern Ghana small-scale agriculture?



Figure 1.3: A simplified visualization of the desired results of ASR-system improvements (At present a single poly tank is filled on daily dry season bases). (visual support by Housin Aziz, Jhun Capaya and Nibras@design from Noun Project - <https://thenounproject.com>)

The main research question can be solved in consecutive parts. Three addition research question are stated that have to be answered:

- *Which range of values for transmissivity (T) and storativity (S) can be obtained from aquifer tests applied at multiple study sites in northern Ghana?*

It might seem trivial, but the functioning of an ASR system is dependent on its surroundings. Locally applicable geohydrological parameters (T and S) have to be determined for the research follow-ups. The desired information is obtained by the application of site-specific measurements at multiple locations within northern Ghana.

- *How and to what extent can improvements of an ASR system increase the water supply to northern Ghana smallholder framers, while sustainability is maintained?*

For northern Ghana smallholder farmers this question is key, but the answer to it is rather challenging. The terms 'how' (types of improvement) and 'to what extent' (limit of sustainability) need further specifications. In order to judge the potential improvements (and sensitivities) of the ASR system, a synthetic northern Ghana base model is defined as reference.

- *With what financial yield levels can a northern Ghana synthetic ASR system potentially be associated?*

The performance of the synthetic ASR system and system improvements is generally expressed in water volumes. Transformations towards financial yields are desired to provide more insight into the magnitude of a locally applicable ASR system. The implementation of pumping costs and crop-specific yield roughly uncovers the ASR systems financial feasibility in northern Ghana conditions.

Methodology

In northern Ghana, a total of five ASR-systems are subjected to in-field aquifer tests. The generated data is analysed in a transient analytical element modelling environment; TTIm (Bakker, 2013a,b). Locally obtained values for transmissivity (T) and storativity (S), are used as conditional (aquifer) input in the subsequent research models. Multiple research simulations take the basic performance of an ASR-system, the impact of (step-wise) improvements and the system's sensitivity to changing natural conditions into account. The models are created in the finite difference environment for groundwater flow; MODFLOW (Harbaugh, 2005; Niswonger et al., 2011). The simulated results on the (improved) ASR system performances are expressed in

both water volumes and financial returns.

* Detailed descriptions of the applied research methods on aquifer test application (e.g. data generation and processing), synthetic ASR-system model definition and water volume-to-yield transformations are included as individual method-sections in the successive chapters (Section 2.2, 3.1 & 4.1).

Reader's guide

Chapter 2 presents the northern Ghana research locations and describes the derivation (process) of the locally applicable geohydrological parameter values (T and S). The performances of simulated ASR-system improvements and the system sensitivities to nature are explained in Chapter 3. In the business case of Chapter 4, the (increased) ASR system groundwater extraction volumes are roughly transformed to financial returns. A farmers guideline in the implementation of ASR system improvements is discussed in Chapter 5. This Chapter also includes the research limitations. Chapter 6 contains the concluding answers to the research questions and recommendations for further research.

2

Aquifer test

The performance of an ASR system is dependent on the physical properties of its surroundings (Bakker, 2010). In the north of Ghana, subsurface characteristics can vary at short mutual distances (Owusu et al., 2017). Representative information on the local geohydrology is obtained through site-specific measurements. Aquifer tests are performed at multiple locations in northern Ghana.

The research locations are presented in Section 2.1. Section 2.2 describes the aquifer test methodologies in measurement set-up and data analysis. Appendix B contains the raw measurement results. The aquifer test data is analysed in Section 2.3. In Section 2.4 the conclusions on the site visits and the data analysis are described. The chapter concludes with the derivation of locally applicable values for T and S . These parameters are the input for the study on potential ASR system improvements in northern Ghana.

2.1. Research locations in northern Ghana

Multiple ASR systems are present in the Upper East Region (UER) and the Northern Region (NR) of Ghana. Commissioned by the NGO Conservation Alliance (CA), some of these systems are installed in the summer of 2016. Pumping tests are performed at four (CA) ASR systems, located in Bingo; Nungo; Nyong Nayili and Janga. At the location Ziong an ASR system is used for the monitoring of the system practical use by farmers. Figure 2.1 shows a map of the research locations in northern Ghana.

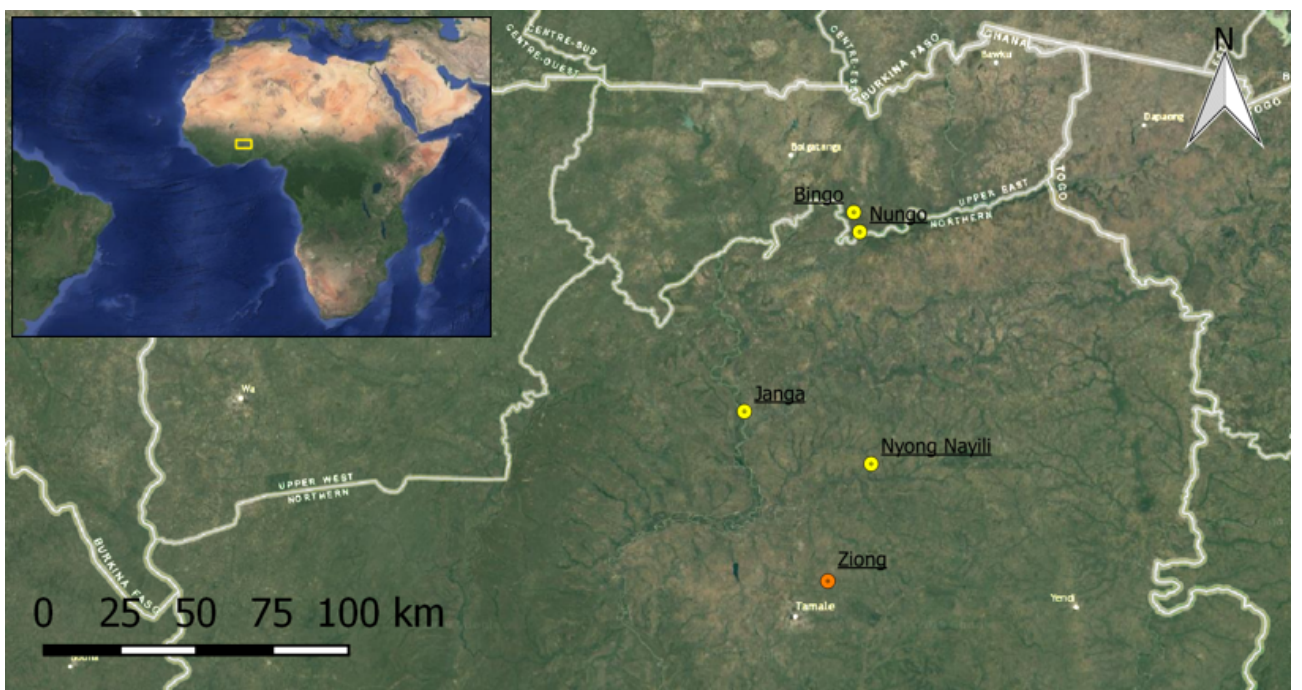


Figure 2.1: The northern Ghana research locations

2.2. Methods - Set-up & analysis

The five northern Ghana study sites (Section 2.1) are subjected to aquifer tests. A complete description of the test process (from measurement data generation to geohydrological parameter values derivation) is described below. The raw results (measurement data) can be found in Appendix B. Data analysis (Section 2.3 & 2.4) is possible by the implementation of the here presented methodologies.

2.2.1. Measurement set-up

This section contains the ins and outs of the practical aquifer test set-up. The aquifer tests accommodates both pumping-recovery tests and the monitoring of the system use by farmers. Due to differences in ASR systems encountered, the data collection is designed by a hybrid measurement approach. The stated approach can be used as input for data (re)production (transparency).

Pump installation

Based on the (2016) original log sheets (Appendix A), site-specific borehole depths are known in advance. The ASR system inspection showed, the accumulation of sedimentation at the borehole bottom. To prevent pump damages and make sure properly functioning is maintained, actual borehole depths are measured before pumping tests are executed. Outcomes of the measurements are taken into account for each individual set-up. To prevent the excessive spread of soil particles, the submersible pump is positioned at least 5 m above the measured borehole bottom (sediment). In practice, this resulted in a pump suction depth of approximately 30-35 m.

Pump discharge & measurement

A single 100 m hose is directly connected to the outlet of the submersible pump. Based on the pump position (deep inside borehole), a distance of circa 65 m is applied for the horizontal displacement of water. At this distance, water is discharged on the surface. The head of the hose is equipped with a nozzle to roughly regulate the discharge rate. By the use of this nozzle, discharge rates in the range of 50-75 m³/d are obtained during the pumping tests. Rates are measured by the use of a stopwatch and a 50 l bucket. Starting at the moment of pump operation, the duration of filling is measured twice every 15 minutes. The obtained 15 minute average is used to calculate the time dependent discharge rates. More detailed discharge information can be found in the site-specific fact sheets (Appendix B).

Groundwater table (GWT) measurement

Groundwater level reductions caused by pumping tests are preferably measured in multiple piezometers, located at a certain known horizontal distance from the discharge well (Kruseman and de Ridder, 2000). In the northern Ghana surroundings, close range monitoring options are absent. Due to a lack of time and/or resources these facilities could not be arranged either. Moreover, the implementation of such facilities do not match research nature. Aim of this research is to collect fieldwork data by the use of minimal resources. The absence of widespread measurement options strengthens this approach. As a consequence, the time dependent GWTs (drawdowns) are measured in the discharge well only.

A water tape is used as hand equipment. First of all to determine the initial (static) GWT. Subsequently, the device is applied as a real time indicator of drawdown. During the pumping tests, multiple hand measurements are applied at randomly picked moments to monitor the test progress. Gathered data functions as verification and back-up of the pressure sensors (divers), which are normative.

Two types of divers (different brands) are used as GWT measurement devices. Product specifications show that these divers can respectively measure pressures up to 10 m (Van Essen) and 9 m (In-Situ) water column (Appendix C). The northern Ghana regional subsurface is characterized as highly heterogeneous. The pumping test GWT drawdown magnitude is therefore unpredictable. To prevent the occurrence of missing drawdown data, the single borehole is equipped with multiple divers at ascending depths. The water column between the initial static water table and pump position is filled with about four divers, with a mutual distance that meets the divers range specifications. To make sure the divers stay in position they are leashed to a rope which runs from well top to pump. This measurement set-up forms a robust network for the collection of drawdown data (figure 2.2a).

However, practical circumstance can cause the application of a more simplistic set-up (figure 2.2b). One can think of a situation in which the pump is already installed and/or will not be removed at the end of

the pumping test. In this case, the (rope) attachment of the divers to the pump is not possible. Adverse effect of the simplistic set-up is a more vulnerable data collection. To prevent the occurrence of undesired diver movement, a minimum distance of 5-10 m between the pump and lowest diver is implemented in this set-up. A complete overview of the borehole measurement set-up (general and simplistic) can be found in figure 2.2.

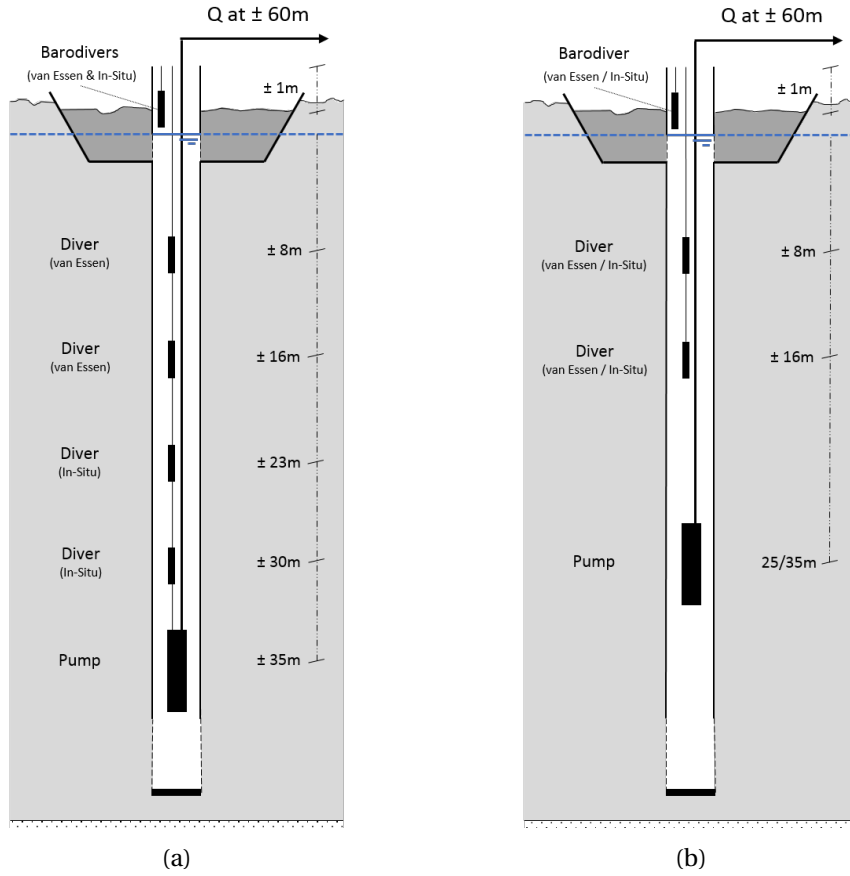


Figure 2.2: Fieldwork (measurement) set-up (a) general, (b) simplistic

Besides the divers, the measurement set-up also accommodates two baro-divers (van Essen & In-Situ). The baro-divers are positioned in the borehole top section. Drawdown is by definition expressed as time dependent GWT reductions relative to the initial status. Short-term atmospheric fluctuations in pressure are compared to the water pressures negligible small. Nonetheless, these minor atmospheric influences are also included in the data collection.

Pumping test duration & time measurement

For each individual pumping test the exact start of pump operation could not be determined in advance. As a consequence, the total pumping test duration differs per pumping test as well. In every single measurement, a minimum of four hours of pumping and one hour of recovery is pursued.

To avoid unnecessary risks in missing out on the collection of drawdown data, all pressure sensors are programmed to start logging in time (08:00:00, local time, at pumping test days). All divers are set to log with a similar linear interval of 10 seconds. As a single exception, the In-Situ BaroTROLL is programmed to linear log once a minute (its minimum sample interval).

* An overview of the aquifer test results for each individual research location can be found in Appendix B. More details on the applied equipment can be found in Appendix C.

2.2.2. Data analysis

Raw drawdown time series are the result of in-field measurements. The data sets are more or less meaningless on its own. The methods below describe the required components in analysis to transforms the obtained aquifer test data to the desired transmissivity (T) and storativity (S) values.

Simplified theoretical models

The original borehole log sheets (appendix A) are the most reliable source of local geological information available. Although the sheets contain site-specific information, similarities in stratification are present. In each case (2.1) the upper 50 m is divided into two or three layers, consisting of a (semi-)impermeable top layer and below that one or two high(er) permeable layers (aquifers). Groundwater tables are predominantly positioned slightly below the bottom of (semi-)impermeable layer, in the top aquifer (labelled as layer 1 in the figure below). Strictly seen, the conditions are therefore unconfined. But given the small interval (relative to total model thickness) between the the aquifer top and the GWT, the situation is close to confined. Based on the borehole log sheets three simplified theoretical models for the analysis of fieldwork data are proposed, as depicted in Figure 2.3.

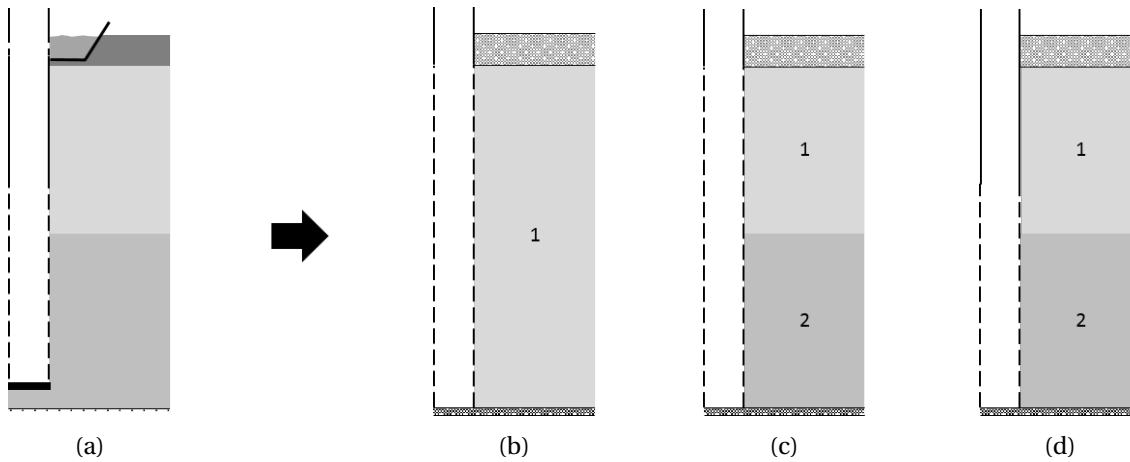


Figure 2.3: Schematic cross-sectional view of (a) generalized northern Ghana soil stratification and simplified representations: (b) a single layer system, (c) a double layer system, and (d) a system with two layers and partial penetration of the well

These simplified models (Figure 2.3b - 2.3d) mimic local conditions, making the derivation of representative hydraulic subsurface characteristics (T and S) potentially possible (Kruseman and de Ridder, 2000). Double layered models are applied to provide more degrees of freedom, perhaps resulting in more accurate solutions. To limit the chances of equifinality (abundant degrees of freedom) a maximum of two soil layers are implemented in data analysis.

Parameter derivation method's & model environment

It lacks a single best approach in the derivation of the geohydrological parameter values (T and S). A widespread variety of analyses (e.g. analytical and computational) can be applied on the pumping test data. The details of the (analytical) models and methods used in this research are described below.

- Theis's method

Groundwater drawdown due to the withdrawal of water can be determined analytically with Theis's equation (Equation 2.1). Theis's method is applicable on the situation depicted in Figure 2.3b; a constant rate pumping test applied on a well that is fully penetrating a single layer aquifer (Kruseman and de Ridder, 2000). Confined conditions are assumed in Theis's method. Therefore, this analytical solution is suitable for obtaining a first indication (approximation) of the research geohydrological parameters.

$$s = \frac{Q}{4\pi K D} E_1(u) \quad (2.1)$$

$$u = \frac{r^2 S}{4 K D t} \quad (2.2)$$

Where s (m) is the drawdown at distance r (m) from the well, Q (m^3) is the constant well discharge, KD (m^2/d) is the aquifer transmissivity ($KD = T$), S (-) is the aquifer storativity, t (d) is the time measured from the start of pumping and E_1 is the exponential integral. The drawdown measurements in this research are limited to in-well measurements. The distance r in Theis's equation is assumed to be the length of the well radius (0.0635 m). Appendix D.1 shows the implementation of Theis's method in Python.

- Analytic Element Modelling in TTIm

TTim is a computer program based on analytic elements and designed for the analysis of transient groundwater flow. The analysis can be applied on a single or multiple layer(s). Several analytical elements (and types of elements) can be added to model layers. The use of TTIm makes it possible to take additional well characteristics into account. Groundwater heads can be determined inside the well and the model optionally accounts for borehole storage and well skin resistance. Moreover, well discharge can be toggled on and off multiple times. This allows for simulations of both single pumping-recovery tests and long-term well operations (Bakker, 2013a,b).

This research fieldwork data is analysed within the TTIm Model3D configuration. A single well (analytical element) is included in the model environment. The groundwater heads are determined inside the well. Aspects as actual borehole storage, optimal borehole storage and/or optimal well resistance are alternately accounted in different compositions of analysis. Moreover, the three types of simplified theoretical models (Figure 2.3) are consecutively considered. A complete overview of all approaches in data analysis (25x) can be found in Appendix D.2.

The top layer (aquifer 1 in Figure 2.3) is configured as being a phreatic layer. In other words, the top layer storage coefficient (S) is a phreatic storage coefficient (S_y). This model assumption is based on the observed initial groundwater tables, which are located below the bottom of the (semi-)impermeable top layer. In analysis, each simplified model layer has a hypothetical thickness of 1 m. The derived hydraulic conductivities (k) can therefore be interpreted as transmissivities (T) and the storage is expressed as the layer storage coefficient (S). This is done to directly derive T and S values. Additionally, this approach automatically corrects for the absence of knowledge on the thickness of the deepest soil layer in which the well is screened. There is no information about soil conditions beyond the bottom of the wells in the borehole log-sheets (Appendix A).

Optimization functions

As a final step in the determination of values for T and S , the analytical solution (Theis's method) and composed TTIm models are linked (fitted) to the fieldwork data. Two optimization functions are applied.

- Fmin-RMSE function

Differences between the measured and modelled drawdown (curves) can be expressed by the Root-Mean-Square-Error (RMSE) objective function (Equation 2.3). The Fmin function (part of Python's `scipy.optimize` package) is applied to minimize the RMSE value. In other words, the function is applied to minimize the difference between modelled and observed drawdowns. The optimization results in (RMSE based) optimal T and S values (and optionally values for borehole storage and/or well skin resistance). These values theoretically represent local conditions. An example Python implementation of the Fmin-RMSE optimization function is depicted in Appendix D.1.

$$RMSE = \sqrt{\frac{\sum (s_{mod} - s_{field})^2}{N}} \quad (2.3)$$

Where s_{mod} is the modelled drawdown (m), s_{field} is the observed drawdown (m) and N is the number of data points.

- Calibration function

TTim has a built-in calibration function for the derivation of parameter values. Application of this second method improves the research robustness (reference values). An example of the Python implemented TTim Calibrate optimization function is part of Appendix D.1.

Both optimization methods require initial parameter estimations. More than one suitable solution is possible, which makes the outcome of the optimization dependent on the choice of the initial values. Other studies found that T and S values are commonly low in northern Ghana (e.g. Owusu et al., 2017, 2015). Based on these other studies the following initial conditions are applied: k_{aq0} is 10 (m/d), k_{aq1} is 10 (m/d), S_{aq0} is 0.01 (-), S_{aq1} is 0.001 (-) and well resistance is 0.1 (d). The well radius (measured in-field) is used as the (initial) borehole storage: 0.0635 (m). Boundary conditions are applied to avoid the optimization resulting in physically improbable parameter values, i.e. negative parameter values and unnaturally high storativity values (greater than 0.3 (-)).

2.3. Data processing

The findings of the site visits are described in this section. Moreover, the section contains the analysis of the aquifer test data. The most important outcomes for each of the five locations are discussed below. A complete overview of all simulations in data analysis (25 per location) can be found in Appendix D.

2.3.1. Location: Bingo

Site inspection

The surroundings of Bingo are characterized by a mildly sloping landscape. (Bed)rock appears occasionally at the surface. Site inspection showed an abundance of charred vegetation. The area is exposed to bush fires. As a consequence of these bush fires the agricultural field is not in operation. Map inspection shows the presence of the Volta river within several kilometres from Bingo. However, no indications of surface water (water-bodies and/or ponds) were observed. Bingo inhabitants experience inundation levels up to 1-2 m, usually lasting for days. The inhabitants label wet season flooding as high. Flooding is not always directly caused by rain. Sometimes rainfall collects to fill up depressions in the landscape at a certain moment in time. Inspection on the infiltration well revealed the presence of a steel lid. Above surface level no well screen perforations were observed.

Measurement quality

A malfunctioning power converter postponed the pumping test start. Since nightfall was a time limiting factor, the delay resulted in a shortened total test duration. Well turbulence caused the rope to which the divers were tied to tangle, which meant the sensor depths changed over the course of the experiment (see measurement set-up in Appendix C). Additionally, because of the tangle, hand measurements also became unreliable. The direct result is a long-term gap in pumping test drawdown data (yellow dotted line in Figure 2.4). The exact drawdown at the last moment of pumping is missing.

Fit analysis

The absence of data has its effects on the parameter fitting capabilities. As visible in Figure 2.4, Theis's method encounters difficulties here. Drawdown most definitely exceeded the measurement limit of 8 m. This is not reflected in the parameter outcome of Theis's method. Defective fitting capabilities, due to a gap in data, are clearly less emphatically present in the analysis by the use of TTim. Optimal parameter values are found at which drawdown curves exceed the drawdown measurement limit. Taking borehole storage and/or well resistance in consideration may potentially underlie this. This example shows it is not by definition required to feature complete drawdown data. By the use of TTim incomplete time series can result in adequate optimal parameter values. In order size the values found are low but align initial conditions. Furthermore, it can be appointed that the double-layered transmissivity values found, suggest the presence of only one layer of groundwater flow.

Table 2.1: Bingo - overview best fit parameters

	Method	Stor [m]	Res [d]	T1	T2 [m²/d]	S1	S2 [-]	RMSE [m]
Analytical	fmin	-	-	10.83	-	2.0e-04	-	0.798
1 lay	fmin	0.0647	5.6e-02	26.23	-	6.6e-03	-	0.163
2 lay	fmin	0.0635	-	2.8e-04	8.25	3.0e-03	2.1e-06	0.107
2 lay (pp)	fmin	0.0597	-	8.6e-04	7.44	7.1e-03	6.3e-06	0.078

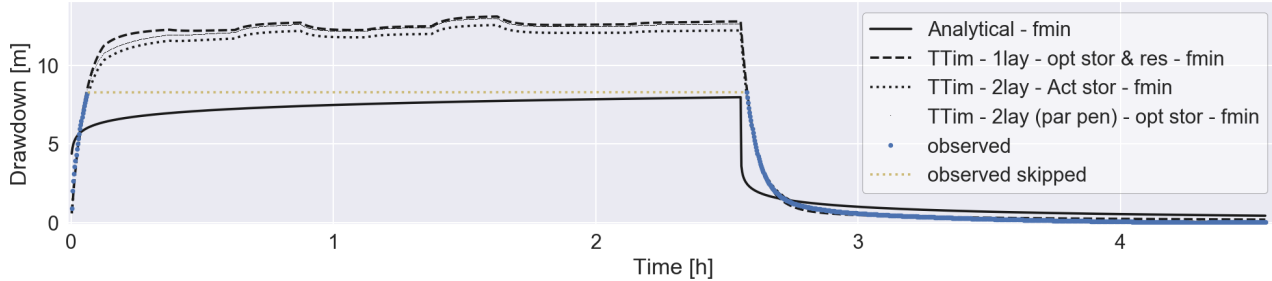


Figure 2.4: Bingo - Simplified models best fit

Effect of model complexity

Both parameter optimization functions (`Fmin` and `Calibrate`) are able to derive reasonable solutions. Results of the `Calibrate` optimization function reveal that an increase in model degrees of freedom does not necessarily lead to better performance (Appendix D). By looking at the TTIm best fit solutions (Figure 2.4) only minor distinction can be made in the performance between the models with a single layer, double layer or double layer with a partially penetrating well. Overall, model accuracy slightly increases (Root-Mean-Square-Error slightly decreases) with an increase in model complexity. However, this increase is not significant.

2.3.2. Location: Nungo

Site inspection

The remote community of Nungo is located in the Upper East Region (UER) of Ghana. Access is only possible by an unpaved road. The landscape is mildly sloping to flat. Low vegetation is interspersed by plains. Adjacent to the village an out of use agricultural field is present. The Volta river is located at approximately 400 m. Wet season flooding occurs due to riverbank over-topping. Inhabitants label inundation levels as extreme. Water levels of 3 m and higher persist for the entire rainy season. The infiltration well has perforations above surface level. At the moment of inspection the top of the well was deformed by heat, which meant it was not possible to close it off by a lid.

Measurement quality

Installation of the test set-up was affected by difficulties with pump immersion. From the first moment of pumping, discharge rates were effectively zero. An inspection revealed the well was filled with a liquid consisting of water, sandy clay and debris. The pumping test was restarted twice with an increased pump elevation. This did not result in an improvement. It was not possible to perform a pumping test at this location.

Remark

The well is clogged and should be cleaned before measurements can be done. No pumping test was performed and no data was acquired.

2.3.3. Location: Nyong Nayili

Site inspection

The landscape of Nyong Nayili and its surroundings is mostly flat. A mix of bushes, low vegetation and crop fields is present. During site inspection, no agricultural fields had been delineated. The local community estimated that wet season inundation levels reach up to 1 m. Throughout the season inundation fluctua-

tions occur, caused by rainfall. No river or water flow was observed in the area. A muddy, stagnant pond is present at close well range (approximately 40m). The infiltration bed was still inundated (approximately 0.2 m) during the pumping test. Well perforations were observed above the infiltration bed. The presence of water on the infiltration bed definitely had an impact on the measurements of the pumping test.

Measurement quality

The start of the pumping test was delayed because the well could not immediately be located, and because of a clogged discharge hose. Since nightfall was a time limiting factor, the delay resulted in a shortened total test duration. In addition, the inundated infiltration bed affected the pumping test. The first 20 minutes of drawdown measurements are affected by an (unknown) additional inflow (see Appendix B). This period is not taken into account in further analysis. The noise of dripping water during pumping test application suggests the interference of additional inflow even beyond the first 20 minutes.

Fit analysis

Theis's method encounters difficulties in finding parameter values leading to a reasonable good fit. The optimal solution does not result in a reasonable curve fit. The resulting storativity is equal to the predefined upper bound. The solution is unreliable and can be neglected. The use of TTIm has a positive impact on the outcome in data analysis. Found transmissivity values are not analogous, but potentially represent nature. The resulting storativity values can be interpreted as low. The obtained optimal borehole storage values are considerably high compared to the initial conditions. Values upto five times the actual borehole storage are encountered. These values potentially reflect the presence of additional inflow. Overall curve fitting performances are moderately good. The absence of a decent fit can potentially be attributed to the data that was left out and/or the unknown additional inflow of water over time.

Table 2.2: Nyong Nayili - overview best fit parameters

	Method	Stor [m]	Res [d]	T1	T2 [m^2/d]	S1	S2 [-]	RMSE [m]
Analytical	fmin	-	-	6.00	-	3.0e-01	-	0.752
1 lay	cal	0.2419	-	13.35	-	7.8e-05	-	0.457
2 lay	cal	0.2436	-	6.95	6.98	4.6e-06	3.6e-05	0.457
2 lay (pp)	fmin	0.2659	1.7e-02	1.7e-04	28.61	1.1e-02	4.4e-06	0.450

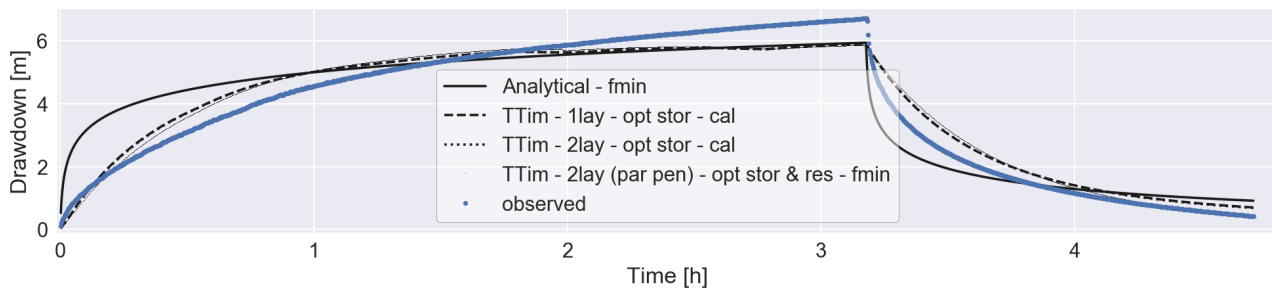


Figure 2.5: Nyong Nayili - Simplified models best fit

Effect of model complexity

The choice of optimization function did not significantly impact the values of the optimized parameters. An increase in the number of parameters did not improve model performance, it even worsens model performance in some cases. In all the model simulations the Root-Mean-Square-Error is substantial. The accuracy of the optimal parameter values is questionable. Further research on the impact of missing starting data and/or the impact of water inflow during a pumping test is recommended.

2.3.4. Location: Janga (1/2)

Site inspection

The infiltration system near Janga is located at the bank of a dry river bed. The Volta river is located at approximately 1000 m (see fact-sheet visualisation, Appendix B). A stagnant pond is present at a distance of

approximately 70 m from the well. Wet season flooding is caused by the river. The flooding was described as a constant inundation of over 4 m and lasts for the four months of wet season. During field visit no agricultural farm was seen. The infiltration well above surface level has perforations and is equipped with a plastic/concrete cover.

Measurement quality

Bush fires are frequent occurrences in the region. Due to close range appearance of fire at the time of measurement, the test is aborted early. The duration of the recovery process monitoring is affected. The color change in water discharged during the pumping test was noteworthy. The water switched color from brownish to grey to white to clear several times.

Fit analysis

The magnitude of the parameter is in line with the values found at the other research locations. The RMSE values are significantly larger, indicating the drawdown curve was not correctly modelled. The large RMSE-values can be attributed to the pumping test drawdown part. The shape of the drawdown curve shows an initial lowering of the groundwater level, which becomes more steady as time progresses. But then after approximately 90 minutes, the groundwater level starts dropping more quickly again before levelling off slightly. None of the methods used in the analysis of the pumping test data is able to mimic the behaviour observed during this pumping test.

Table 2.3: Janga first attempt - overview best fit parameters

	Method	Stor [m]	Res [d]	T1	T2 [m²/d]	S1	S2 [-]	RMSE [m]
Analytical	fmin	-	-	8.84	-	3.0e-01	-	1.339
1 lay	fmin	0.0635	-9.7e-03	9.09	-	1.6e-02	-	1.382
2 lay	fmin	0.1287	-	12.48	1.3e-04	1.9e-02	1.1e-08	1.445
2 lay (pp)	fmin	0.0635	-	9.1e-05	15.19	4.3e-08	3.1e-03	1.530

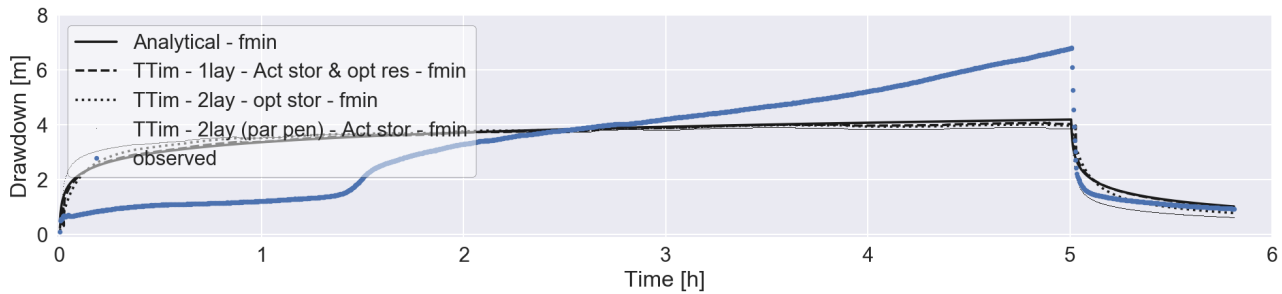


Figure 2.6: Janga first attempt - Simplified models best fit

Effect of model complexity

The shape of the drawdown curve is striking. There is a sudden increase in drawdown after 90 minutes of pumping. Towards the end of pumping period (four to five hours) the curve does not show the characteristic behaviour of reaching a new equilibrium. The variable rates of drawdown observed during the pumping test are not observed during the recovery test. As stated by Kruseman and de Ridder (2000), most of the time there is not a unique theoretical solution for these well-flow problems. This makes the identification of the right (theoretical) system even more difficult. Additional fieldwork could provide more information as to which local characteristics are causing this behaviour. A second pumping test was performed to verify whether the first test was done correctly.

2.3.5. Location: Janga (2/2)

Measurement quality

The initial (first two hours) pumping test discharge rates vary slightly (Appendix B). The drawdown curve is potentially affected by these variations. Similar to the first test, the extracted water changed color several

times. Compared to the previous research, the recovery period was monitored for longer.

Fit analysis

Despite the application of a pumping test with a lower discharge (compared to first attempt) the drawdown data shows similar behaviour. The lower values in Root-Mean-Square-Error can be attributed to the lower absolute drawdown (test with lower discharge rate) and the increased duration of recovery monitoring. The RMSE values still indicate the models are not able to describe the observed behaviour. The resulting parameters are shown in Table 2.4.

Table 2.4: Janga second attempt - overview best fit parameters

	Method	Stor [m]	Res [d]	T1	T2 [m ² /d]	S1	S2 [-]	RMSE [m]
Analytical	fmin	-	-	15.97	-	3.0e-01	-	0.571
1 lay	fmin	5.4e-07	-9.7e-03	13.54	-	1.9e-02	-	0.551
2 lay	fmin	0.2228	-2.2e-02	2.05	8.13	2.1e-02	4.1e-04	0.545
2 lay (pp)	fmin	0.2005	-3.1e-02	6.59	0.86	9.4e-05	2.1e-03	0.545

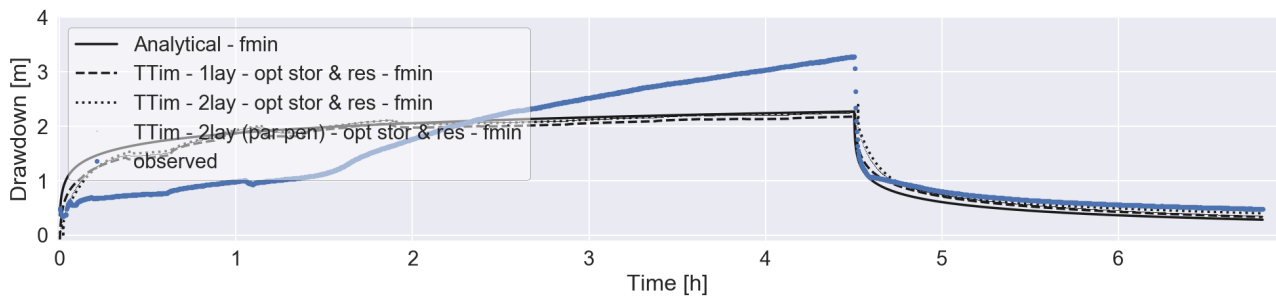


Figure 2.7: Janga second attempt - Simplified models best fit

Effect of model complexity

The second test confirms the behaviour observed in the first test. There are multiple explanations for this behaviour, i.e. one can think of the subsurface layers that are emptied as pumping continues, hydraulic interaction with the river bed or fracture zones drawdown and more.

2.3.6. Location: Ziong (monitoring)

Site inspection

In the study site surroundings of Ziong, no rivers, water flows or ponds were observed. Wet season inundation depths were said to be less than 2 m. Daily level variations occur as flooding is caused by rainfall. The landscape is flat. Occasionally, (bed)rock is observed at the surface. High grasses and bushes are present. There are several crop fields nearby. The infiltration system does not have perforations above surface level. A steel lid is present to cover the top of the well. The agricultural field and the ASR-system were fully operational.

Measurement quality

During the observed period the system was in daily operation. The system was monitored over multiple days. The divers had to be installed above the lowest groundwater levels because of the presence of the pump and the fact that the system was already in operation. This meant that the largest drawdowns could not be measured. The estimated discharge rate of 20 m³/d is based on multiple measurements of the volume meter. In analysis it is assumed to be constant. The exact time at which the recovery starts is unknown because the lowest groundwater levels could not be measured. Based on the comparable test situation at the location Bingo, it is assumed the recovery starts 4 minutes before the first measurement indicating the recovery has started.

Fit analysis

The analytical Theis method was not applied in this monitoring test situation. Analysis with TTim show rea-

sonable results. The modelled drawdown corresponds closely with the observations. This example shows the advantages of TTIm. The obtained transmissivity values of approximately $1 \text{ m}^2/\text{d}$ are low.

Table 2.5: Ziong - overview best fit parameters

	Method	Stor [m]	Res [d]	T1	T2 [m^2/d]	S1	S2 [-]	RMSE [m]
1 lay	fmin	0.0382	-	1.76	-	1.1e-03	-	0.255
2 lay	fmin	0.0635	-0.05	0.38	1.05	2.9e-02	1.2e-03	0.240
2 lay (pp)	fmin	0.0147	-0.08	0.23	0.78	2.6e-02	1.3e-03	0.243

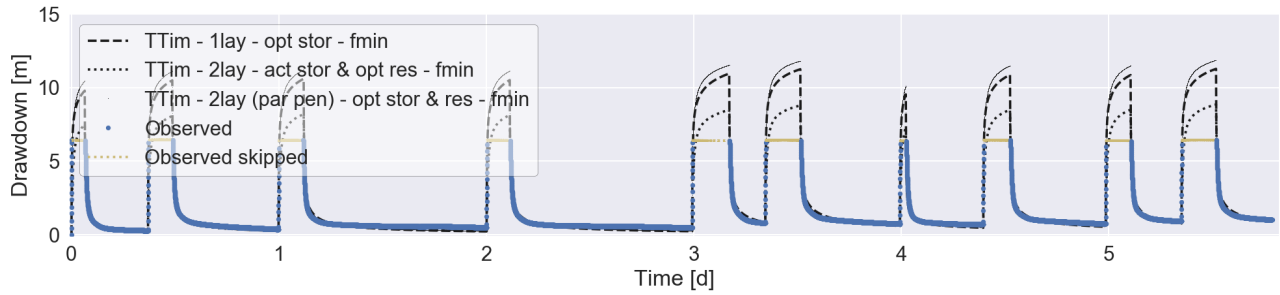


Figure 2.8: Ziong - Simplified models best fit

Effect of model complexity

Both optimization functions (Fmin and Calibrate) yield comparable parameters. When applying a simplified model with an increased number of degrees of freedom, the Fmin optimization function tends to score slightly better on values for the Root-Mean-Square-Error (Appendix D). This however concerns a single measurement analysis, with a single set of predefined initial parameters. No other objective functions are taken into account. The performance of the different models does not show any trend. Models with an increased number of degrees of freedom do not necessarily describe the observed data better. All three theoretical models are able to describe the observed data at Ziong to a certain extent.

2.4. Results & conclusions

This section contains the conclusions that can be drawn from the site visits and the analysis of pumping test data. The final part of this section describes how this data was used to derive parameters for soil scenarios to study potential methods for improvements of ASR systems in northern Ghana.

Maintenance of ASR systems

- ASR-system cleaning

One year after construction (2016) the penetration depth of all five boreholes has decreased (significantly) due to the deposition of sand at the bottom of the well. The impact differs per location, but at each location a minimal depth decrease of 6 m is observed. The most striking example is the borehole at location Nungo, where a complete clogging has occurred (over 40 m decrease in depth). Measures should be taken to prevent the occurrence of clogging. It is recommended to seal off each borehole with a plastic/concrete lid. The tube penetrations above the infiltration bed should be sealed off permanently to avoid inflow of undesired sand and clay. In addition, annual maintenance of the borehole and infiltration bed is desirable.

- Additional research

The results obtained through the analysis of the pumping tests seem to yield plausible estimates of subsurface characteristics. However, the models are not able to closely match the observations in all cases. Additional research could be done to expand the models to include processes that were left out in this analysis, e.g. inflow from the infiltration bed and irregularities (sudden additional decrease)

in the drawdown time-series. Methods to deal with missing data (gaps in time series) could also be improved upon.

- Recommendations for future pumping tests

Pumping tests should be performed with at least one (preferably more) observation well at a certain distance from the well (Kruseman and de Ridder, 2000). These tests potentially give insight in well skin behaviour (degree of resistance) and increase the amount of data from which subsurface parameters can be derived. The installation of one or more divers is recommended if complete ASR system understanding is required. This can provide more insight into how these system function throughout the year.

Applicability of methods & models

- Performance (analytical) methods; Theis & TTIm

Compared to the simplest pumping test interpretation (Theis's method), TTIm offers more model options (borehole storage, well skin resistance, multiple layers) in drawdown data analysis (Bakker, 2013a,b). In this research TTIm outperforms Theis's method. However, TTIm also encounters limitations, e.g. when there is a variable inflow at the start of a pumping test or when an additional sudden drop in drawdown occurs.

- Performance of optimization functions; Fmin & Calibrate

Obtained geohydrological parameters represent local nature to a certain extend. This is confirmed by the Root-Mean-Square-Error values (objective function). Application of the two optimization functions generates outcomes. The results of different optimization functions can lead to differences in parameter size, while goodness of the fit statistics (RMSE) are comparable. However, the resulting parameters are generally similar. Therefore, it can be concluded that both optimization functions (Fmin and Calibrate) are applicable for the determination of suitable T and S values.

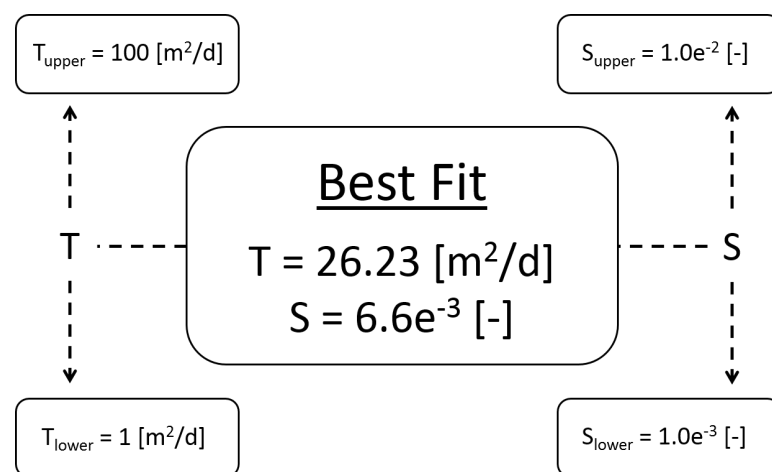
- Performance of proposed subsurface models

Three simplified system models were used: a single layer model, a double layer model and a model with two layers and partial penetration of the well (Figure 2.3b - 2.3d). Based on the Root-Mean-Square-Error objective function, none of these systems performs consistently better or worse than any of the others. Therefore, the most simple (the single layer) model is applied in the rest of this research.

T & S values

Drawdown measurements are taken in the extraction well. This set-up deviates from the desired common standard (Kruseman and de Ridder, 2000). It should be kept in mind that the quality of the data can be questioned. At each location different combinations of parameters yielded similar drawdown curves. This is likely a consequence of only having measurements inside the extraction well. The different models that were applied in the analysis of the data did not yield significantly different results. It is clear that due to the lack of groundwater measurements in the vicinity of the pumping wells, there is some uncertainty in the derived subsurface parameters.

The results from Bingo are used in further analysis. A bandwidth is defined to deal with the uncertainties mentioned in Section 2.3. Upper and lower limits for T and S values are derived. The bandwidth is presented in Figure 2.9. Transmissivity limits are based on the obtained values in Section 2.3 and some factor of safety. For the definition of the storativity values a different approach was used. The parameters limits are based on more commonly found values. The chosen lower limit storativity (S_{lower}) corresponds with the situation of a confined aquifer, while the upper limit (S_{upper}) related more to the specific yield of a phreatic storage (Fitts, 2012; Strack, 1989).

Figure 2.9: T & S bandwidth selection

3

ASR system - Improvements & sensitivities

In the north of Ghana farmers are in search of sources to increase the water availability during dry season. This chapter investigates to what extent an Aquifer Storage and Recovery (ASR) system, and the potential improvements of the system, can provide solutions. The options are explored by the use of a hypothetical ASR system. The synthetic model is adapted to potential northern Ghana conditions by the use of the geo-hydrological parameters found in aquifer test data analysis (Chapter 2.4).

In Section 3.1, the applied soil scenarios are presented and a base model ASR system simulation is defined. Moreover, the types of ASR system improvements, sensitivities and test criteria are included in this section. The year-round performances of the synthetic ASR system are explained in Section 3.2. Section 3.3 contains the results of three types of ASR system improvements; (a) the extension of daily pumping time, (b) the enlargement of the borehole cross-sectional dimension and (c) the reduction of the well skin resistance. In Section 3.4, the ASR systems interaction with nature is explored by a sensitivity analysis on; (a) the degradation of well depth by clogging; (b) the shortening of the wet season inundation time-span and (c) the reduction of the wet season inundation levels. The relations between soil conditions and the different ASR system improvements and sensitivities are presented in Section 3.5. The Chapter ends with a discussion on the obtained results, Section 3.6.

3.1. Methods - ASR system simulation

In this methodology part a synthetic ASR system is presented to explore and access the system (improved) performances. The applied representations of (northern Ghana) natural conditions are defined. The section contains information on: soil scenarios; the ASR system base model (reference); the types of ASR system improvement/sensitivity and the research test criteria. The methods are implemented in the subsequent parts of this Chapter (Section 3.2 - 3.6). Additional information on the modelling environment (MODFLOW) is included in the Appendices E - F.

3.1.1. Soil scenarios

The northern Ghana geohydrological conditions are potentially represented by the results from the aquifer test data analysis in Chapter 2. The derived parameter bandwidth (Figure 2.9) is used to adapt the synthetic ASR system to locally applicable conditions. Transmissivity (T) values in the scope of 1 - 100 (m^2/d) and storativity (S) values between $1e-3$ - $1e-2$ (-) are taken into account by the definition of five soil scenarios. An overview of the research soil scenarios is presented in Figure 3.1.

3.1.2. ASR system - Synthetic base model definition (reference)

The research is provided with an ASR system base model. Unsurprisingly, the base model accommodates basic conditions. The applied conditions are based on the northern Ghana study site inspections and the gathered borehole log sheets (Appendix A). The simplified model represents a hypothetical 'standard' ASR system, potentially applicable in northern Ghana. The base model is a reference, a starting point to which the impact of system improvements can be compared. The distinctive modelled components (e.g. subsurface, well characteristics and simulation time frame) are one-by-one described. The overall representation

of the base model (with the inclusion of the soil scenarios) is presented in Figure 3.1.

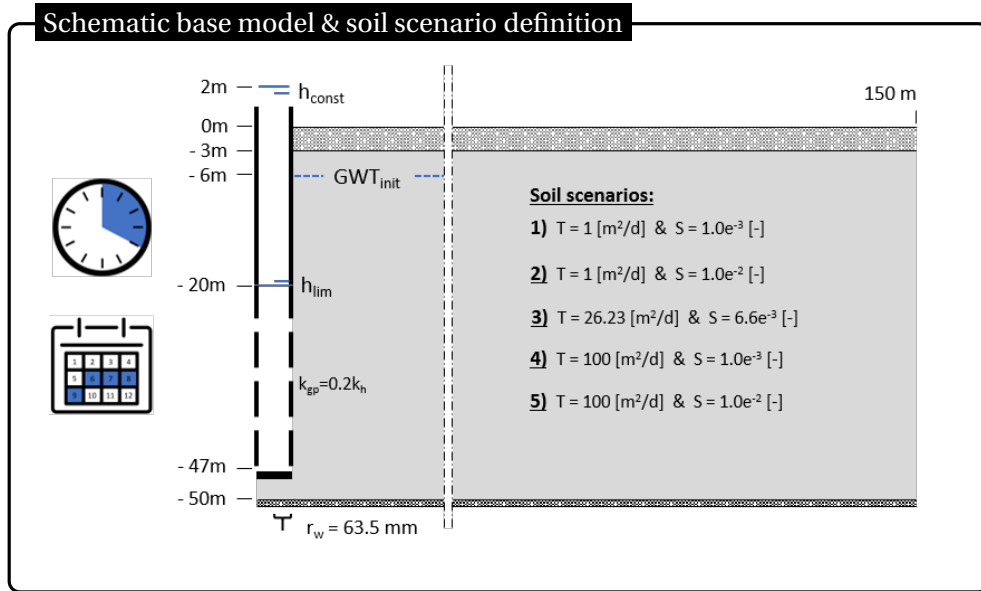


Figure 3.1: Schematic base model & soil scenario definition

Subsurface

The interaction between the ASR system and the upper 50 m of subsurface is simulated. The model top is bounded by a 3m-thick poor permeable soil layer. The well penetration (partially) occurs in the underlying 47m-thick single aquifer. With an elevation of -6 m the initial groundwater table (GWT) is positioned just under the aquifer top. Unconfined conditions are applicable. The characteristic T and S values, defined in the soil scenarios of Section 3.1.1, apply to this aquifer. The aquifer is assumed to be homogeneous and horizontally isotropic, while the vertical anisotropy is 1/4 (-). The model extent is defined in correspondence with the obtained results from fieldwork data analysis. With a radial length of 150 m, the model scope is assumed to be sufficient. More information on the derivation of the extent can be found in Appendix E.2.

Well dimensions & pump placement

The base model design accommodates a single well with a radius of 0.0635 m (2.5 inch) and a total length of 47 m. It is assumed, in-well accumulation of sedimentation is absent. The displacement of water between well and aquifer is possible through a partially penetrating screen. Well screen perforations are present from 20 m to 47 m below the model top (screen length 27 m). More details on the well hydraulic conductivity can be found below. Dry season groundwater withdrawal is possible through the installation of a pump. The model contains a submergence pump positioned in the well at an elevation of -30 m. The maximum drop in GWT is limited to an elevation of -20 m (14 m drawdown relative to initial conditions). In this way the occurrence of well screen dry-out and pump malfunctioning is prevented.

Well hydraulic conductivity

Due to the tiny nature of screen perforations (and constructional soil around the borehole), a well skin resistance (hydraulic conductance) is taken into account. In this research the well hydraulic conductance is defined by the use of Equations 3.1 - 3.4.

$$cond = \frac{2\pi r_w b}{c_{skin}} \quad (3.1)$$

$$c_{skin} = \frac{\Delta r_{skin}}{K_{skin}} \quad (3.2)$$

where $cond$ (m²/d) is the well hydraulic conductance, r_w (m) is the radius of the well, c_{skin} (d) is the well skin resistance, Δr_{skin} (m) is the well skin (radial) length and K_{skin} (m/d) is the well skin hydraulic conduc-

tance.

As stated by Houben (2015), the hydraulic conductivity of a sequence of materials (i.e. well screen, gravel-pack and aquifer) can be calculated by Equation 3.3 (1D flow assumed). The model well cells are in this research defined in correspondence with the (radial) well dimensions (Appendices E & F). Therefore, the well skin conductance is assumed to be dependent on the materials of the well screen and the gravel-pack only. In this case, the well skin hydraulic conductivity corresponds with the simplified variant of Equation 3.3; Equation 3.4.

$$K_{tot} = \frac{\Delta r_{tot}}{\frac{\Delta r_{sc}}{K_{sc}} + \frac{\Delta r_{gp}}{K_{gp}} + \frac{\Delta r_{aq}}{K_{aq}}} \quad (3.3)$$

$$K_{skin} = \frac{\Delta r_{skin}}{\frac{\Delta r_{sc}}{K_{sc}} + \frac{\Delta r_{gp}}{K_{gp}}} \quad (3.4)$$

where K_{tot} , K_{skin} , K_{sc} , K_{gp} and K_{aq} (m/d) are respectively the total, the well skin, the well screen, the gravel-pack and the aquifer hydraulic conductivities and Δr_{tot} , Δr_{skin} , Δr_{sc} , Δr_{gp} , Δr_{aq} (m) are the corresponding (radial) length intervals of these materials.

The well skin length (Δr_{skin}) equals the summed up length of the well screen Δr_{sc} and the gravel-pack Δr_{gp} . An ASR system well screen length of 0.005 m is measured in-field. The radius of the soil around the well, the gravel-pack, is undetermined. As stated by (Bot, 2016), for proper installation a minimum length of 0,125 m is required. This length is assumed and implemented in research.

The well skin hydraulic conductivity (K_{skin}) accounts for the combined conductivity of the well screen (perforations) and the gravel-pack around the well. The hydraulic conductivity of the well screen (K_{sc}) is based on research done by Houben (2015). Perforation sizes (screen slot width) of 2 mm are measured (study site investigation). These screen sizes correspond with a (clean) hydraulic conductivity (K_{sc}) of 1 m/s (Houben, 2015). As stated by Konikow et al. (2009), the well skin hydraulic conductivity (K_{skin}) is typically expected to be lower than the aquifer hydraulic conductivity (K_h). To meet this requirement, the gravel-pack is interpreted as mildly clogged. The gravel-pack hydraulic conductivity (K_{gp}) is assumed to be 1/5 of the, soil scenario dependent, aquifer hydraulic conductivity (K_h).

Time frame

As stated by the Canadian International Development Agency (2011), the northern Ghana regions encounter a single wet season of approximate four months (dependent on the year and altitude) annually. Randomly applied interviews with local inhabitants (site visits) confirmed the temporal resolution of the wet season. Inundation levels of 0.5 m - 4 m are perceived with a timespan varying from weeks till the four months duration of the wet season (Appendix B).

Seasonal system performance is simulated by a year-round (long term) temporal model resolution. In the synthetic (simplified) model it is assumed the region encounters flooding for as long as the wet season. A flood duration of four months is taken into account, starting on June 1st and ending on September 30th. The flooding is simulated by gravity based infiltration on top of the ASR system. A constant (122 days) 2 m inundation level is assumed (Figure 3.1). In the subsequent eight months of dry season (October-May) no flooding or rainfall is taken into account. In accordance with the data obtained in the ASR system monitoring and interviews with farmers, groundwater withdrawal takes place by four hours of pumping daily. Intermediate day time offers time-space for recovery of the local GWT. For the purposes of this research it is assumed the hypothetical groundwater withdrawal last for as long as the dry season (243 days).

Model discussion

The research base model results do not apply to a single research location (depicted in Figure 2.1). The applied simplified model conditions serve research purposes. Assumptions made, are not by definition realistic. One can for example imagine the actual wet season inundation levels will fluctuate over time. And in practice, groundwater withdrawal needs day-specific tuning (not constant for 243 days) with respect to

agricultural needs. Aspects advisable to take into account in further research.

Modelling environment - MODFLOW

The computational modelling of the research synthetic ASR system is done with Modular Ground-Water Flow Model (MODFLOW), a finite difference model for groundwater flow developed by the U.S. Geological Survey (USGS). MODFLOW is the international standard in groundwater simulation (Harbaugh, 2005; Niswonger et al., 2011). More information on the applied inputs can be found in the Appendices E - F.

3.1.3. ASR system improvements

A free interpretation of the term 'improvement' learns that multiple directions of ASR system modifications are applicable. As stated by Bakker (2010) and Ward et al. (2007), the success and sustainability of an ASR system is amongst others dependent on the length of injection, storage and recovery; the well dimension; and potential clogging of the well screen. In correspondence, the synthetic model of this research is exposed to three types of ASR system improvement:

- a) Extension of daily pumping time:

In a consecutive order the base model dry season pumping time (4 hours daily) is increased (by 1 hour steps) up to a maximum daily (dry season) pump operation of 8 hours.

- b) Enlargement of borehole cross-sectional dimension:

The base model radius (0.0635m) is stepped up (doubled, tripled, etcetera) to in total five times its original radius: 0.3175 m.

- c) Reduction of well skin resistance:

This type of synthetic model improvement is designed by the application of enlarged gravel-pack hydraulic conductivities. In four equal steps (steps of $(2/5)*K_h$) the base model gravel-pack hydraulic conductivity (K_{gp}) is increased to a maximum of $(9/5)*K_h$. Note, well skin hydraulic conductivities larger than the aquifer hydraulic conductivities are considered in this way.

3.1.4. ASR system sensitivities

The forces of northern Ghana's nature can highly fluctuate spatially and temporarily. Nonetheless, the base model houses multiple assumptions that are more or less fixed representations of nature (3.1.2). A sensitivity analysis is part of the research to balance the impact of these assumptions. Three types of model modifications are part of the sensitivity analysis:

- a) Degradation of well depth (clogging):

The study site observations imply that ASR systems in northern Ghana can be vulnerable for the power of nature. Due to the accumulation of sedimentation the well penetrations depths can decrease over time. The reduction is (simplified) simulated by a decrease in the well screen length. An hypothetical initial screen length of 30 m (longer than base model) is reduced in 5 m steps to a total screen length of 10 m.

- b) Shortening the wet season inundation timespan:

Within northern Ghana the duration of the wet season is spatially dependent (Canadian International Development Agency, 2011). Besides, season durations naturally differ between years. Through the application of three research steps, the synthetic base model wet season duration is reduced from four months (Jun-Sept) till one (Aug).

- c) Reduction of wet season inundation level:

The impact of lower inundation levels is analysed in combination with increased initial groundwater tables. Relative to the base model (Δh is 8m) the Δh is reduced (in steps of 2 m) to a minimum of Δh is 2 m.

3.1.5. Test criteria - sustainability

As mentioned in Section 3.1.2, the synthetic ASR system performance is simulated in the time-frame of a year. A distinction can be made between the wet and dry season. The wet season ASR system functionality

is characterized by the groundwater recharge. Analysis is pointed at the inflow volumes and the impact of these volumes on the GWT. In the subsequent eight months of dry season, the system works in reverse. In this time of year, maximum pump operation and the accompanied impact on GWT is of key interest. As a supplement, the mutual relation between recharge and discharge is considered. This is done by the introduction of the 'Recovery ratio' $R\%$ (Equation 3.5). The Recovery ratio is similar to Recovery Efficiency (RE) applied by Ward et al. (2007). Ward et al. (2007) mentions the RE ($R\%$) is a measure to indicate the degree of recovery, i.e. RE = 1 (-) (100%) implies complete recovery.

$$R\% = \frac{V_{out,tot}}{V_{in,tot}} \quad (3.5)$$

Where $R\%$ is the year-round Recovery Ratio (-), $V_{in,tot}$ (m^3) is the wet season total volume recharged and $V_{out,tot}$ (m^3) is the dry season total volume discharged.

The ASR system sustainability is discussed through the Recovery ratio. A $R\%$ smaller than 1 (-) indicates a year round net inflow. In this case, the interaction between system and nature is positive. For the purposes of this research 'sustainability' is defined as a situation where the $R\%$ is smaller than or equal to 1 (-). The potential increase in groundwater withdrawal, due to synthetic improvements, is bounded by sustainability. In other words, a 100% recovery is set as an upper system limit.

3.2. ASR system base model performance

In the methodology all the model components are set to simulate and study the potential improvements of an ASR system. As a reference, this section contains a description of the year-round base model performance in combination with the different soil scenarios.

3.2.1. Wet season

The four months of wet season are simulated by the instantaneous occurrence of a (2 m constant) flooding on top of the ASR system. The difference between the level of inundation and the groundwater table (GWT initially -6 m) results in a gravity based groundwater recharge. At simulation start the head difference (hydraulic gradient) is highest. In correspondence, the initially observed inflow is above average. Due to the mutual interaction, the recharge causes the GWT to increase. The hydraulic gradient mutates over time. In the first days (approximately five days) the hydraulic gradient declines fast. Thereafter, the decline remains present but progresses excessively slow. Although the inflow does not reach a steady state, the rate of water accumulation in the aquifer is close to constant for the time-scope of this research (four months). This system performance is visualized for soil scenario 3 in the Figure G.4 and G.5, but takes place in all soil scenarios. As an visual example of the wet season flood impact on groundwater, the soil scenario 3 radial cross-sectional head contours at the begin (day 5) and absolute end of wet season (day 122) are presented in Figure 3.2.

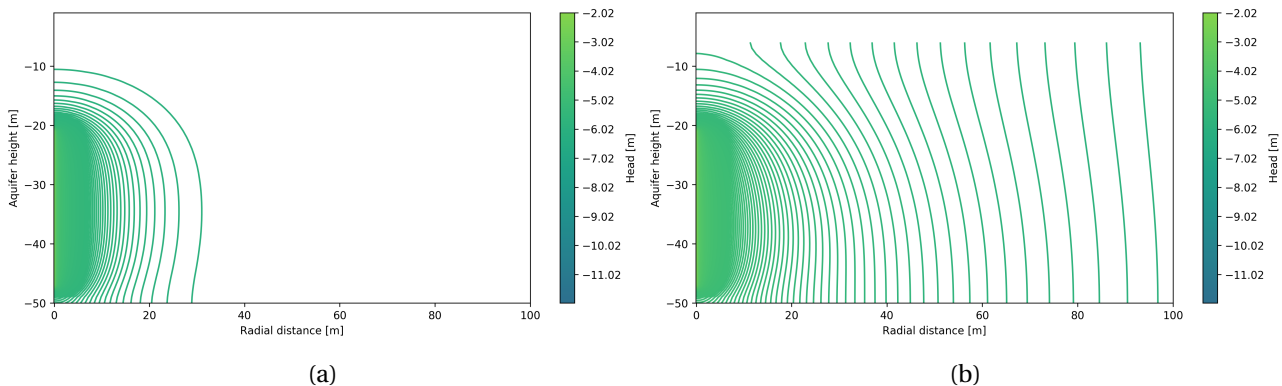


Figure 3.2: Base model soil scenario 3- Cross-sectional contour head after (a) five days and (b) 122 days of infiltration

A significant (more or less instant) head increase is encountered at close well (screen) range. The ground-

water head does not reach the predefined flood level, not even at end of the wet season. A performance that can be attributed to the implemented well skin resistances. In terms of radial distance the system impact (on GWT) remains limited. After 122 days of infiltration the head increase is not quite substantial at a distance of approximately 60-80 m (in all scenarios). More visualizations on the base model performance can be found in Appendix G.1.

The scenario dependent results on total wet season inflow volumes are included in Table 3.1. Differences between the soil scenario 1 and 2 as well as the scenarios 4 and 5 are small. These soil scenarios only differ in the applied storativity (S) values. The variance in storativity (defined in bandwidth) appears to have only limited influence on the inflow of water, most definitely during the application of higher transmissivities. Nonetheless, the obtained absolute recharge volumes show significant differences between the entire spectrum of soil scenarios. These differences can be attributed to the applied soil scenario transmissivity values.

Table 3.1: Base model scenarios - Wet season recharge (m³)

	Sc 1	Sc 2	Sc 3	Sc 4	Sc 5
Volume in (m ³)	207.57	208.68	5357.45	20330.33	20333.15

3.2.2. Dry season

The simulated well discharge (four hours dry season daily) originates by a predefined sustainable maximum withdrawal. In all soil scenarios, the obtained (base model) discharges do not exceed the limits of sustainability (visualized for soil scenario 3 in Figure 3.3). Instead, the system performance is limited by the maximum allowed drawdown. The head bound (-20 m in well) is reached almost instantaneously after the start of pumping operation. In the subsequent hours of pumping (within day) the head bound keeps active. The simulation compensates by a decrease in discharge over time. In practice pumping takes place at a more or less constant rate. It suggests, modelled outcomes overestimate the discharge volumes slightly. Mutual comparison between the days shows a difference in total discharge between the first and all other days of pumping. The first day of pumping generates somewhat higher volumes. In the subsequent days discharge volumes are by approximation equal.

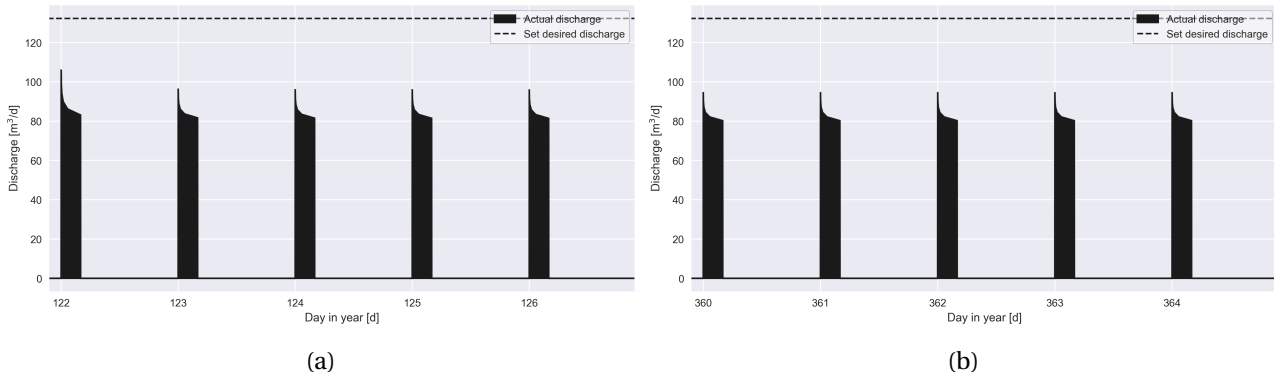


Figure 3.3: Base model soil scenario 3 - Discharge performance for (a) the first five days and (b) the last five days of dry season

The impact of well discharge on groundwater (example soil scenario 3) is presented in the cross sectional contour plot of Figure 3.4. After the first day of pumping the transition from wet (recharge) to dry season (discharge) is still observable. Towards the end of the year this impact is no longer present. Over the entire dry season, the head bound (-20 m) is not reflected in the contour range. This can be justified by the influence of the well skin resistance. The maximum allowed drawdown is reached in the well. As a result, the consequences on nature (groundwater) are less distinctive. More visualizations on the base model performance can be found in Appendix G.1.

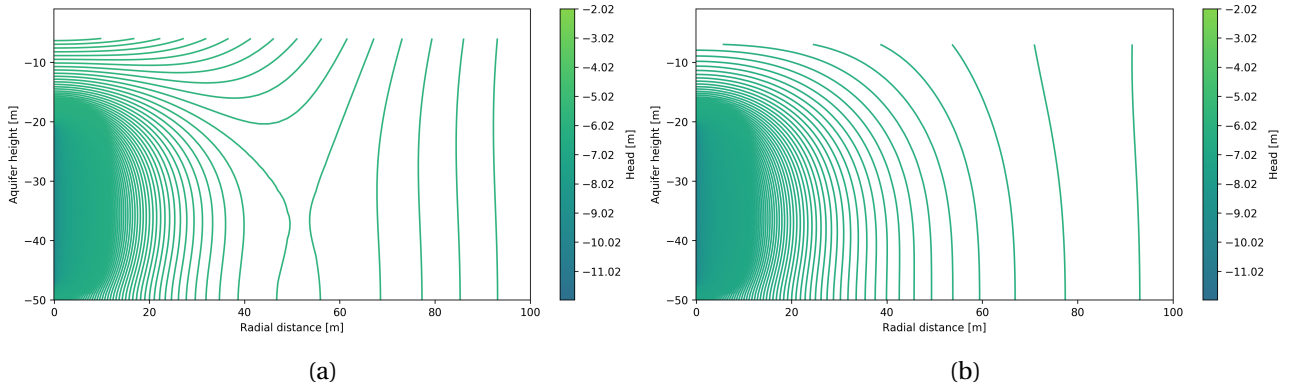


Figure 3.4: Base model soil scenario 3 - Cross-sectional contour head after four hours of pumping on (a) the first day (day 123) and (b) the last day (day 365) of dry season

Unlike the outcomes in recharge, all different soil scenarios show (minor) distinctive results in total volumes discharged. The variation in storativity is possible more pronounced for discharge (after a certain time of recharge) than for recharge. However, the total volumes withdrawn are still in the same order of size for the scenarios 1 and 2, and the scenarios 4 and 5. The obtained discharges are in absolute terms more emphatically determined by the (range of) transmissivity values.

Table 3.2: Base model scenarios - Dry season discharge (m³)

	Sc 1	Sc 2	Sc 3	Sc 4	Sc 5
Volume out (m ³)	129.84	137.76	3299.99	12080.08	12353.58

3.2.3. Recovery ratio $R\%$

The Recovery ratios $R\%$ are for all base models scenarios in the same order of size (Table 3.3. Nonetheless, the positive outlier of soil scenario 2 is worth-mentioning. Mutual differences in performance can potentially be attributed to the varying storativity values (in combination with different transmissivity values). The ratios are also affected by the (soil scenario dependent) well skin resistances. As a consequence, no conclusions can be drawn on the scenario distinctive Recovery ratios.

Table 3.3: Base model scenarios - Recovery ratio $R\%$

	Sc 1	Sc 2	Sc 3	Sc 4	Sc 5
$R\% (-)$	0.626	0.660	0.616	0.594	0.608

In all base model soil scenarios the recovery ratio stays below 100%. In eight months of daily (4 hours) pump operation it is not possible to fully recover the volumes infiltrated due to four months of constant inundation (2 meter) on top of the well. A reason for this is that the inflow bubble may level out over the aquifer due to the hydraulic gradient (Bakker, 2010). The discharge water is not by definition the 'original' recharge water. Under the defined conditions of system composition and use, the found Recovery ratios suggest a sustainable system use and impact on nature.

3.3. ASR system improvements

This section presents the impact of potential improvements of an ASR-system. One-by-one, different types of improvement are taken into account. The model performances are described by the test criteria: total recharge, discharge and Recovery ratio ($R\%$). The results can be weighted to the base model.

3.3.1. Extension of daily pumping time

The extent of the daily (dry season) pumping operation is an easily applicable variant to improve the ASR system yield. Except from additional fuel and possibly temporal storage requirements (poly tanks), no further modifications are required. Base model pump operation is set to be four hours daily (243 days, dry season). This study is pointed at a maximum time-scope of pumping for 8 hours daily. As visualized in Figure 3.5, the system improvement is implemented in four simulation steps.

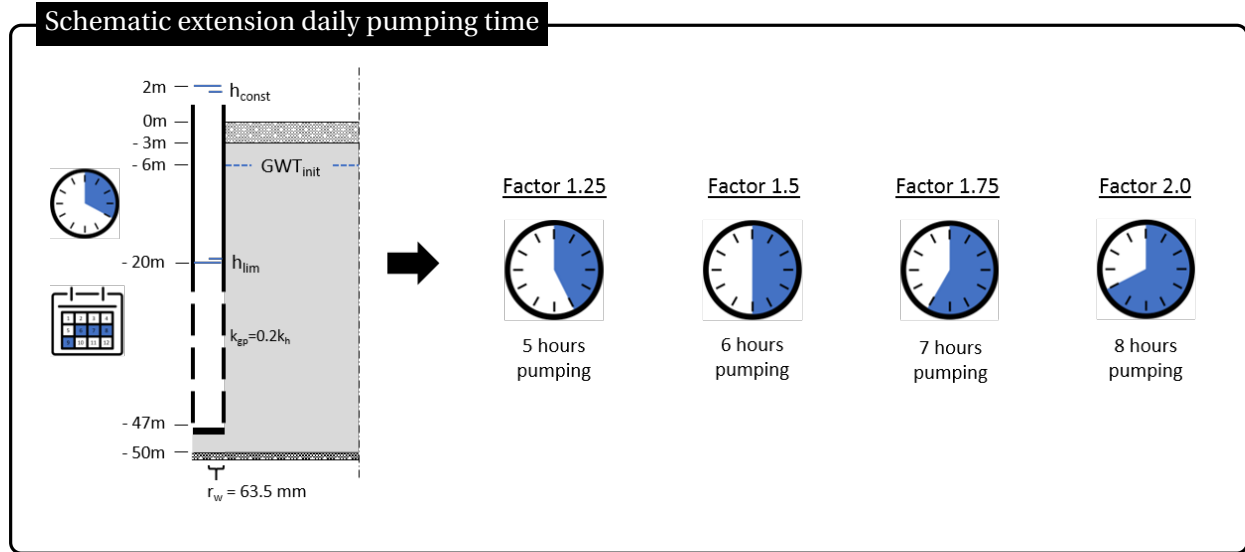


Figure 3.5: Schematic extension daily pumping time

Deviations in wet season recharge are not applicable to this type of system improvement. Pump operation is only in effect during dry season. As visible in Figure 3.6, discharged volumes are most definitely affected by the duration of pumping. An approximately linear ascending relation is observed in all soil scenarios. The relation can be justified by the daily discharge performance, as depicted for the base model in Figure 3.3. After four hours of pumping a more or less equilibrium (maximum) discharge rate is present. Extension by adding active hours of pumping daily will not make any significant change in discharge rates. Moreover, the discharge pattern is repeated daily. Except from the first day, mutual differences between the dry season days of pump operation are small.

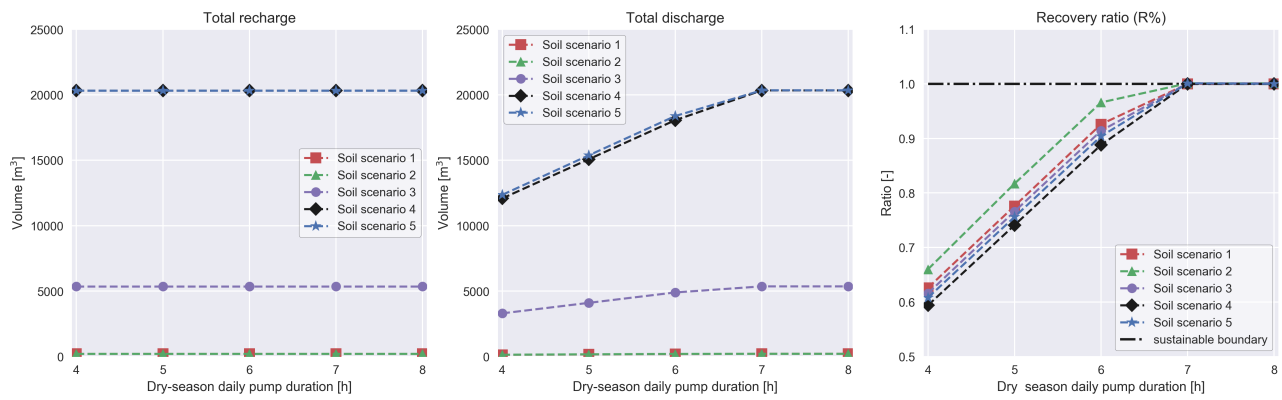


Figure 3.6: Results of yearly total volumes (in, out, ratio) by extension daily pumping time

By the extension of the daily pumping time, the total discharge volumes (eight months) can equal (or exceed) the total inflow volumes (four months). A 100% Recovery is in all soil scenarios obtained in the situation of 6 till 7 hours of dry season daily pumping operation. When base model conditions (2 m constant inundation for four months) apply, it is advisable pumping operations should not exceed the 6 till 7 hours duration (on daily basis). In this way, a sustainable system use can potentially be retained.

3.3.2. Enlargement of borehole cross-sectional dimension

The enlargement of the borehole cross-sectional dimension is a rigorous approach in the improvement of an ASR system. An adjustment that can not be applied on existing systems. If the appropriate equipment is present (e.g. drilling machinery), the enlargement can be applied by new constructions. To take implementation in consideration, it is of extra interest to gain knowledge on potential effects. The enlargement is tested by a stepwise (4 steps) multiplication of the original borehole radius (Figure 3.7).

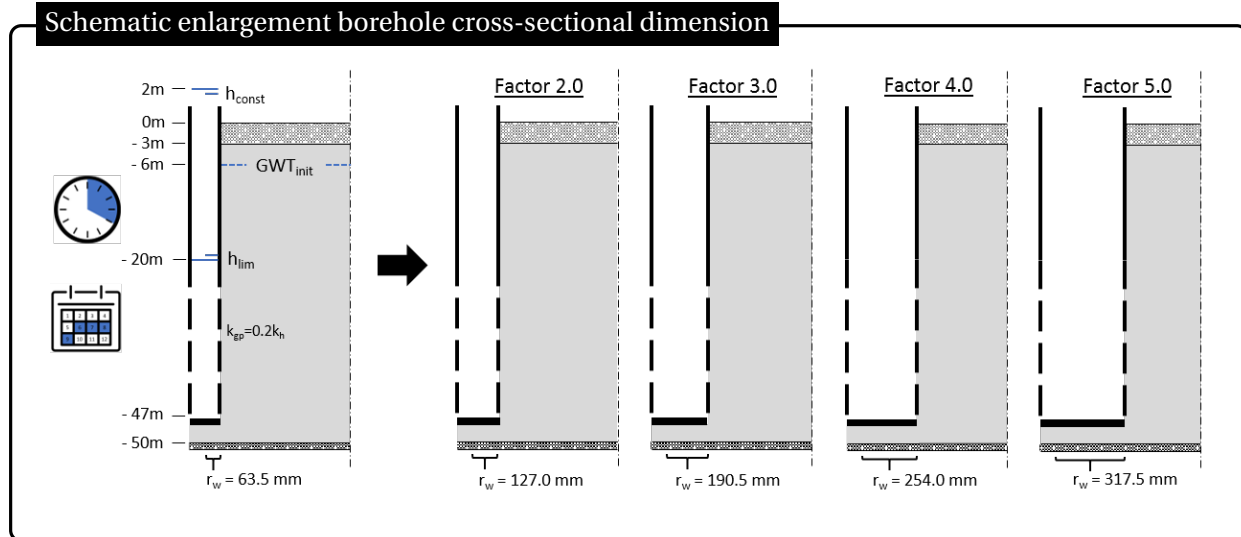


Figure 3.7: Schematic enlargement borehole cross-sectional dimension

The magnification of the borehole diameter is beneficial for both groundwater recharge and discharge. In Figure 3.8, it can be seen that a non-linear ascending relation is present between the ASR system diameter and the total inflow, outflow and Recovery ratio. Well-size improvement is beneficial, but an increasingly less positive effect is obtained. The cross-sectional enlargement is not endless, both in terms of volumes and practical application. In the scope of this research (five times the base model size) a volume increase well over two times its original is acquired.

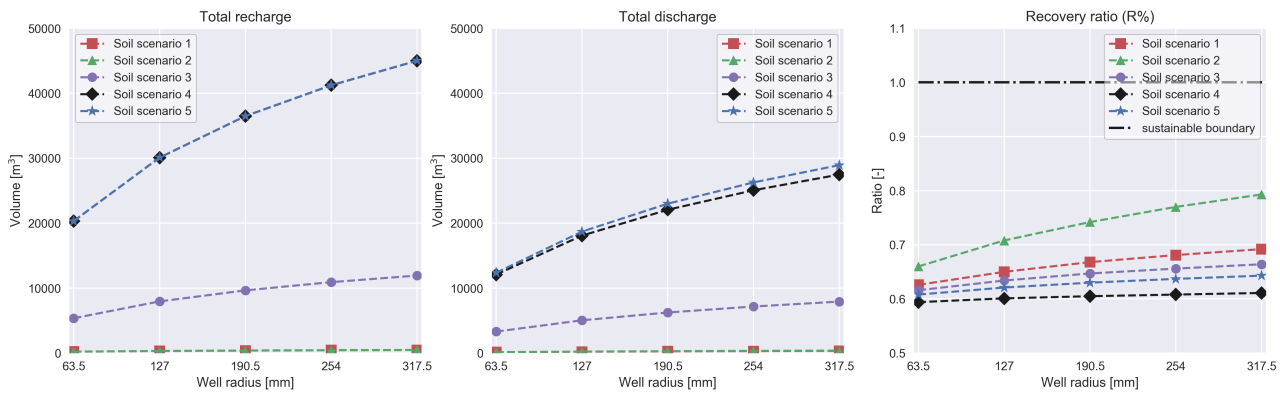


Figure 3.8: Results of yearly total volumes (in, out, ratio) by enlargement well cross-sectional dimension

3.3.3. Reduction of well skin resistance

This type of improvement is characterised by its applicability on existing ASR systems. Fieldwork showed, some already installed systems performed better than others. If the right cleaning equipment is present, a reduction of well skin resistance can potentially offer solutions. Based on the statements done by Konikow et al. (2009) and Houben (2015), the base model is designed with a gravel-pack that is moderately permeable. The (simulated) improvements are implemented by a stepwise increase of the the gravel-pack hydraulic conductivities. As visible in Figure 3.9, gravel-pack hydraulic conductivities that exceed the soil (scenario dependent) hydraulic conductivities are considered.

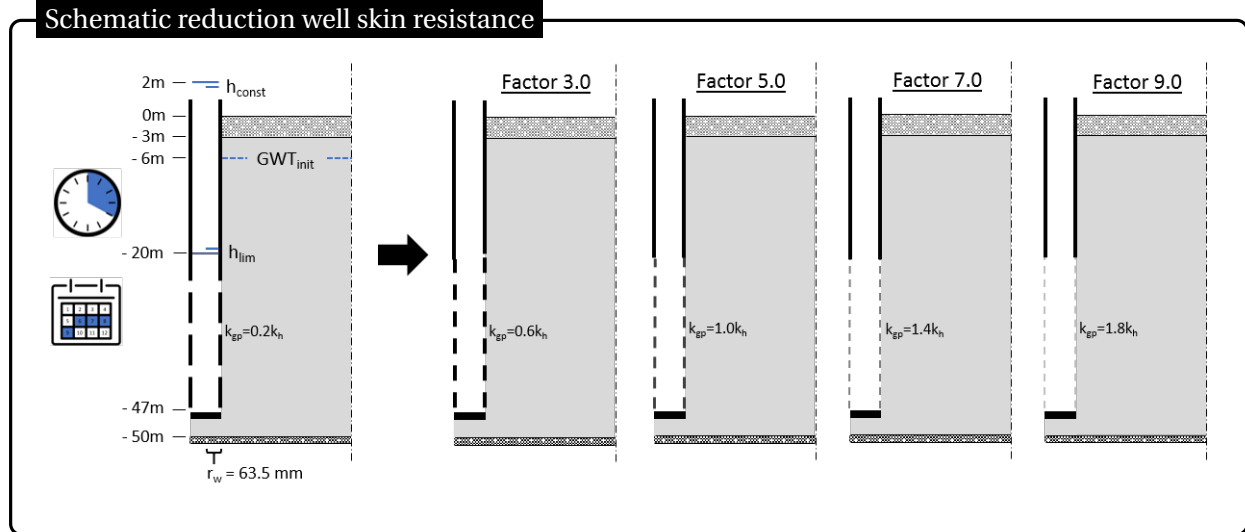


Figure 3.9: Schematic reduction well skin resistance

Figure 3.10 presents the results of the (simulated) improvement of an ASR system by the modification of the gravel-pack hydraulic conductivity. It can be seen that the ASR system performance (on total recharge, discharge and Recovery ratio) increases by improved gravel-pack permeabilities. A non-linear ascending relation is present. In the scope of this research (upto nine times the base model gravel-pack permeability) in- and outflow volumes of approximately two times the original values are achieved. Significant improvements can be made, especially in the lower interval of well permeabilities. In the contrary, system degradation in skin performance can be devastating.

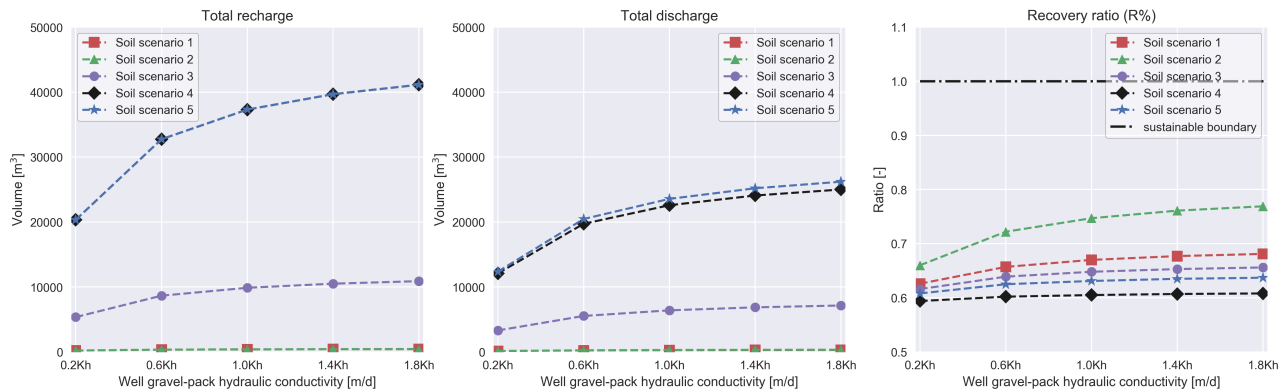


Figure 3.10: Results of yearly total volumes (in, out, ratio) by reduction well skin resistance

* Note, although not clearly visible (especially, when total recharge volumes are taken into account) all soil scenarios are included in the presented figures.

3.4. ASR system sensitivity

The performance of an ASR system is dependent on the natural circumstances of its surroundings. This section explores the impact of changing natural conditions on the system performance. The system sensitivity is expressed by the test criteria: total recharge, discharge and Recovery ratio ($R_{\%}$).

3.4.1. Degradation of well depth by clogging

Prior simulations (Section 3.2 - 3.3) are executed by the implementation of a borehole that is fully function in depth. Fieldwork inspection revealed that sand and/or clay can accumulate at the borehole bottom. The presence of debris can reduce the well penetration depth. By a decrease in model screen length, the borehole clogging of an ASR system is simulated (3.11). In four successive steps the 30 m screen length of an already partially penetrating well is reduced to a minimum of 10 m.

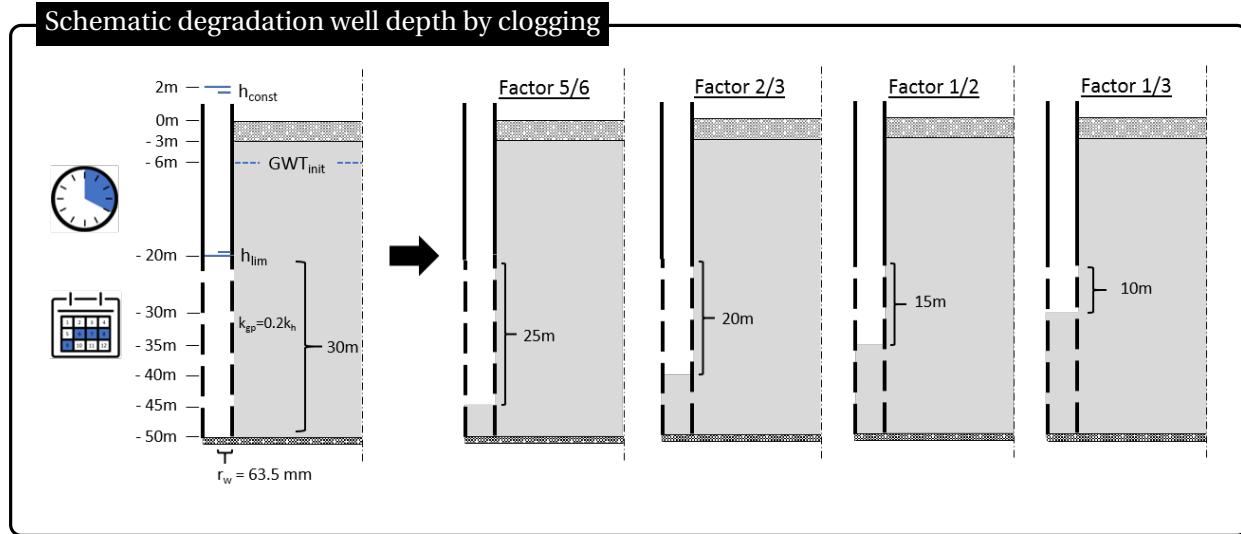


Figure 3.11: Schematic degradation well depth by clogging

The data in Figure 3.12 shows the system performance while the borehole screen length is stepwise reduced. Under the defined model condition (e.g. homogeneous aquifer), the observed relation between the active screen length and the test criteria (recharge, discharge and Recovery ratios) is close to (but not precisely) linear. In relative perspective, the average specific recharge and discharge volumes (m^3/m screen) increase while the length of well penetration is reduced. As stated in Table G.1, this increase is not significant. Moreover, the total inflow and outflow volumes are increasingly negative affected by a further reduction of the well screen length (Table G.2). The preservation of maximum borehole depth should be pursued, to obtain highest system functionalities. This can be achieved by the (preventive) use of a 'pulse drill'.

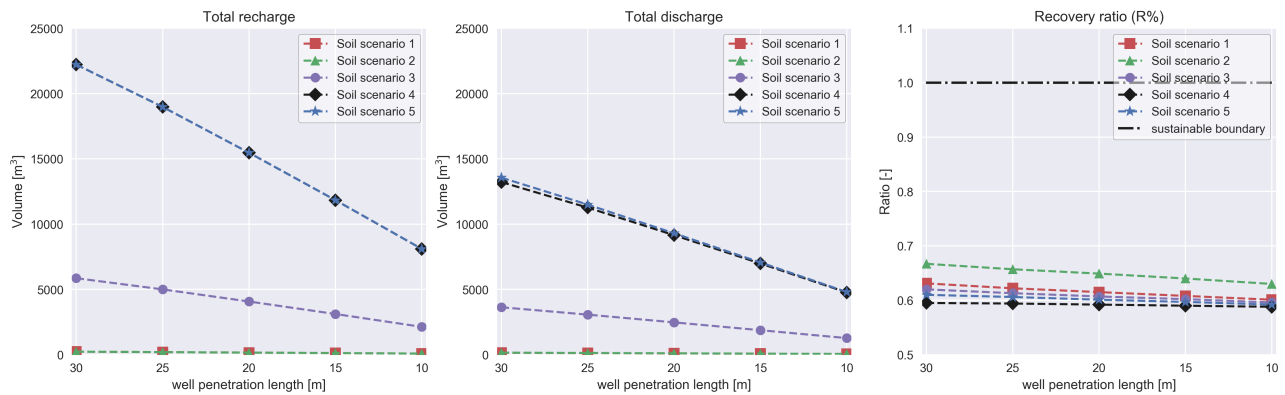


Figure 3.12: Results of yearly total volumes (in, out, ratio) by degradation well depth

As an example, a more precise distribution of the soil scenario 3 recharge volumes over the (variable) well screen length is presented in Figure G.3 (Appendix G).

3.4.2. Shortening wet season inundation time-span

Within northern Ghana the duration of the wet season is spatially dependent. At higher latitudes the wet season time-span is generally less than four months (Canadian International Development Agency, 2011). Besides, wet season duration differs annually. The relation between the wet season duration and the ASR system performance is described in this part of the sensitivity analysis. Through the application of three steps the synthetic base model flood duration (four months: June-September) is reduced. In successive order, the following shortened wet seasons are simulated: July-September, July-August and August.

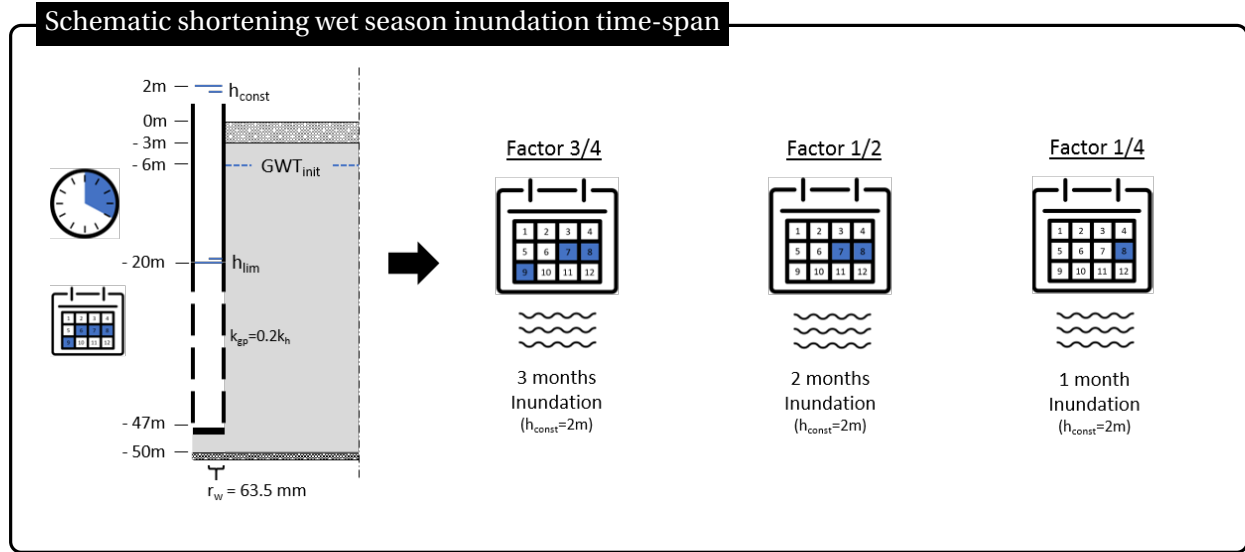


Figure 3.13: Schematic shortening wet season inundation time-span

The data in Figure 3.14 shows an approximately linear relation. A fractional reduction of the (constant level) flood duration, causes an almost equal fractional decrease in the total volumes recharged. This ASR system performance can be explained by the fact that shortly after the inundation start (after approximately 5 days) the inflow rate is close to constant (but not steady) for as long as the research time-scope (four months). For each of the four time-span durations, the wet season performance is visualized in Figure G.4 (Appendix G.2). In the simulation, the desired discharge (dry season) is retained. Nonetheless, the obtained model discharges are affected in the situation of a flooding that lasts for two months (and less). A development caused by the predefined boundaries of sustainable system use (maximum allowed Recovery ratio of 100%).

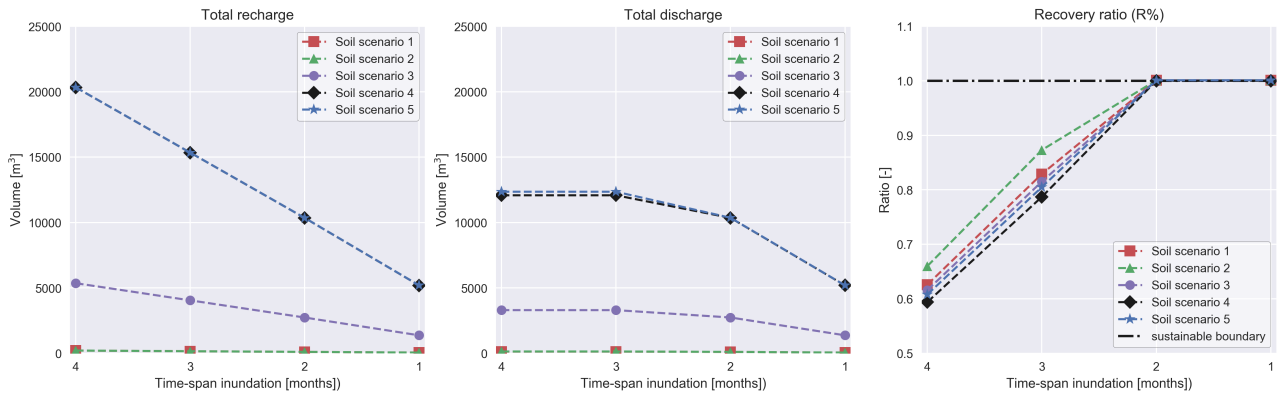


Figure 3.14: Results of yearly total volumes (in, out, ratio) while shortening wet season inundation time-span

3.4.3. Reduction wet season inundation level

As mentioned by the Canadian International Development Agency (2011), within northern Ghana the wet season is variable in terms of duration and intensity. Different flood levels are encountered by local inhabitants (Appendix B). Moreover, the (initial) groundwater tables are not fixed. Based on fieldwork inspection it can be confirmed that the GWT in northern Ghana varies (Appendix B). The impact of lower flood inundation levels is analysed in combination with increased initial groundwater tables. Relative to the base model (Δh is 8m) the Δh is reduced (in steps of 2 m) to a minimum of Δh is 2 m.

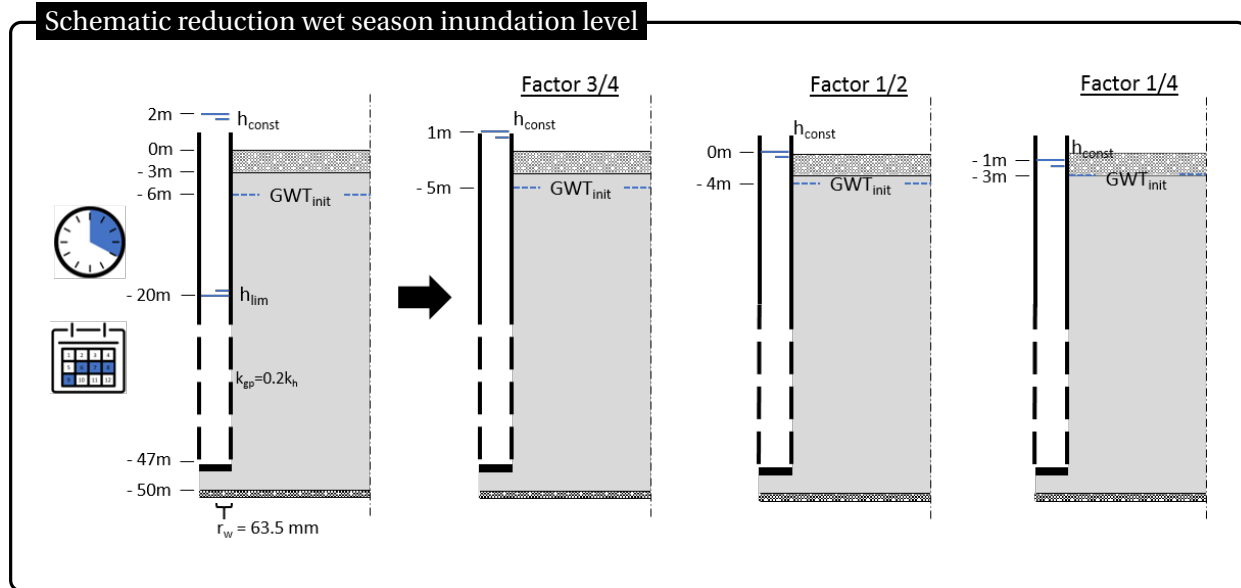


Figure 3.15: Schematic reduction wet season inundation level

Figure 3.16 presents the impact of the (simulated) reduced flood levels. It can be seen that the total recharge volumes corresponds approximately linear with the constant level of inundation. The results can be justified by the differences in hydraulic gradient. Shortly after the flood starts a by approximation constant groundwater head (very slow reduction hydraulic gradient) is obtained. As a consequence the rate of inflow becomes approximately constant for the research time-scope (four months). The performance is visualised in Figure G.5 (Appendix G.2).

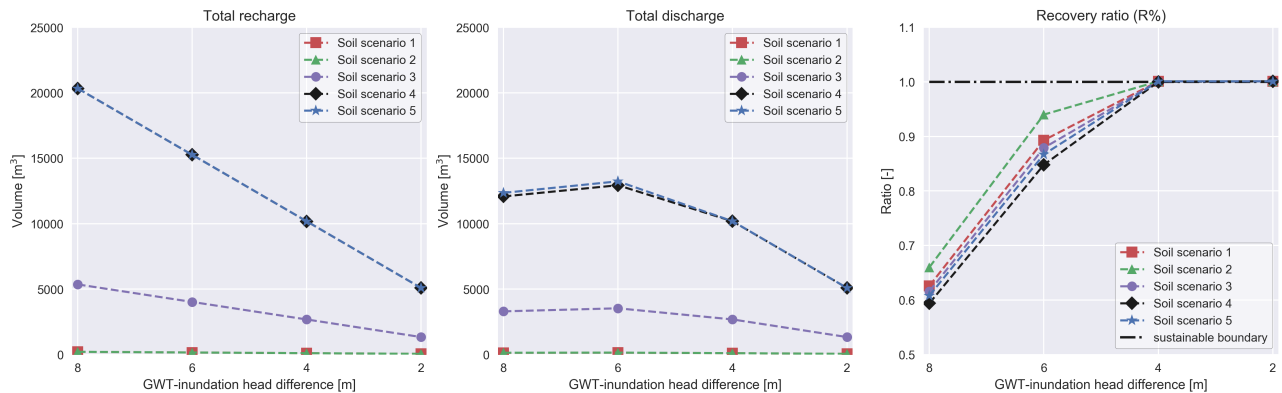


Figure 3.16: Results of yearly total volumes (in, out, ratio) by reduction of wet season inundation level

Note, compared to the base model (Δh is 8 m) the total discharge volume is slightly higher for the situation with a Δh is 6 m. A system performance that can be justified by the defined initial groundwater table. The higher GWT of latter situation (-5 m instead of -6 m) ensures higher groundwater pressure, causing a (although minor) higher well discharge rate.

* Note, although not clearly visible (especially, when total recharge volumes are taken into account) all soil scenarios are included in the presented figures.

3.5. The dimensionless ASR system recharge factor

The prior research sections (3.3 - 3.4) contain an abundance of model modifications. The modifications are related to both the ASR system (3.3) and natural conditions (3.4). Regardless its origin, this section tries to enclose the ASR system performance in terms of recharge in a single 'dimensionless ASR system recharge factor'.

3.6. Results & Conclusions

This section contains conclusions about the performance of an hypothetical ASR system, potentially applicable on northern Ghana conditions. The conclusions on system performance are drawn from the synthetic base model, the simulated ASR system modifications and the system sensitivity analysis.

Performance of a simulated ASR system in northern Ghana

- Recharge & discharge volumes

The total inflow and outflow volumes are both affected by the magnitude of the transmissivity value. An increase of the transmissivity value, in the range of 1 - 100 (m^2/d), results in acquired volumes that are significantly higher. The presence of a well skin resistance (transmissivity dependent) may play a role in this context. The bandwidth variance in storativity values, $1e-3$ - $1e-2$ (-), appears to have only limited influence on the obtained volumes. The shift in storativity values applied (within bandwidth range), sorts minimal effects on the total inflow volume. While, the discharge volumes are somewhat positively affected by an increased storativity. The (small) storativity bandwidth-scope is insufficient to draw further conclusions.

- Sustainable use

Under the applied conditions of subsurface composition and ASR system use, recovery ratios (for all soil scenarios) stay within the limits of sustainability. In eight months of daily (4 hours) pump operation, with a discharge bounded by a maximum drawdown (Δh of 14 m), it is not possible to fully recover the water volumes recharged due to four months of constant inundation (Δh is 8 m).

ASR system improvements

- Preservation of sustainable use

Higher total discharge volumes can be obtained by an extension of the dry season daily pumping time. By considering the predefined conditions (e.g. wet season constant 2 m flooding, dry season daily pumping operation of 4 hour), it is advisable pumping operation should not exceed a 6 till 7 hour daily duration (8 months). Independently from the soil scenario, a sustainable system use can in this way potentially be retained.

- Increase in recharge & discharge volumes

In terms of volumes (and Recovery ratios), an ASR system can be improved by both the enlargement of the borehole cross-sectional dimension and the reduction of the well skin resistance. Within the research scope ($r_w = 0.0635\text{-}0.3175$ m and $k_{gp} = 0.2\text{-}1.8*K_h$), the obtained base model volumes are more than doubled by these types of improvement. A non linear relation exists between the 'size' of the system improvement and the magnitude of obtained volumes. A significant water profit can be obtained by relative small base model modifications.

ASR system sensitivity to nature

- Recharge volumes

The relation between the partially penetrating well screen length (research scope: 10 - 30 m) and inflow and outflow is slightly off from linear. When the active screen length reduces (more accumulation of sediment), the essence of cleaning becomes not only in absolute terms but also relatively more important. Within the research time-span, the system recharge volumes are by approximation linear related (positively) to the duration of the constant level flooding (range 1 - 4 months) and the depth of the inundation level. In the latter case, it is more precisely the difference between the flood level and (initial) groundwater table (hydraulic gradient) that is normative (Δh range 2 - 8 m).

4

ASR system - Business case

The Aquifer Storage and Recovery (ASR) system performances are so far expressed in water volumes. The volumetric results are desirable, but it is hard to get a good picture of it. By the introduction of simplistic rules of thumb, the obtained volumes can be expressed in financial yield. This chapter offers a rough glimpse in the financial feasibility of an ASR system in northern Ghana.

The methodology of section 4.1 specifies the crops of interest and describes the derivation process of the pumping costs. Section 4.2 presents the financial yield of respectively the first dry season crop-cycle (tomatoes) and the subsequent crop-cycle (groundnut). In Section 4.3 the ASR system operational pumping costs are discussed. The agricultural yield is weighted up against the pumping costs in Section 4.4.

4.1. Methods - From water volume to financial considerations

This research methodology contains the required information to make a simplified financial balance on an operational ASR system. The section is split in two. On the one hand, the section presents yield information. Components as the crops of interest, the irrigation efficiency and the applied exchange rate are addressed. On the other hand, the operation costs are defined. The process from power consumption, due to water withdrawal, to the determination of fuel costs is specified.

4.1.1. Yield - crops of interest

Some crops need more water than others. Some crops thrive better in northern Ghana climate than others. Some crops are financially more beneficial than others. And so, many more elements are decisive in the process of crop type determination. This research is not about crop type decisions. The crops are purely included in the study to gain knowledge on hand-on possibilities in the agricultural use and financial feasibility of an ASR-system in northern Ghana. It is chosen to consider the tomato and groundnut crops.

Crops of interest

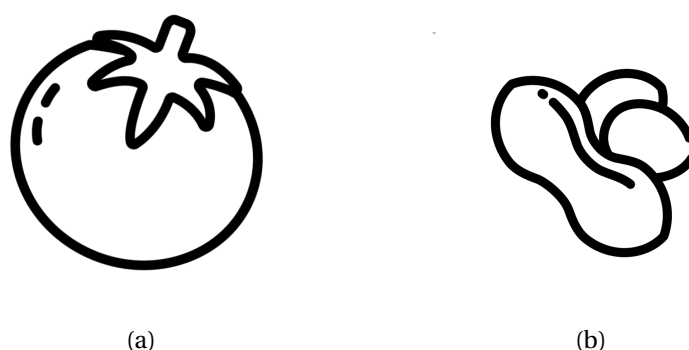


Figure 4.1: Crops of interest: (a) Tomatoes and (b) Groundnuts
(visual support by Ben Davis and Lemon Liu from Noun Project - <https://thenounproject.com>)

- Tomato

The worldwide second most important vegetable crop (after the potato) concerns the tomato. Because of its relative high (financial) yield, the vegetable is a desired crop for cultivation. After a period of approximately 90 to 120 days the seeds are grown to fully-fledged crops, the tomatoes are ready for harvesting. Over the growth season the crop thrives best by the supply of 400 to 600 mm of water (rain-fed). To reduce the chances of deceases (pests and infestations) the crop should be cultivated in rotation with other crops. Under the conditions of irrigation the tomato yield is approximately 45 to 65 ton/ha (FAO, 2018b). Because of the broad ranges in agricultural yield and water requirements (moreover, only rain-fed statistics), these specific crop competences are not taken into account in research. The derivation of agricultural yield is based on the average 'water utilization efficiency' (E_y). For the transformation of agricultural yield to financial benefits, the Esoko march 2018 Ghana average wholesale price is used. The tomato wholesale price is set at a value ranging from 217.86 to 220.43 GHS for a 52 kg crate (Modern Ghana, 2018). For the purposes of this research the highest average value is applied. To summarize:

- Length growth season: 120 (d)
- Water utilization efficiency: $E_y = 11 \text{ (kg/m}^3\text{)}$
- Wholesale price: 4.239 (GHS/kg)

- Groundnut

The groundnut is an above average profitable crop grown in Ghana. Production is often the responsibility of small holder farmers in the North. Almost the complete Ghana groundnut production originates here (Ghana-made, 2018). Growth season length is dependent on the varieties (sequential or alternately). In general harvesting can take place after a period of 90 to 140 days. For a proper single season production, groundnut crops require approximately 500 to 700 mm of water. Rain-fed crops can produce average yields of 2-3 ton/ha unshelled nuts. By the introduction of irrigation these values even reach 3.5-4.5 ton/ha (FAO, 2018a). At the contrary, a 2016 Ghana average agricultural yield of 1.25 ton/ha unshelled groundnut is perceived (FAO, 2018c). In other words, groundnut crop yield are not unambiguous. The FAO (2018a) average water utilization efficiency (E_y) is adapted as normative. Financial yields are highly fluctuating over time. Market forces are dominant in actual returns. The march Esoko 2018 Ghana average unshelled groundnut wholesale price is set at a value ranging from 247.50 to 282.50 GHS for a 82 kg bag (Modern Ghana, 2018). For the purposes of this research the highest average value is applied and interpreted as the unshelled groundnut price. To summarize:

- Length growth season: 123 (d)
- Water utilization efficiency: $E_y = 0.7 \text{ (kg/m}^3\text{)}$
- Wholesale price: 3.445 (GHS/kg)

As stated before, the time frame of the synthetic simulation consist of 243 days of dry season. It is assumed two consecutive growth seasons fit this period. The tomato growth season is succeeded by a growth season labelled for the production of groundnut. This complies with the desire of rotational crop cultivation.

The applied crop specifications are dominated by supreme rough assumptions in e.g. quantity (kg) and prices. The obtained (financial) yields should solely be interpreted as indicative. In other words, "All rights reserved".

Irrigation efficiency

The dry season agriculture is assumed to be purely dependent on irrigation for the supply of water. Different types of irrigation are suitable in northern Ghana. One can think of border strip/furrow irrigation; simplistic but inefficient. Higher degrees of efficiency can be achieved by the use of sprinkler irrigation. In the particular case of ASR-system use, minimum water losses are pursued. Therefore, drip irrigation is applied. Drip irrigation is the type of irrigation with the highest efficiencies. Systems are standard paired with facilities as poly-tank(s), pipes and drip hoses. Distances between extraction and irrigation are small, resulting in

limited losses. However, water losses are present due to pipe connections and potential evaporation. All-encompassing, a irrigation system efficiency of 0.8 (-) is considered. 80% of all water withdrawn is assumed to be net usable for crop growth (van de Giesen, 2013). Note, this efficiency number also accounts for the in practice required schedule in irrigation water amounts. Over the growth season the required water volumes are here hypothetical and assumed to be daily equal.

Financial yield

Based on the described crop specification, the simulated water volumes withdrawn can be expressed in financial returns. The agricultural yield (kg/m^3) and the weighted crop prices (GHS/kg) are defined. From consistence considerations it is chosen to express the financial returns in US dollars. The July 7th Bloomberg financial exchange rate is applied: 0.2081 USD/GHS (Bloomberg, 2018).

4.1.2. Costs - water withdrawal

Profits are accompanied by costs. For this research all Capital Expenditures(CAPEX) are unknown and ignored. The same applies for large parts of the Operating Expenses (OPEX), e.g. farmer wage and fertilizer costs. The only costs accounted are related to the energy (diesel) consumption. Outcomes are purely focused on the feasibility of the daily system operation. An impression is generated, whether or not regular ASR-system operation on its own is profitable.

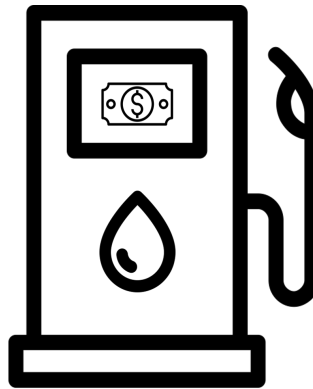


Figure 4.2: Schematic of the ASR system operational pumping costs
(visual support by Nociconist, Quan Do and Phonlaphat Throngsriphong from Noun Project - <https://thenounproject.com>)

Synthetic pump application

The Pedrollo 4" submergence pump is applied in fieldwork measurements. The same pump, i.e. its specifications, is used a standard in the subsequent parts of research. General specification can be found in Appendix H. The results of the synthetic simulations contains time dependent (4 hours daily, 243 days) discharge rates. As soon as the maximum pumping capacity is exceeded, it is assumed the specific simulation is carried out by the implementation of an extra (same) pump. By a parallel pump configuration the same heads and efficiencies are ensured, while discharge capacities are doubled (van de Giesen, 2013).

Energy Consumption

The available groundwater has to be lifted to the surface. Depends on the obtained discharges, the lifting action requires a certain magnitude of power (Equation 4.1). For water displacement the difference between pump position and surface level (30m) is retained. An extra lift of 15 m is added to account for friction losses and the higher position (above surface) of the poly tank(s). A total head lift of 45 m is applied.

$$N_{net} = g * Q * \Delta H \quad (4.1)$$

Where N_{net} (kW) is the net power required, g (m/s^2) is the gravitational acceleration ($9.81 \text{ m}/\text{s}^2$), Q (m^3/s) is the discharge (total extracted volume of water over the yearly sum of pumping time (in seconds)) and ΔH (m) is the net head (total lift) required. In this equation it is assumed the water has a density of $1000 \text{ kg}/\text{m}^3$.

In general, the use of power gets accompanied by losses (for example due to friction and turbulence). Every single power-related equipment works at a certain level of efficiency. The power generator applied in field-work (Appendix C) is used over years. Due to its datedness, a generator efficiency of 70% is estimated. The efficiency of the Pedrollo pump(s) is dependent on the discharge rate. An overview of the efficiency curve is present in Appendix H. In this study, the pump efficiencies are related to the time dependent discharges obtained in the synthetic model simulations. Besides equipment losses, energy get lost due to mutual transmission. An extra efficiency value of 90% is accounted (van de Giesen, 2013). Result is a variable ASR-system efficiency of that never exceeds 36.5 % (based on maximum pump efficiency).

$$\eta_{total} = \eta_{generator} * \eta_{transmission} * \eta_{pump} \quad (4.2)$$

Where η_{total} (-) is the overall power efficiency, $\eta_{generator}$ (-) is the generator power efficiency, $\eta_{transmission}$ (-) is the transmission power efficiency and η_{pump} (-) is the pump power efficiency.

The combination of total ASR-system efficiency and net required power results in a gross power 4.3. The gross power should be delivered by the generator to gain the desired volumes of water at the agricultural fields. Multiplying the gross power required by the total hours of pump operation returns the total energy consumed (kWh).

$$N_{gross} = \frac{N_{net}}{\eta_{total}} \quad (4.3)$$

Where N_{gross} (kW) is the gross power required, N_{net} (kW) is the net power required and η_{total} (-) is the overall power efficiency.

Energy costs

The Kipor power generator (Appendix C) contains a 15 litre diesel tank. On a full tank the generator can operate for 6.5 hours. A fuel consumption of 2.31 l/h is taken into account. During operation the generator delivers a continuous power capacity of 4.5 kW (TS24, 2018). Ghana diesel price of 5.03 GHS/l (begin of July) is adopted as normative (GlobalPetrolPrices, 2018). The Bloomberg financial exchange rate (0.2081 USD/GHS) is once again applied on the fuel costs for proper comparison with the agricultural yield (Bloomberg, 2018).

$$Cost_{fuel} = \frac{consump_{gen} * price_{fuel} * rate_{exchange}}{power_{gen}} \quad (4.4)$$

Where $Cost_{fuel}$ (USD/kWh) is the price of fuel, $consump_{gen}$ (l/h) is the generator fuel consumption, $price_{fuel}$ (GHS/l) is the fuel price in Ghana, $rate_{exchange}$ (USD/GHS) is the Bloomberg financial currency rate and $power_{gen}$ (kW) is the generator continuous power capacity.

4.2. Financial yield

* The obtained results are all based on volume-to-yield transformations described in Section 4.1.

The available water volumes are approximately the same for the first four months (tomatoes) and the subsequent four months (groundnut) of dry season. Nonetheless, the obtained yield differ strongly. Note, the y-axis of Figure 4.3 and Figure 4.4 are not the same. The obtained financial yield is highly dependent on the crop of interest and its transfer assumptions.

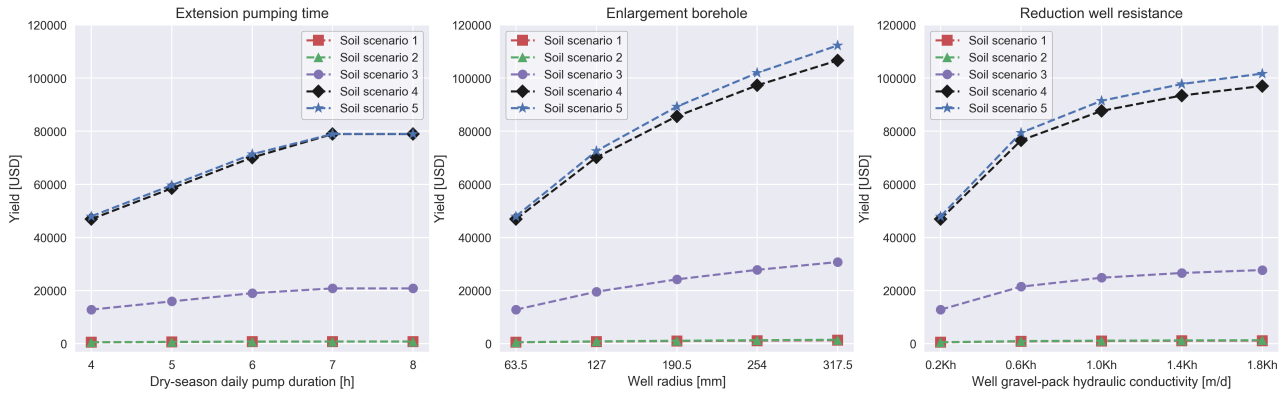


Figure 4.3: Financial yield - Tomatoes (4 months) - three types of ASR system improvement

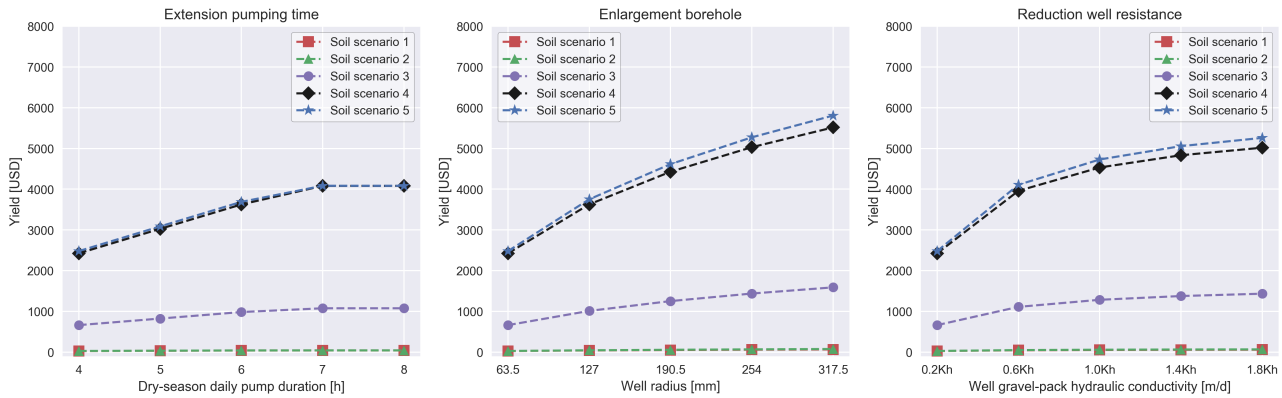


Figure 4.4: Financial yield - Groundnut (4 months) - three types of ASR system improvement

4.3. Pumping costs

The pumping curve of the Pedrollo 4" submergence pump is defined as normative H. In multiple soil scenarios and types of improvement the obtained discharges are far out of pumping range. Based on the predefined approach multiple pumps are set-up in a parallel operation. However, the increase in pump numbers is not reflected in this research costs. As a consequence, unrealistic judgements and comparisons are applied.

The obtained (model) discharges for the soil scenarios 1 and 2 are extremely low. As a consequence, pumping efficiencies (Pedrollo 4" submergence pumping curve) are stated to be almost zero. A situation highly unlikely. In practise, a specific pump type will be applied that suits the circumstances. As a consequence, unrealistic judgements and comparisons are applied.

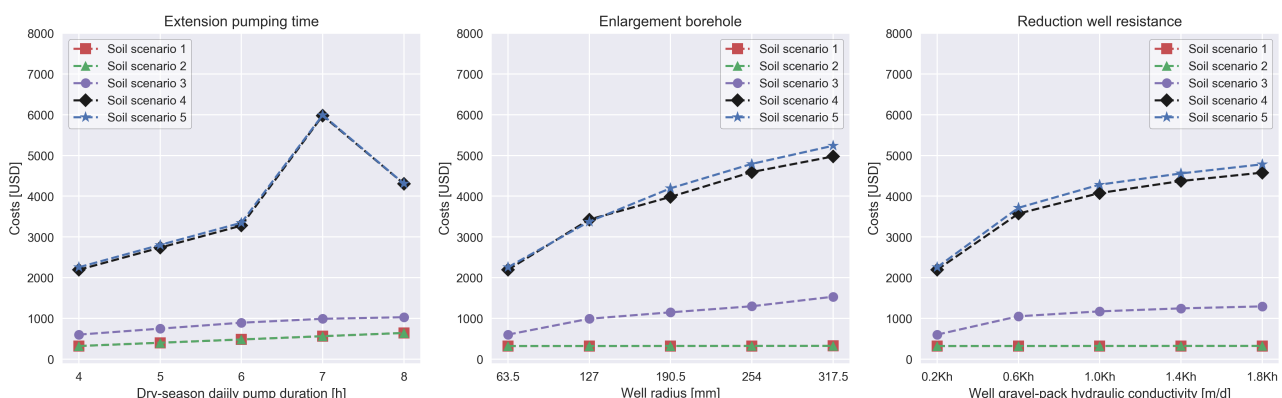


Figure 4.5: Pumping costs - dry season (8 months) - three types of ASR system improvement

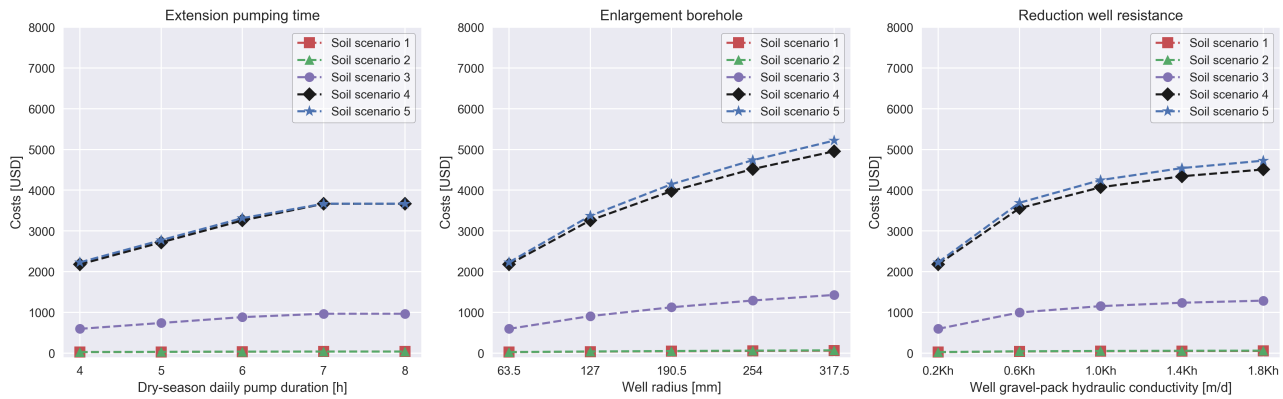


Figure 4.6: Pumping costs - maximum pumping efficiency - dry season (8 months) - three types of ASR system improvement

Note, the outlier in the soil scenarios 4 and 5 for the situation of 7 hours pumping operation can be justified by the application of an unfortunate number of pumps. Efficiencies are in this particular case relatively low (as low as 35%).

4.4. Results & conclusions

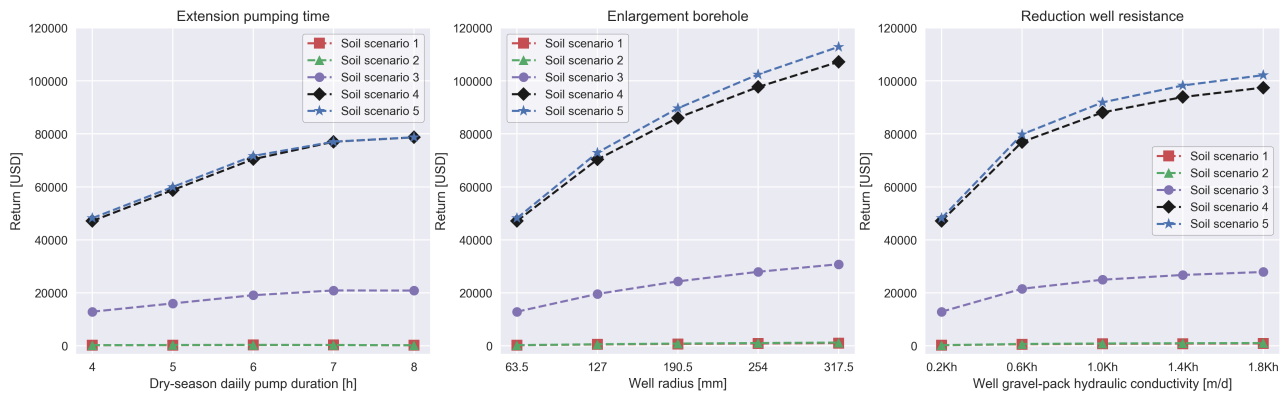


Figure 4.7: Year-round net financial return - three types of ASR system improvement

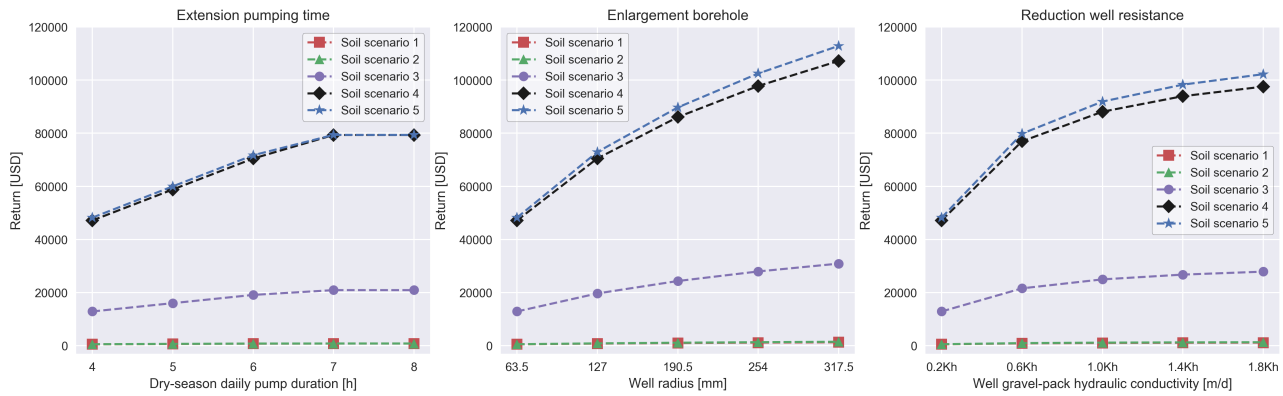


Figure 4.8: Year-round net financial return - maximum pumping efficiency - three types of ASR system improvement

due solely the withdrawal of water, gekozen voor een zeer onrealistische financiële situatie, omdat informatie gewoon afwezig is. Bovendien kunnen onderdelen vanuit (europese) fondsen in aanmerking komen voor een financiële compensatie. waardoor het financiële kostenplaatje al weer iets minder onrealistisch is. nonetheless, business case blijft hoogst onzeker. verder onderzoek dan ook zeker wenselijk.

Before conclusions on this part are drawn, feedback is desired. Feedback items:

- 1. Agricultural yield assumptions - tomato versus groundnut
- 2. pump quantity - in soil scenario 4 and 5: abundant (upto 8)
- 3. pump efficiency - in soil scenario 1 and 2: very low (0.04-0.1)
- 4. inclusion of more OPEX or CAPEX

5

Discussion

In this section, the research content is reviewed. The aspects of moderate quality and potential shortcomings in the fulfilment of the thesis (e.g. fieldwork set-up, model definition, software application, etcetera) are uncovered. If relevant, recommendations for (additional) research improvements are given.

5.1. Farmer's guideline - ASR system implementation

5.2. Fieldwork analysis

- measurement
 - In well
 - Simplistic test set-up (rope tangle)
 - Multiple locations (representative)
- Data analysis
 - Simplified theoretical models - general
 - Simplified theoretical models - confined/unconfined
 - Simplified theoretical models - initial conditions
- T & S bandwidth definition

5.3. ASR system - Improvements & sensitivities

- Model definition
 - Varying flood level and time-frame
 - Homogeneous single layer unconfined aquifer
 - H_{lim}
 - ASR system infiltration bed
 - MODFLOW MNW2 CWC combined with radial scaling
- Well skin resistance
- The dimensionless ASR system recharge factor

5.4. ASR system - Financial magnitude

- Crops of interest
- Irrigation efficiency
- Pump - type/efficiencies/working point

- Power required - head, generator and loss efficiencies
- Fuel - costs/(generator)consumption

6

Conclusions & Recommendations

The conclusion presents the final results and recommendations of this research. An answer will be generated on the main research question:

How can improvements of Aquifer Storage and Recovery (ASR) systems be more beneficial for the availability and sustainable use of groundwater in northern Ghana small-scale agriculture?

In correspondence with the thesis core, the answer will consist of three parts. The answer elaborates on the sub conclusion, to be found in the Sections 2.4, 3.6 and 4.4.

Work In Progress. Final conclusion will follow soon.

Bibliography

- Bakker, M. (2010). Radial Dupuit interface flow to assess the aquifer storage and recovery potential of saltwater aquifers. pages 107–115.
- Bakker, M. (2013a). Analytical Modeling of Transient Multilayer Flow. In Mishra, P. K. and Kuhlman, K. L., editors, *Advances in Hydrogeology*, volume 9781461464, chapter Chapter 5, pages 95–114. Springer Science+Business Media, New York, NY.
- Bakker, M. (2013b). Semi-analytic modeling of transient multi-layer flow with TTIm. *Hydrogeology Journal*, 21(4):935–943.
- Bakker, M. and Anderson, E. I. (2011). Mechanics of Groundwater Flow. In Wilderer, P., editor, *Treatise on Water Science*, pages 115–134. Academic Press, Oxford, United Kingdom, vol. 2 edition.
- Bloomberg (2018). GHS-USD Cross rate currency.
- Bot, B. (2016). *Grondwaterzakboekje Gwz2016*. Bot Raadgevend Ingenieur, Rotterdam.
- Canadian International Development Agency (2011). *Hydrogeological Assessment Project of the Northern Regions of Ghana (HAP)*, volume I. SNC Lavalin international, Montreal (Quebec).
- Dillon, P., Pavelic, P., Page, D., Beringen, H., and Ward, J. (2009). *Managed aquifer recharge : An Introduction*. Number 13.
- FAO (2018a). Crop information - Groundnut.
- FAO (2018b). Crop information - Tomato.
- FAO (2018c). FAOSTAT - download data - crops.
- FAO (2018d). How close are we to #ZeroHunger? - The state of food security and nutrition in the world 2017.
- Fitts, C. R. (2012). *Groundwater Science*. Academic Press, Oxford, United Kingdom, scond edit edition.
- Ghana-made (2018). Groundnut.
- GlobalPetrolPrices (2018). Ghana diesel price (litre).
- Harbaugh, A. W. (2005). MODFLOW-2005 , The U . S . Geological Survey Modular Ground-Water Model — the Ground-Water Flow Process. *U.S. Geological Survey Techniques and Methods*, page 253.
- Harbaugh, B. A. W., Banta, E. R., Hill, M. C., and McDonald, M. G. (2000). MODFLOW-2000 , The U . S . Geological Survey modular graound-water model — User guide to modularization concepts and the ground-water flow process. *U.S. Geological Survey*, page 130.
- Houben, G. J. (2015). Review: Hydraulics of water wells—head losses of individual components. *Hydrogeology Journal*, 23(8):1659–1675.
- Konikow, L. F., Hornberger, G. Z., Halford, K. J., and Hanson, R. T. (2009). Revised Multi-Node Well (MNW2) Package for MODFLOW Ground-Water Flow Model Techniques and Methods 6 – A30. *Methods*, page 80.
- Kruseman, G. and de Ridder, N. (2000). *Analysis and evaluation of pumping test data*. International Institute for Land Reclanation and Improvement (ILRI), Wageningen, The Netherlands, second edi edition.
- Langevin, C. D. (2008). Modeling axisymmetric flow and transport. *Ground Water*, 46(4):579–590.

- Martin, N. (2008). Development of a water balance for the Atankwidi catchment, West Africa – A case study of groundwater recharge in a semi-arid climate. (41):176.
- Ministry of Foreign Affairs, Ministry of Agriculture, and Wageningen UR (2018). Small Business Innovation Research (SBIR) call - Food security in Sub-Saharan Africa - Background note. Technical report.
- Modern Ghana (2018). Esoko market.
- Niswonger, R. G., Panday, S., and Motomu, I. (2011). MODFLOW-NWT , A Newton Formulation for MODFLOW-2005. *USGS reports*.
- Owusu, S., Cofie, O. O., Osei-Owusu, P. K., Awotwe-Pratt, V., and Mul, M. L. (2017). Adapting aquifer storage and recovery technology to the flood-prone areas of northern Ghana for dry-season irrigation. *Working Paper 176*.
- Owusu, S., Mul, M., Ghansah, B., Awotwe-pratt, V., and Osei, P. K. (2015). Technical Report: Identification and selection of suitable sites for Bhungroo and Pave Irrigation Technologies. pages 1–61.
- Strack, O. D. L. (1989). *Groundwater Mechanics*. Prentice Hall, Englewood Cliffs, New Jersey.
- TS24 (2018). KIPOR KDE6700T DIESEL GENERATOR.
- United Nations (2014). International Decade for Action 'WATER FOR LIFE' 2005-2015 - Water and food security.
- United Nations (2018). Sustainable Development Goal 2: End hunger, achieve food security and improved nutrition and promote sustainable agriculture.
- van de Giesen, N. (2013). Dictaat CTB2120 Waterbeheer. Technical report, Delft Univeristy of Technology, Delft.
- Ward, J. D., Simmons, C. T., and Dillon, P. J. (2007). A theoretical analysis of mixed convection in aquifer storage and recovery : How important are density effects ? pages 169–186.
- Wood, T. N. (2013). Agricultural Development in the Northern Savannah of Ghana. pages 1–73.

Appendices

A

Original borehole log sheets

In the first half of the year 2016 Conservation Alliance (CA) commissioned the construction of multiple boreholes in northern Ghana. The boreholes subjected in this research (five locations, visualized in 2.1) are all part of this operation. Valuable information is gained with respect to local soil stratification, during borehole construction. Information is preserved in the original borehole log-sheets, which can be found in this appendix. Besides the local soil stratification, these log-sheets contain information on individual applied well structures. A depth dependent distinction is made in plain versus screened well skin. In terms of content these borehole log-sheets are used as a starting point in the theoretical model determination (section ??).

		CONSERVATION ALLIANCE- THE PAVE PROJECT					BH status:	Successful	<input checked="" type="checkbox"/>			
		BOREHOLE LOG SHEET					Dry					
Community		Bingo	District	Talensi	Borehole ID	BH B1						
Coordinates - Latitude (N) :		Longitude (W)										
Drilling contractor		Drill rig				Method	ROTARY AIR					
Drilling start date		6-8-2016	Compl. date	6-8-2016	Operator							
TEST PUMPING		Date:			Conductivity	us/cm	Top of screen *	0	m			
Dynamic WL *		m	Pump type			Total Iron	mg/l	Static WL *	m			
Static WL *		m	Pumping rate (Q)			m³/h	Manganese	mg/l	Potential drawdown	m		
Drawdown (s)		m	Duration			h	Nitrate	mg/l	Potential yield	25 l/min		
* Levels to ground level datum		Specific capacity (Q/s)				m³/h/m	Fluoride	mg/l	Depth of borehole *	48 m		
BIT SIZE & TYPE	Temporary Casing	SCALE	PROFILE		TIME/DEPTH M/MIN	WATER ZONES CUMULATIVE Q (l/min)	WELL DIAGRAM					
10"			Light brown clay									
Clay cutter												
6.5" hammer bit			Highly weathered light brown sandstone mixed with shaly materials									
			5									3m PVC Screen
			10									5
			15									10
			20									15
			25									20
			30									25
			35									30
			40									40
			45									45
			50									50
			Moderately weathered brownish sandstone						15			
									55			
Gravel for gravel pack		48	LM	Remarks and stoppages:								
Screen Length		30	LM									
Casing length		18	LM									
Installation of grout seal		M	M									
Cleaning & development		2	HRS	Prepared by:								
Centralisers fitted			No									
Safety cap fitted		/	No	Approved:								
Backfill aband. BH			/									
Cement for grout			KG									
Platform construction date												
Distance from last BH			KM									

		CONSERVATION ALLIANCE- THE PAVE PROJECT				BH status:		Successful			
						Dry					
Community		Nungo		District	Talensi	Borehole ID		BH N100			
Coordinates - Latitude (N) :		Longitude (W)									
Drilling contractor				Drill rig				Method	ROTARY AIR		
Drilling start date		6-8-2016		Compl. date	6-8-2016			Operator	Kwaku		
TEST PUMPING		Date:				Conductivity	us/cm	Top of screen *	0	m	
Dynamic WL *		m		Pump type		Total Iron	mg/l	Static WL *		m	
Static WL *		m		Pumping rate (Q)		Manganese	mg/l	Potential drawdown		m	
Drawdown (s)		m		Duration		h	Nitrate	mg/l	Potential yield	80 l/min	
* Levels to ground level datum				Specific capacity (Q/s)		m³/h/m	Fluoride	mg/l	Depth of borehole *	42	m
BIT SIZE & TYPE	Temporary CASING	SCALE	PROFILE		TIME/DEPTH M/MIN	WATER ZONES CUMULATIVE Q (l/min)	WELL DIAGRAM				
10"	Clay cutter	5	Highly weathered light brown sandstone								
6.5"			hammer bit	10			Moderately weathered light grey sandstone mixed with shaly materials (at 18m, 21-24m)			55	
20	15	25			Light grey sandstone			80			
30			35	40							
45	45	50									
Gravel for gravel pack			42	LM	Remarks and stoppages:						
Screen Length			36	LM							
Casing length			6	LM							
Installation of grout seal			M	M							
Cleaning & development			2	HRS	Prepared by:						
Centralisers fitted			No								
Safety cap fitted			/	No	Approved:						
Backfill aband. BH			No	/							
Cement for grout			KG								
Platform construction date			KM								
Distance from last BH											

		CONSERVATION ALLIANCE- THE PAVE PROJECT					BH status:	Successful	<input checked="" type="checkbox"/>		
		BOREHOLE LOG SHEET					Dry				
Community		Nyong Nayili		District	Karaga		Borehole ID	BH NN1			
Coordinates - Latitude (N) :		Longitude (W)									
Drilling contractor				Drill rig			Method	ROTARY AIR			
Drilling start date		31/05/2016		Compl. date	31/05/2016		Operator	Kwaku			
TEST PUMPING		Date:				Conductivity	us/cm	Top of screen *	0	m	
Dynamic WL *		m		Pump type		Total Iron	mg/l	Static WL *	m		
Static WL *		m		Pumping rate (Q)		m³/h	Manganese	mg/l	Potential drawdown	m	
Drawdown (s)		m		Duration		h	Nitrate	mg/l	Potential yield		
* Levels to ground level datum				Specific capacity (Q/s)		m³/h/m	Fluoride	mg/l	Depth of borehole *	54	m
BIT SIZE & TYPE	Temporary Casing	SCALE	PROFILE			TIME/DEPTH M/MIN	WATER ZONES CUMULATIVE Q (l/min)	WELL DIAGRAM			
			Clay	Highly weathered chocolate brown sandstone	Moderately weathered chocolate brown sandstone			3m PVC Screen	21m PVC Plain	54m Gravel pack	
10"											
Clay cutter			5								5
6.5"			10								10
hammer bit			15								15
			20								20
			25								25
			30								30
			35								35
			40								40
			45								45
			50								50
			55								55
Gravel for gravel pack			54	LM	Remarks and stoppages:						
Screen Length			33	LM							
Casing length			21	LM							
Installation of grout seal			M	M							
Cleaning & development			2	HRS	Prepared by:						
Centralisers fitted			No								
Safety cap fitted			/	No	Approved:						
Backfill aband. BH				/							
Cement for grout				KG							
Platform construction date											
Distance from last BH				KM							

		CONSERVATION ALLIANCE- THE PAVE PROJECT				BH status:	Successful	✓								
						Dry										
BOREHOLE LOG SHEET																
Community		Janga 1	District	West Mamprusi	Borehole ID	BH J1										
Coordinates - Latitude (N) :		0°iu	Longitude (W)													
Drilling contractor			Drill rig		Method	ROTARY AIR										
Drilling start date		6-3-2016	Compl. date	6-3-2016	Operator	Kwaku										
TEST PUMPING		Date:		Conductivity	us/cm	Top of screen *	0	m								
Dynamic WL *		m	Pump type	Total Iron	mg/l	Static WL *		m								
Static WL *		m	Pumping rate (Q)	m³/h	Manganese	mg/l	Potential drawdown	m								
Drawdown (s)		m	Duration	h	Nitrate	mg/l	Potential yield	35 l/min								
* Levels to ground level datum			Specific capacity (Q/s)	m³/h/m	Fluoride	mg/l	Depth of borehole *	48 m								
BIT SIZE & TYPE	Temporary Casing	SCALE	PROFILE	TIME/DEPTH M/MIN	WATER ZONES CUMULATIVE Q (l/min)	WELL DIAGRAM										
10" Clay cutter	6.5" hammer bit		Highly weathered light brown sandstone (Very loose formation) Moderately weathered grey shale													
									5							
									10							
									15							
									20							
									25							
									30							
									35							
									40							
									45							
50																
Gravel for gravel pack		Yes	48	LM	Remarks and stoppages:											
Screen Length			48	LM												
Casing length				LM												
Installation of grout seal				M												
Cleaning & development			2	HRS	Prepared by:											
Centralisers fitted				No												
Safety cap fitted			/	No	Approved:											
Backfill aband. BH				/												
Cement for grout				KG												
Platform construction date																
Distance from last BH			KM													

		CONSERVATION ALLIANCE- THE PAVE PROJECT					BH status:	Successful	<input checked="" type="checkbox"/>											
		BOREHOLE LOG SHEET					Dry													
Community		Ziong	District	Savelugu Nanton	Borehole ID	BH Z1														
Coordinates - Latitude (N) :		Longitude (W)																		
Drilling contractor		Drill rig		Method		ROTARY AIR														
Drilling start date		27/05/2016	Compl. date	27/05/2016	Operator															
TEST PUMPING		Date:		Conductivity	us/cm	Top of screen *	0	m												
Dynamic WL *		m	Pump type	Total Iron	mg/l	Static WL *		m												
Static WL *		m	Pumping rate (Q)	m³/h	Manganese	mg/l	Potential drawdown	m												
Drawdown (s)		m	Duration	h	Nitrate	mg/l	Potential yield	25 l/min												
* Levels to ground level datum		Specific capacity (Q/s)		m³/h/m	Fluoride	mg/l	Depth of borehole *	48 m												
BIT SIZE & TYPE	Temporary Casing	SCALE	PROFILE		TIME/DEPTH M/MIN	WATER ZONES CUMULATIVE Q (l/min)	WELL DIAGRAM													
10"			Reddish brown laterite																	
Clay cutter	6.5" hammer bit	5 10 15 20 25 30 35 40 45 50	Highly weathered light brown sandstone mixed with shaly materials Moderately weathered brownish sandstone		15 25															
											5	10	15	20	25	30	35	40	45	50
											10	15	20	25	30	35	40	45	50	50
											15	20	25	30	35	40	45	50	50	50
											20	25	30	35	40	45	50	50	50	50
											25	30	35	40	45	50	50	50	50	50
											30	35	40	45	50	50	50	50	50	50
											35	40	45	50	50	50	50	50	50	50
											40	45	50	50	50	50	50	50	50	50
											45	50	50	50	50	50	50	50	50	50
											50	50	50	50	50	50	50	50	50	50
											50	50	50	50	50	50	50	50	50	50
											50	50	50	50	50	50	50	50	50	50
											50	50	50	50	50	50	50	50	50	50
											50	50	50	50	50	50	50	50	50	50
50	50	50	50	50	50	50	50	50	50											
Gravel for gravel pack		48	LM	Remarks and stoppages:																
Screen Length		36	LM																	
Casing length		12	LM																	
Installation of grout seal		M	M																	
Cleaning & development		2	HRS	Prepared by:																
Centralisers fitted		No																		
Safety cap fitted		/	No	Approved:																
Backfill aband. BH			/																	
Cement for grout			KG																	
Platform construction date																				
Distance from last BH			KM																	

B

Aquifer test - Data results (fact sheets)

In consultation with Conservation Alliance (CA), a total of five pumping tests are applied in boreholes located at Bingo, Nungo, Nyong Nayili and Janga. By the use of a fifth borehole, location Ziong, the day-to-day PIT system-use is monitored for a week. All tests are applied in November-December 2017, shortly after the transition from wet to dry season. Geohydrological data is gathered by the application of the general pumping test set-up (as described above) at the location Nungo, Nyong Nayili and Janga. The simplified set-up is applied at the location Bingo and Ziong. Outcome of the tests are widespread. Detailed site-specific results are displayed in the fact-sheet figures below (Figures B.1 - B.6).

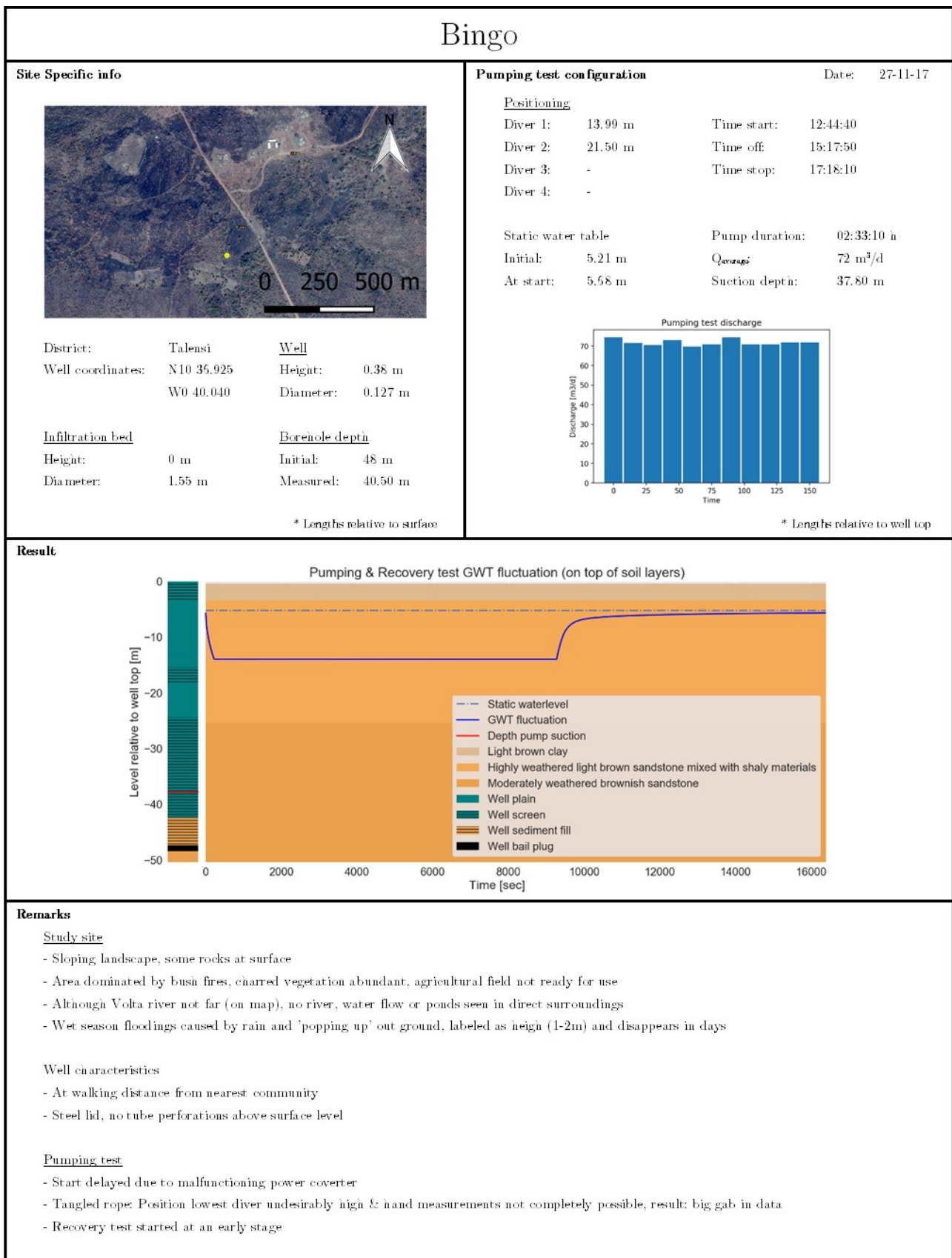


Figure B.1: Fieldwork fact sheet: Bingo

Nungo		
Site Specific info	Pumping test configuration	Date: 28-11-17
	<u>Positioning</u> Diver 1: 9.05 m Time start: 09:45:00 Diver 2: 17.90 m Time off: 11:00:00 Diver 3: 26.05 m Time stop: 11:15:00 Diver 4: - <u>Static water table</u> Initial: 3.02 m Pump duration: 01:15:00 h At start: 3.00 m Q _{average} : < 5 m ³ /d Suction depth: 31.20 m	
District: Talsi Well Well coordinates: N10 33.419 Height: 0.51 m W0 38.990 Diameter: 0.127 m		Pumping test aborted
<u>Infiltration bed</u> Height: -0.35 m Initial: 42 m Diameter: 1.50 m Measured: 9.80 m		
* Lengths relative to surface		* Lengths relative to well top
Result -		
Pumping test aborted		
Remarks		
<u>Study site</u> - Mildly sloped till flat landscape - Vegetation abundant, agricultural field present but not ready for use - Volta river in close range (approximately 400 m) - Wet season floodings caused by riverbank overtopping; labeled as extreme (>3m) and constant; duration as long as wetseason		
<u>Well characteristics</u> - At short walking distance from nearest community - No lid, and tube perforations present above surface level		
<u>Pumping test</u> - Pump hard to descend in well; well clogged due to combination of clay, sand and water - Discharge rates very low during test - To improve discharge, test multiple times applied with increased position of pump suction - No drawdowns perceived, pumping test aborted		

Figure B.2: Fieldwork fact sheet: Nungo

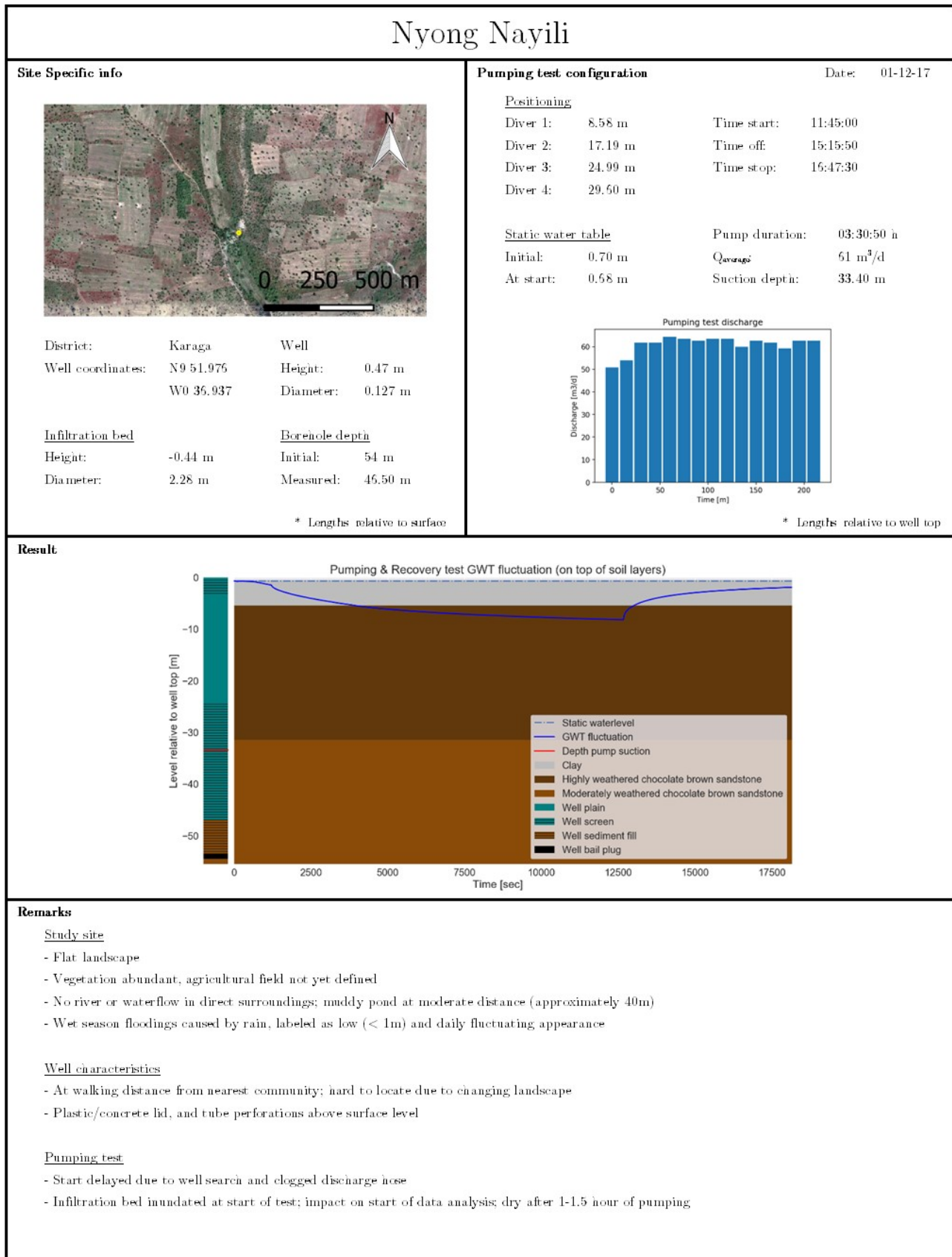


Figure B.3: Fieldwork fact sheet: Nyong Nayili

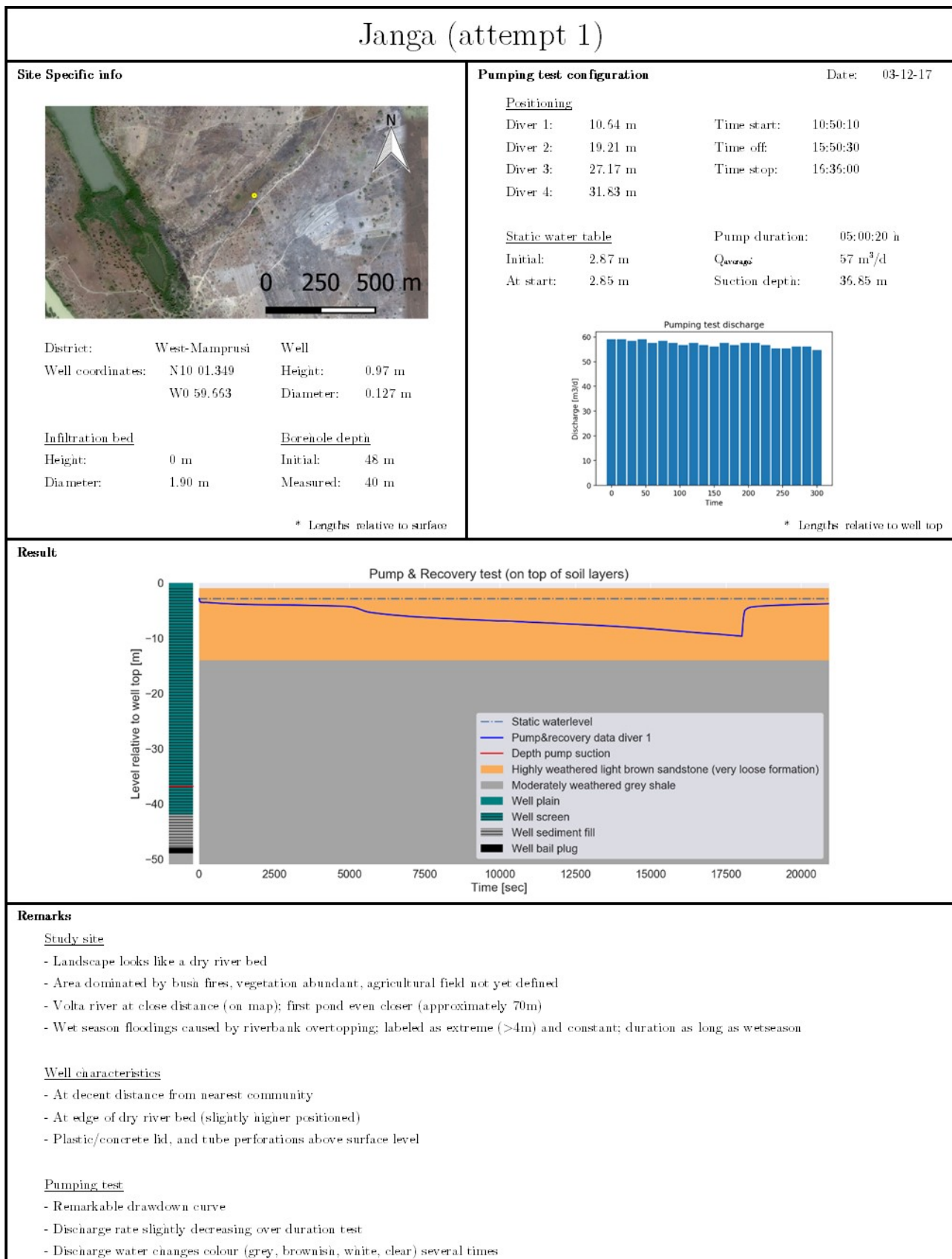


Figure B.4: Fieldwork fact sheet: Janga (attempt 1)

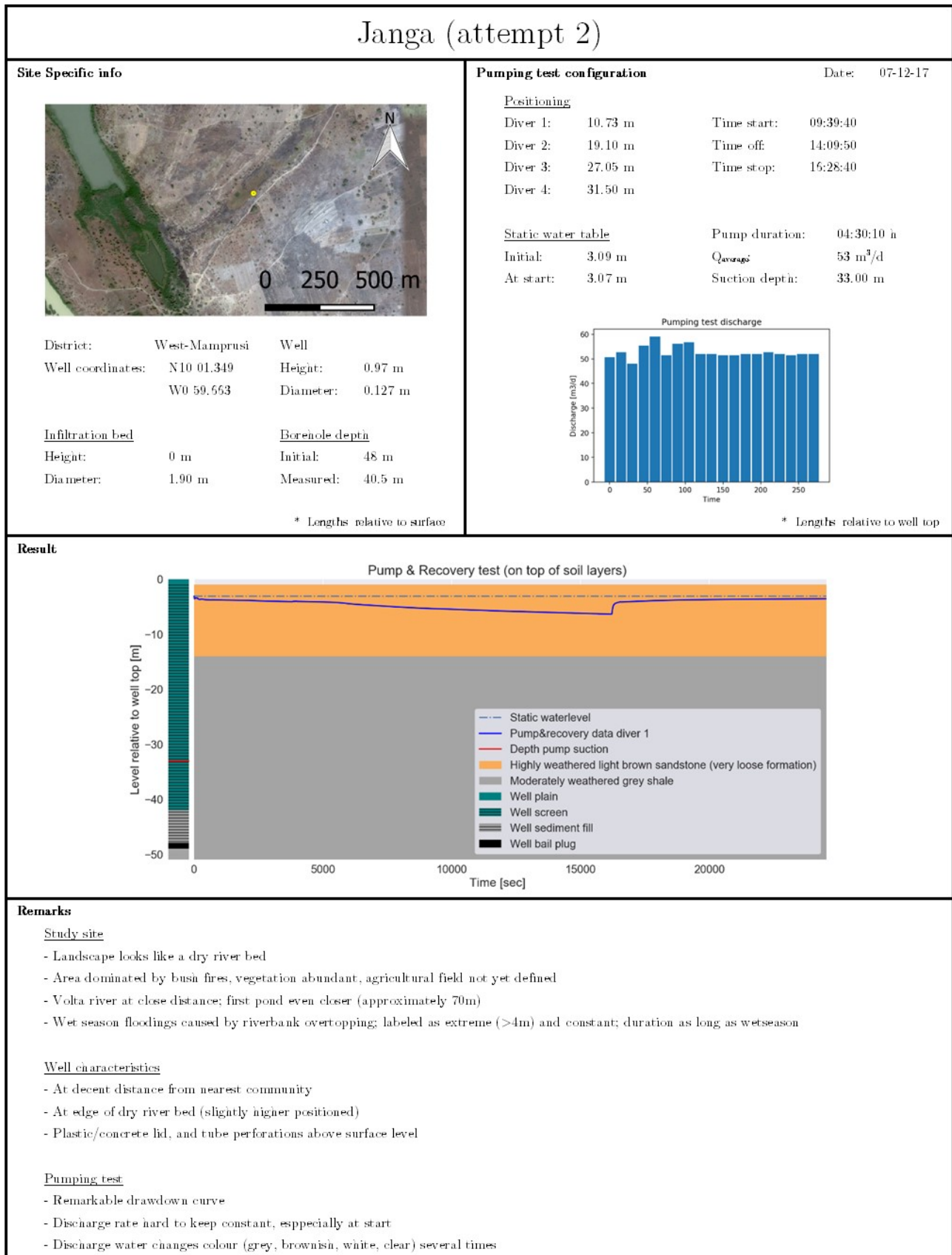


Figure B.5: Fieldwork fact sheet: Jamga (attempt 2)

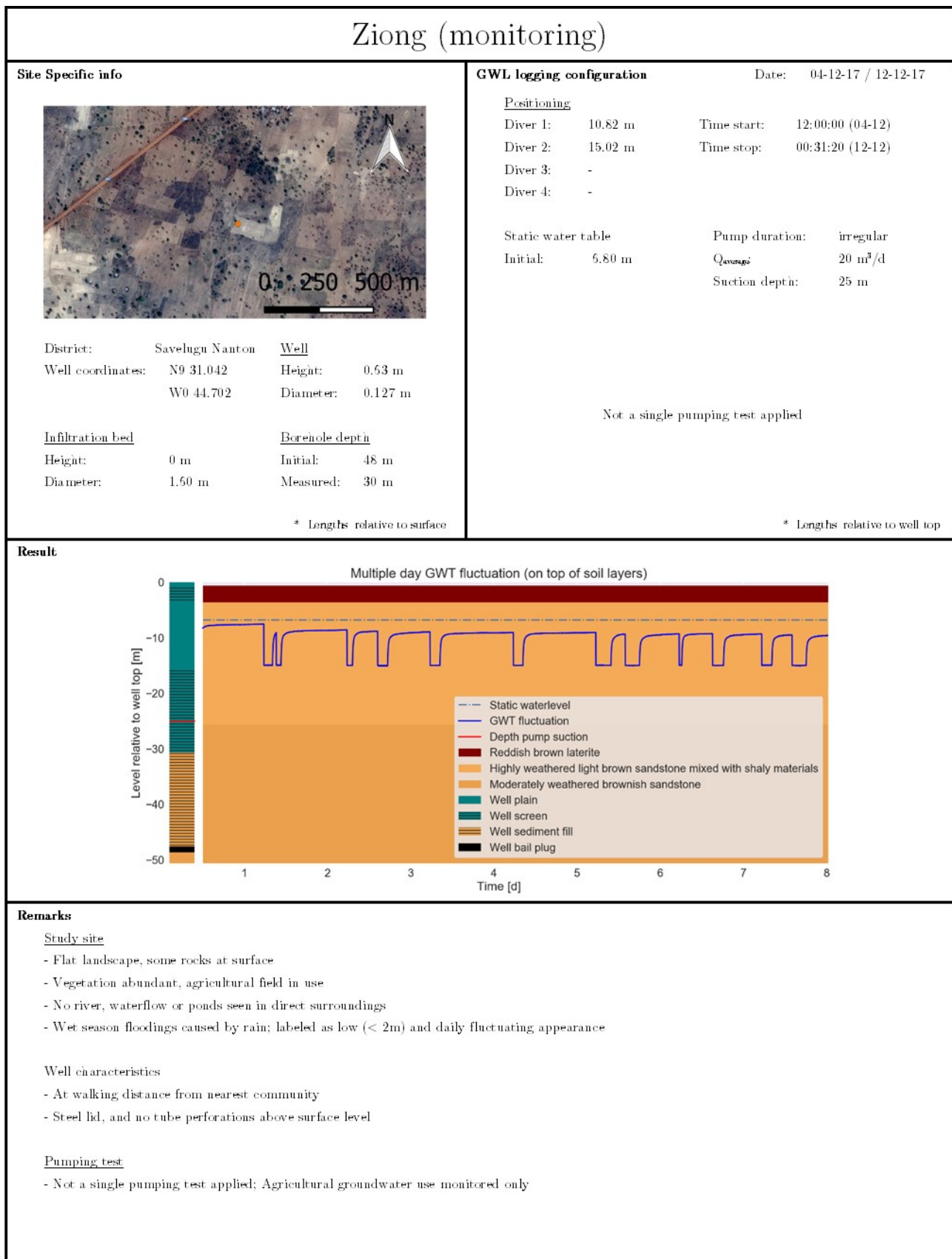


Figure B.6: Fieldwork fact sheet: Ziong (location of monitoring)

C

Aquifer test - Equipment

The northern Ghana in-field geohydrological data collection would not have been possible without the interference of Conservation Alliance (CA). Spread over the Upper East and Northern Region the NGO holds multiple PIT locations. Five locations, visible in figure 2.1, are appointed as measurement locations for the purposes of this research. Besides the research locations, CA provided transport, an interpreter and pumping test equipment. The section below contains detailed information on the equipment applied. A distinction has been made between the equipment for the pumping tests and the actual groundwater measurements. Moreover small equipment as pliers, screwdrivers, gloves and robes are ignored. Purposes and use of these tools are taken for granted.

C.1. Pumping test

- Pump: Pedrollo 4" submersible pump; Type 4SR4/18

A 2 HP pump, for example usable for the supply of water to irrigation fields. While pumping the water should preferably not exceed 35 °C and should not contain too many particles; no more than 150 g/m³. The pump can be submerged in water up to 100 meters. Installed in the right way, the pump can deliver 20-100 l/min with an head difference of 112-45 m. More specific information regarding the pump can be found on the Pedrollo webpage.



Figure C.1: Comparable example of the fieldwork submersible pump
(source: <https://www.pedrollo.com/en/4sr-4-submersible-pumps/150>)

- Generator & power converter: Kipor diesel generator - 5 kVA

A mobile generator has been used as a pump power source. The Kipor generator is a relatively small model, easy to handle and meets the pump requirements by the use of the 230 V connection. A power converter is placed between generator and pump to manually switch on and off the pump. To facilitate a flawless transfer between generator and pump one should be aware the cables and connections

towards the pump should be waterproof. Moreover these power cables should be of a decent length to allow the pump to submerge.



Figure C.2: Comparable example of the fieldwork generator
(source: <https://www.kipor-power.eu/winkel/kipor-kde6700t-diesel-generator-5-kva/>)

- Hose:

As a transport line towards the location of discharge a flexible water hose has been attached to the pump. The hose has been manufactured in Polyethylene, has an external diameter of $1\frac{1}{4}$ " and is approximately 100 m long.



Figure C.3: Actual fieldwork hose & bucket

- Bucket:

As a rough estimation for discharge an plastic bucket has been used. This oversized measuring cup stores volumes up to 50 l and contains 5 l level indicators.

C.2. Water table monitoring

- Pressure sensor data loggers:

- Van Essen; TD-Diver Type DI801 (2x) & Baro-Diver Type DI800 (1x):

TD- and Baro-Divers are applied for the measuring and recording of time dependent fluctuations in (ground)water levels, atmospheric pressures and temperatures. The TD-Divers can record a water column up to 10 m. Baro-Divers can be used to measure atmospheric pressures and shallow water levels, approximately up to a range of 0.9 m. Based on the internal memory these devices can store up to 72.000 measurements per parameter. Measurement logging can be programmed by the use of a USB-Unit and the Diver-Office software. With a battery life of 10 years, long and/or short term measurements can be applied with a sample interval of 0.5 seconds to 99 hours. Moreover the sample interval can be linear or logarithmic.



Figure C.4: Comparable examples of Van Essen TD- & Baro-Divers
(source: <https://www.vanessen.com/images/PDFs/TD-Diver-DI8xx-ProductManual-nl.pdf>)

- In-Situ; RuggedTROLL100 (2x) & BaroTROLL (1x):

Rugged TROLL 100 and BaroTROLL divers are applied for the measuring and recording of time dependent fluctuations in (ground)water levels, atmospheric pressures and temperatures. The RuggedTROLL100 divers function in a pressure range up to 9 m water column. BaroTROLL divers can be used for the measurement of atmospheric pressures, up to 1 bar. The internal memory of 2.0 MB accommodates the storage of 120.000 data records. A record contains a set of three items; date & time, pressure and temperature. The internal battery has a lifetime of approximately 10 years. By the use of the Rugged TROLL docking-station and the Win-Situ 5 software, linear logging can be programmed. Fastest logging rate is 1 log per second for the Rugged TROLL 100 divers and 1 log per minute for the BaroTROLL divers. Optionally it is possible to display the pressure in units of Psi, Bar, Pascal or mH₂O.



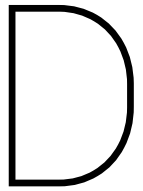
Figure C.5: Comparable examples of In-Situ TD- & Baro-Divers
(source: <https://in-situ.com/product-category/water-level-monitoring/level-temp-data-loggers/>)

- Hand measurement device: Heron water tape

The water tape is applied to hand measure static water levels and verify drawdown water levels during the pumping tests. The water tape has a length of 300 ft (100 m). A water level sensing probe is attached to the tail of the tape. Probe water contact results in an instant auditory signal, after which the depth can be determined by eye. Product specifications can be found on the Heron webpage.



Figure C.6: Comparable example of the fieldwork water tape
(source: <https://envirotechonline.com/water-level-interface-meters/the-heron-water-tape.html>)



Aquifer test - Data analysis overview

This appendix accommodates an overview in fieldwork data analysis. Section D.1 contains multiple distinctive python script applied in fieldwork data analysis. The results of all determined geohydrological parameter values (25 approaches for each pumping test / location) can be found in Section D.2.

D.1. Example Python scripts

Example Python script - Theis's method

```
def drawdown(t, T, S):
    s = Q / (4 * np.pi * T) * exp1(r ** 2 * S / (4 * T * t))
    s[t > toff] -= Q / (4 * np.pi * T) * exp1(r ** 2 * S / (4 * T * (t[t>toff] - toff)))
    return s
```

Where s (m) is the drawdown at distance r (m) from the well, Q (m^3) is the constant well discharge , KD (m^2/d) is the aquifer transmissivity ($KD = T$), S (-) is the aquifer storativity, t (d) is the time measured from the start of pumping and exp1 is the exponential integral. The drawdown measurements in this research are limited to in-well measurements. The distance r in Theis's equation is assumed to be the length of the well radius (0.0635 m).

Example Python script - Fmin-RMSE optimization

An example Python implementation of Fmin optimization is given below. It shows an optimization of a two layered model, containing five parameters (T and S values for two model layers and well skin resistance).

```
def optimTTim_Qvar(params, t, meas):
    kaq = np.zeros(2)
    Saq = np.zeros(2)
    kaq[0] = params[0]
    kaq[1] = params[1]
    Saq[0] = params[2]
    Saq[1] = params[3]
    res = params[4]
    s = drawdownTTim_Qvar(t, kaq, Saq, res)
    error = np.sqrt(np.mean((s-meas)**2))
    return error

xopt = fmin(optimTTim_Qvar, x0=[10, 10, .01, .001, 0.1], args=(to[mask], do[mask]),
            xtol=1e-4)
```

Where $kaq[0]$ and $kaq[1]$ (m/d) are respectively the hydraulic conductivities of the first and second layer, $Saq[0]$ and $Saq[1]$ (m/d) are the storativities (-) of the first and second layer, res (d) is the well skin resistance, s (m) is the modelled (optimal) drawdown, $error$ (m) is the RMSE objective function and $x0$ contains the ordered initial parameter conditions.

Example Python script - TTIm Calibrate optimization

In the Python script below, an example of the TTIm Calibrate function is given. It is the same example as mentioned in the Fmin optimization above.

```
cal = Calibrate(mlc)
cal.parameter(name='kaq0', layer=0, initial=10, pmin=0)
cal.parameter(name='kaq1', layer=1, initial=10, pmin=0)
cal.parameter(name='Saq0', layer=0, initial=.01, pmin=0, pmax=0.3)
cal.parameter(name='Saq1', layer=1, initial=.001, pmin=0, pmax=0.3)
cal.parameter(name='res', par=wc.res, initial=0.1)
cal.series(name='obs3', x=ro, y=0, layer=[0,1], t=to[mask], h=do[mask])
cal.fit()
```

Where '*kaq0*' and '*kaq1*' (m/d) are respectively the hydraulic conductivities of the first and second layer, '*Saq0*' and '*Saq1*' (m/d) are the storativities (-) of the first and second layer, '*res*' (d), *x* (or *y*) (m) is the radius of the well, *layer* contains the layer numbers of the 'active' connected layer, *initial* is the initial parameter condition and *pmin* and *pmax* are the predefined 'allowed' minimum and maximum values for that particular parameter.

D.2. Data analysis overview

Each dataset (location specific) is analysed by multiple distinctive simulations. The simulations are distinctive in: theoretical model (single layer, double layer and double layer and partial penetration of the well), method (analytical Theis's method (single layer only), TTIm) and optimization function (Fmin-RMSE and TTIm Calibrate). In the TTIm analysis an additional distinction is made between analysis by the use of (a) actual borehole storage and no well resistance, (b) optimal borehole storage and no well resistance, (c) actual borehole storage and optimal well resistance, (d) optimal borehole storage and optimal well resistance. Summarized, the location specific datasets are subjected to 25 different approaches in analysis; analytical (1x), Fmin-RMSE (4x3 = 12x) and TTIm Calibrate (4x3 = 12x). Table D.1 contains an overview of the approaches in fieldwork data analysis.

Table D.1: Overview - approaches in fieldwork data analysis

		Actual bor stor	Opt bor stor	Opt well res
Analytical		-	-	-
Fmin-RMSE	a	x	-	-
	b	-	x	-
	c	x	-	x
	d	-	x	x
TTIm Cal	a	x	-	-
	b	-	x	-
	c	x	-	x
	d	-	x	x

* where the different approaches of the Fmin-RMSE and TTIm Calibrate (a-d) are analysed in combination with a single layer system, a double layer system and a system with a two layers and partial penetration of the well.

The results of all determined geohydrological parameter values can (by location) be found below.

D.2.1. Location: Bingo

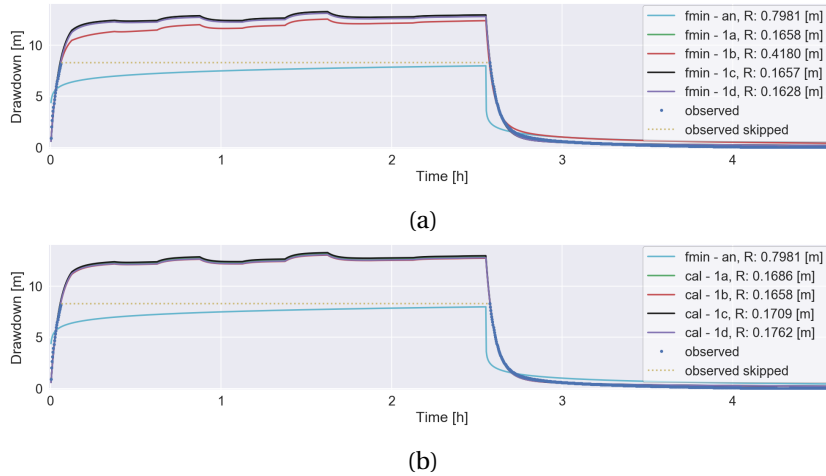


Figure D.1: Bingo single layer fieldwork data analysis by the optimization (a) fmin-RMSE method and (b) TTIm calibration method

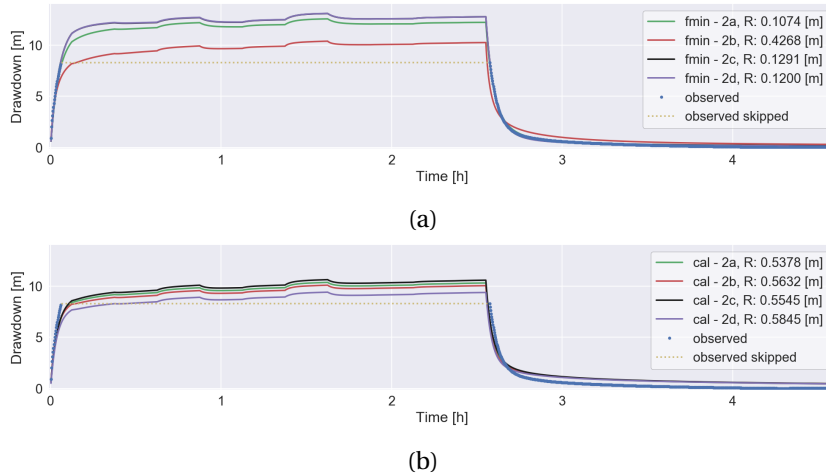


Figure D.2: Bingo double layer fieldwork data analysis by the optimization (a) fmin-RMSE method and (b) TTIm calibration method

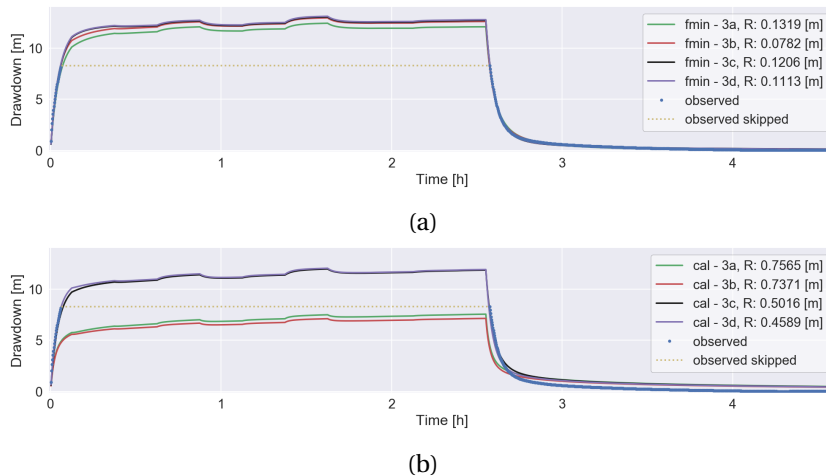


Figure D.3: Bingo partially penetrating double layer fieldwork data analysis by the optimization (a) fmin-RMSE method and (b) TTIm calibration method

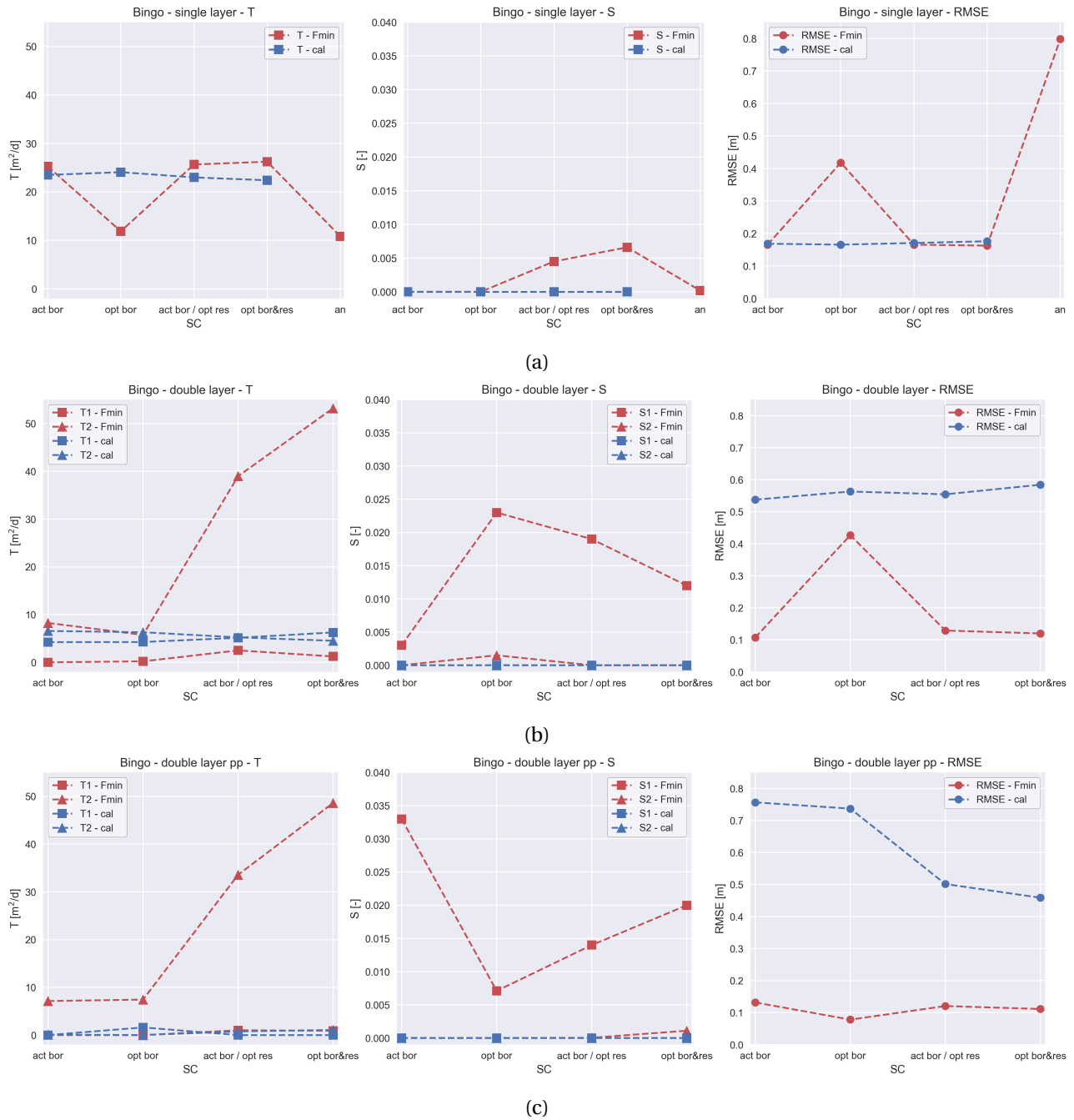


Figure D.4: Bingo - overview determined (F_{\min} and Cal) optimal parameter values of (a) a single layer system, (b) a double layer system, and (c) a system with two layers and partial penetration of the well

D.2.2. Location: Nungo

bigskip Gained fieldwork data at the location Nungo not sufficient for the analysis of geohydrological parameter values.

D.2.3. Location: Nyong Nayili

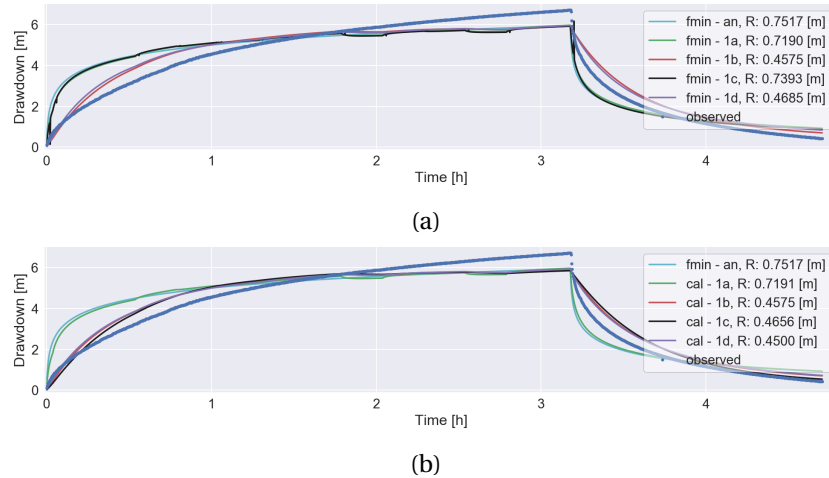


Figure D.5: Nyong Nayili single layer fieldwork data analysis by the optimization (a) fmin-RMSE method and (b) TTIm calibration method

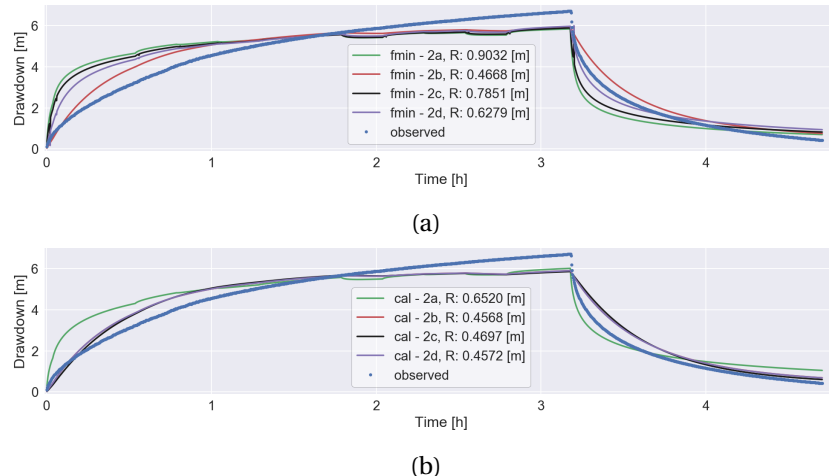


Figure D.6: Nyong Nayili double layer fieldwork data analysis by the optimization (a) fmin-RMSE method and (b) TTIm calibration method

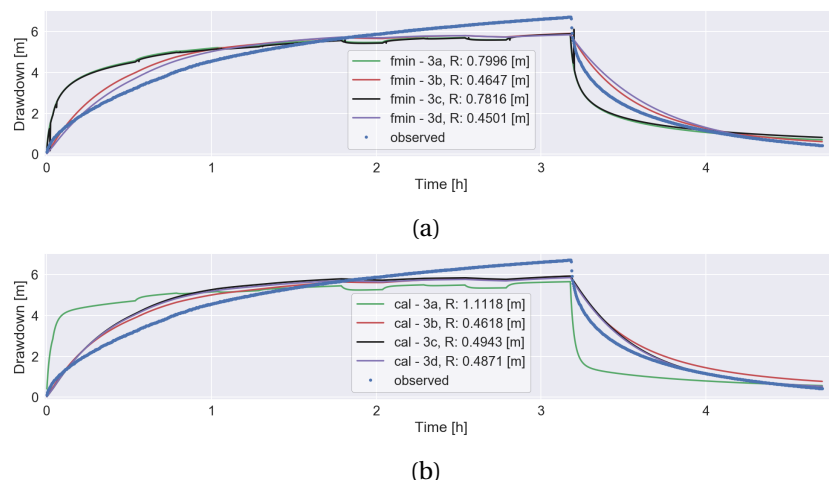


Figure D.7: Nyong Nayili partially penetrating double layer fieldwork data analysis by the optimization (a) fmin-RMSE method and (b) TTIm calibration method

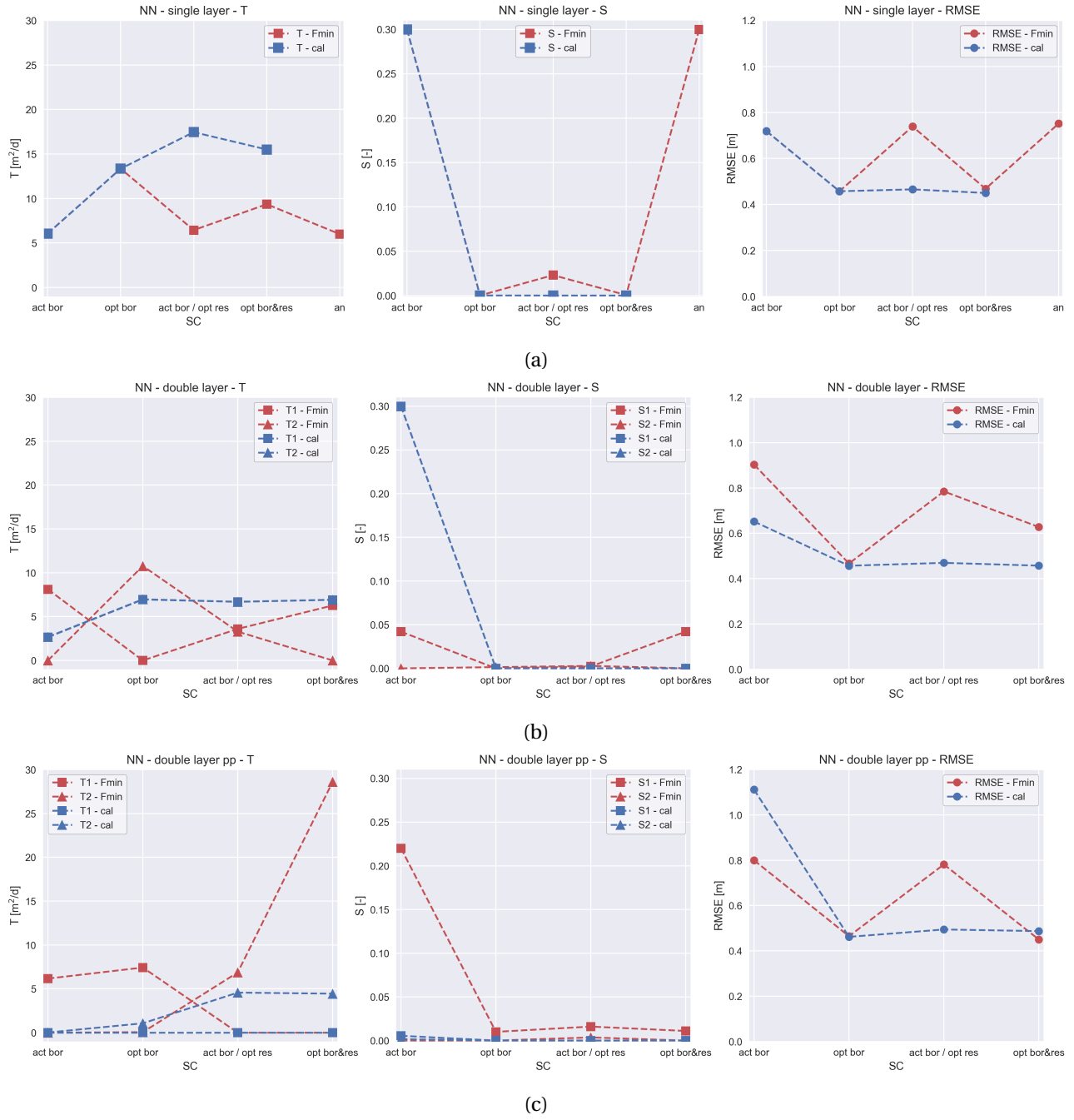


Figure D.8: Nyong Nayili - overview determined (Fmin and Cal) optimal parameter values of (a) a single layer system, (b) a double layer system, and (c) a system with two layers and partial penetration of the well

D.2.4. Location: Janga (1/2)

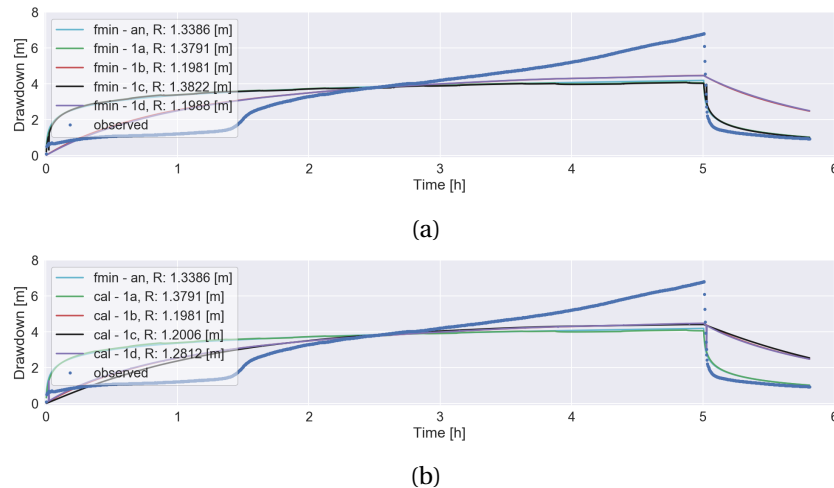


Figure D.9: Janga first attempt single layer fieldwork data analysis by the optimization (a) fmin-RMSE method and (b) TTIm calibration method

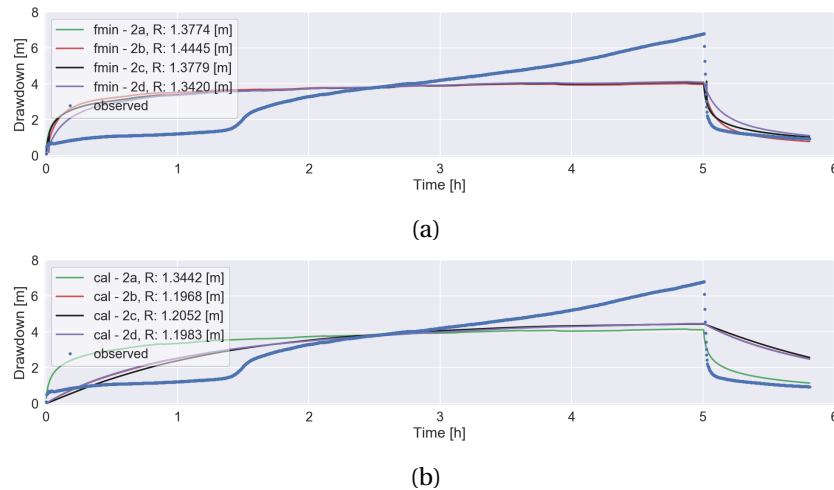


Figure D.10: Janga first attempt double layer fieldwork data analysis by the optimization (a) fmin-RMSE method and (b) TTIm calibration method

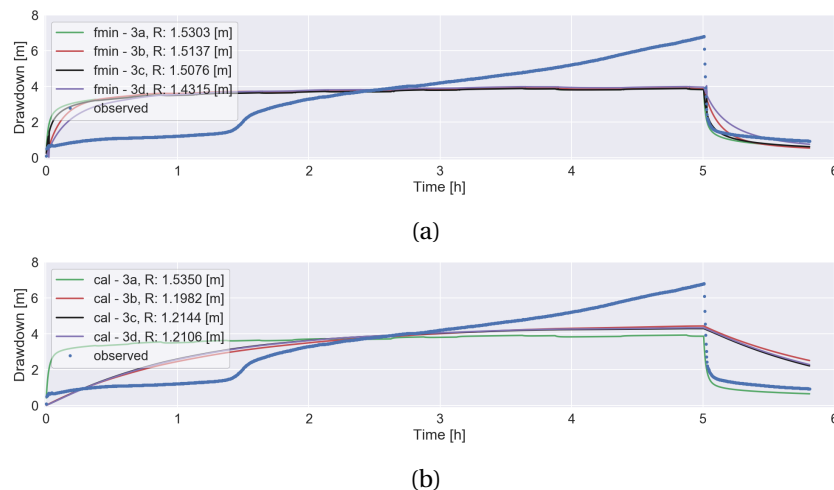


Figure D.11: Janga first attempt partially penetrating double layer fieldwork data analysis by the optimization (a) fmin-RMSE method and (b) TTIm calibration method

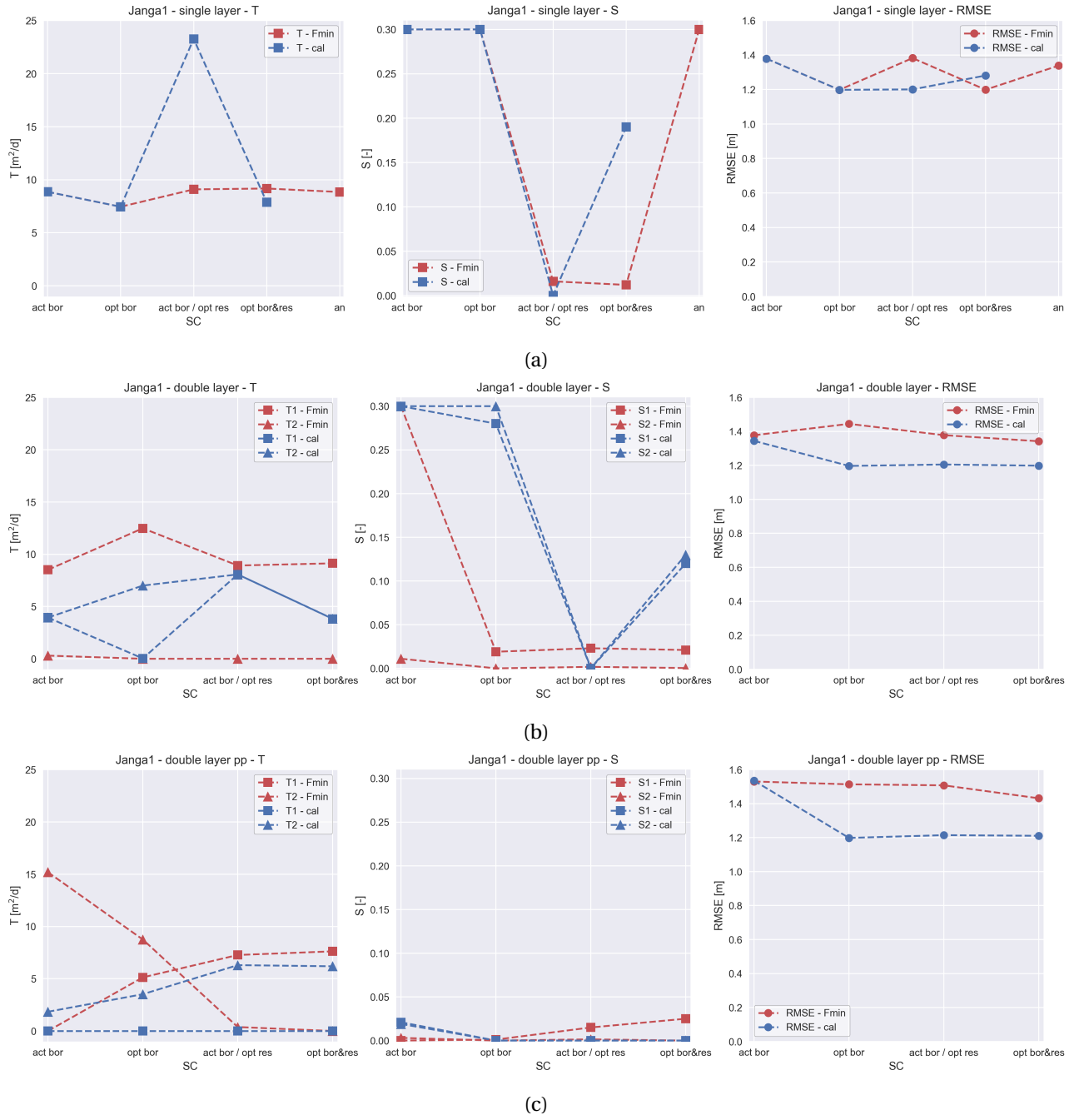


Figure D.12: Janga first attempt - overview determined (Fmin and Cal) optimal parameter values of (a) a single layer system, (b) a double layer system, and (c) a system with two layers and partial penetration of the well

D.2.5. Location: Janga (2/2)

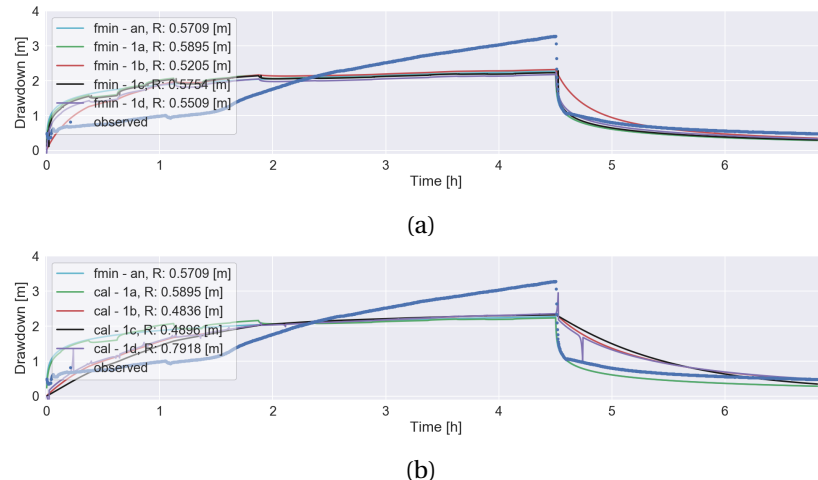


Figure D.13: Janga second attempt single layer fieldwork data analysis by the optimization (a) fmin-RMSE method and (b) TTIm calibration method

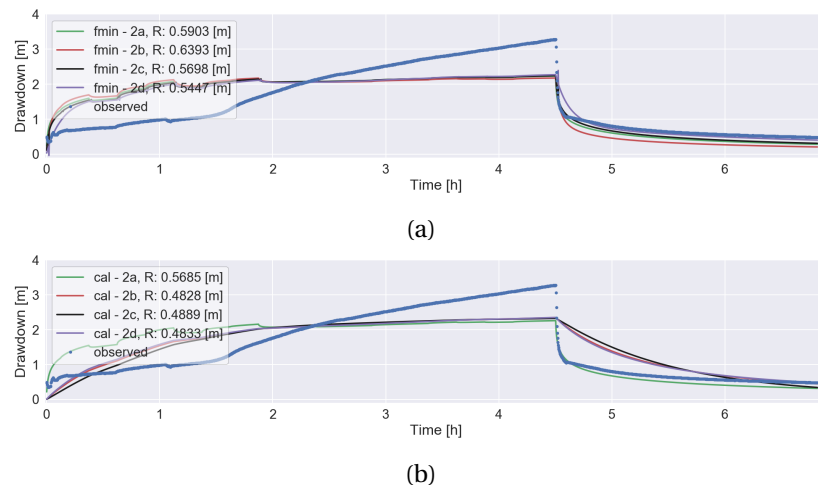


Figure D.14: Janga second attempt double layer fieldwork data analysis by the optimization (a) fmin-RMSE method and (b) TTIm calibration method

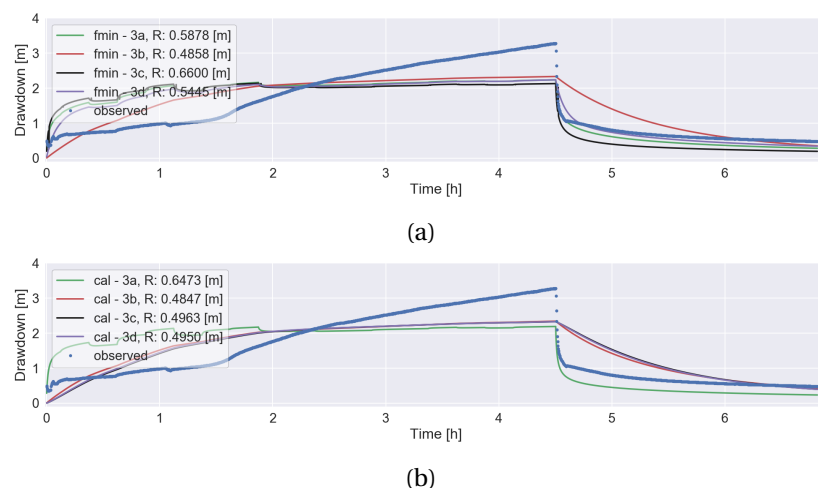


Figure D.15: Janga second attempt partially penetrating double layer fieldwork data analysis by the optimization (a) fmin-RMSE method and (b) TTIm calibration method

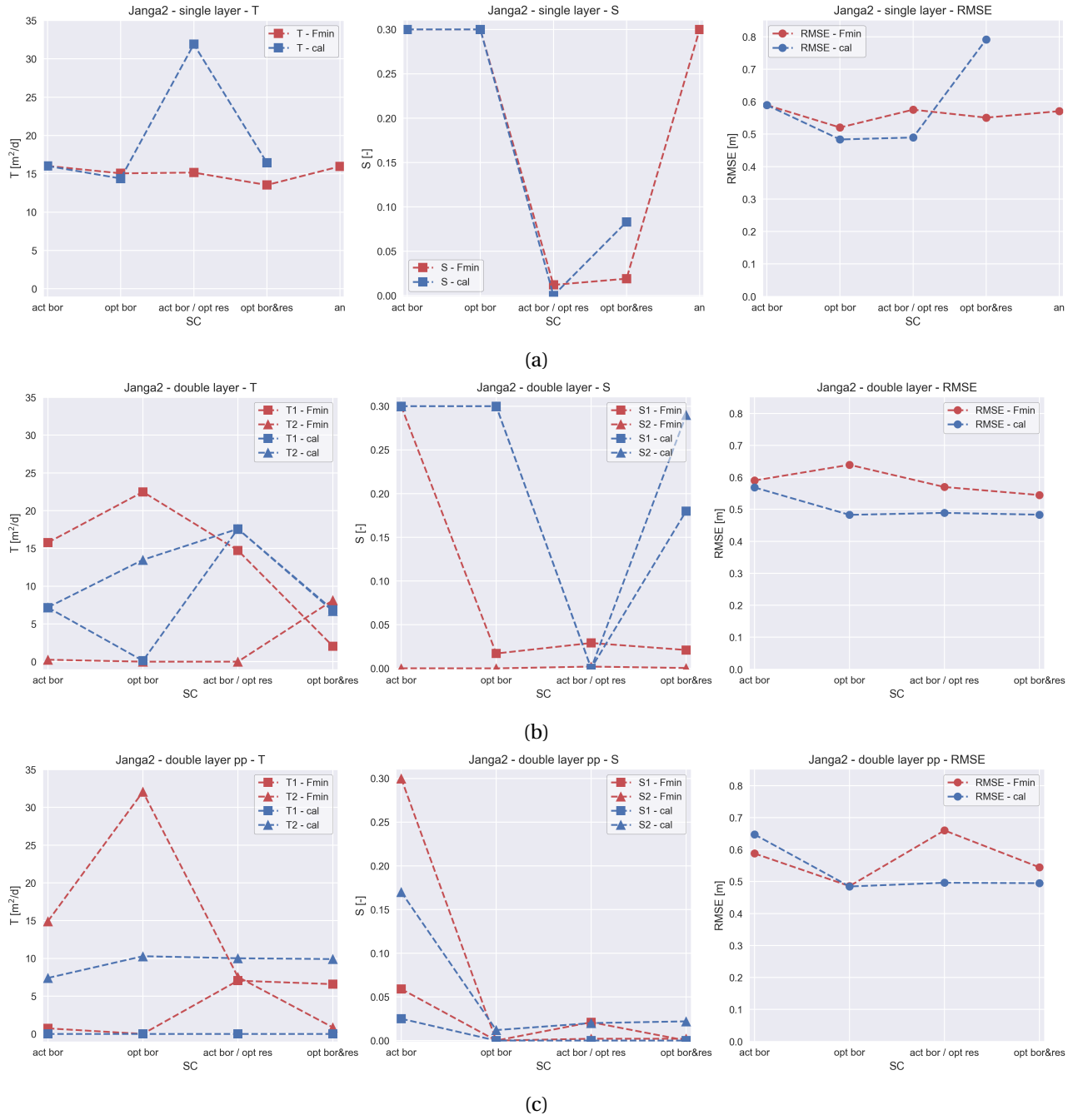


Figure D.16: Janga second attempt - overview determined (Fmin and Cal) optimal parameter values of (a) a single layer system, (b) a double layer system, and (c) a system with two layers and partial penetration of the well

D.2.6. Location: Ziong

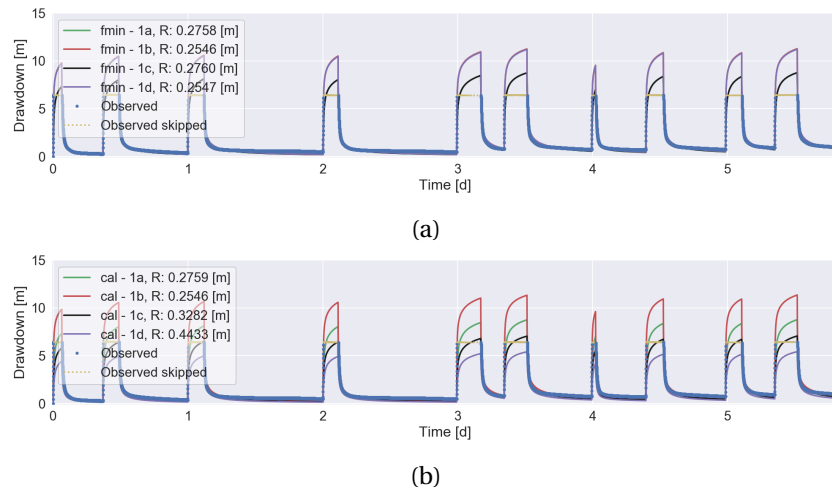


Figure D.17: Ziong single layer fieldwork data analysis by the optimization (a) fmin-RMSE method and (b) TTIm calibration method

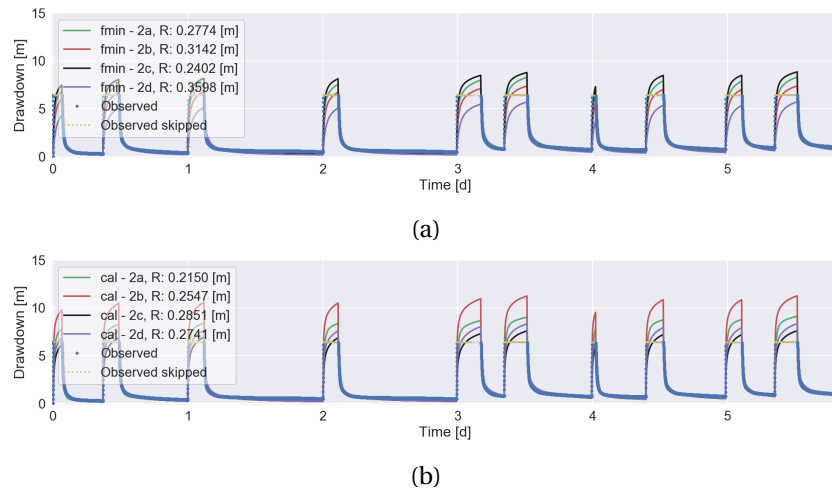


Figure D.18: Ziong double layer fieldwork data analysis by the optimization (a) fmin-RMSE method and (b) TTIm calibration method

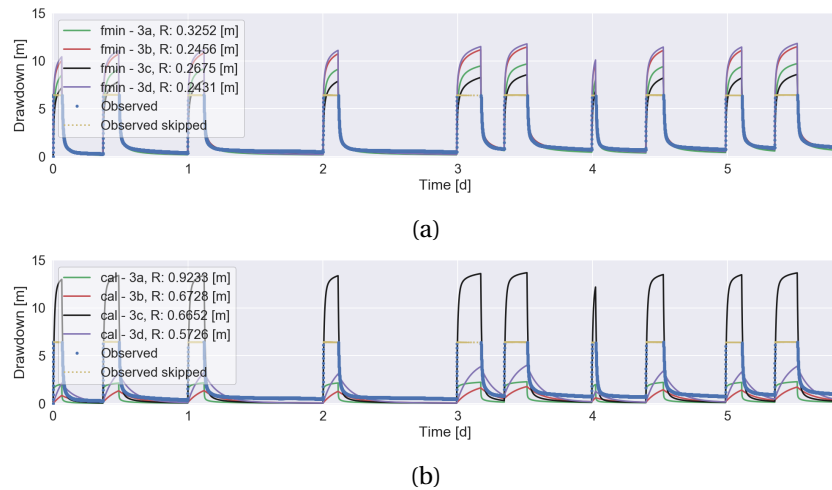


Figure D.19: Ziong partially penetrating double layer fieldwork data analysis by the optimization (a) fmin-RMSE method and (b) TTIm calibration method

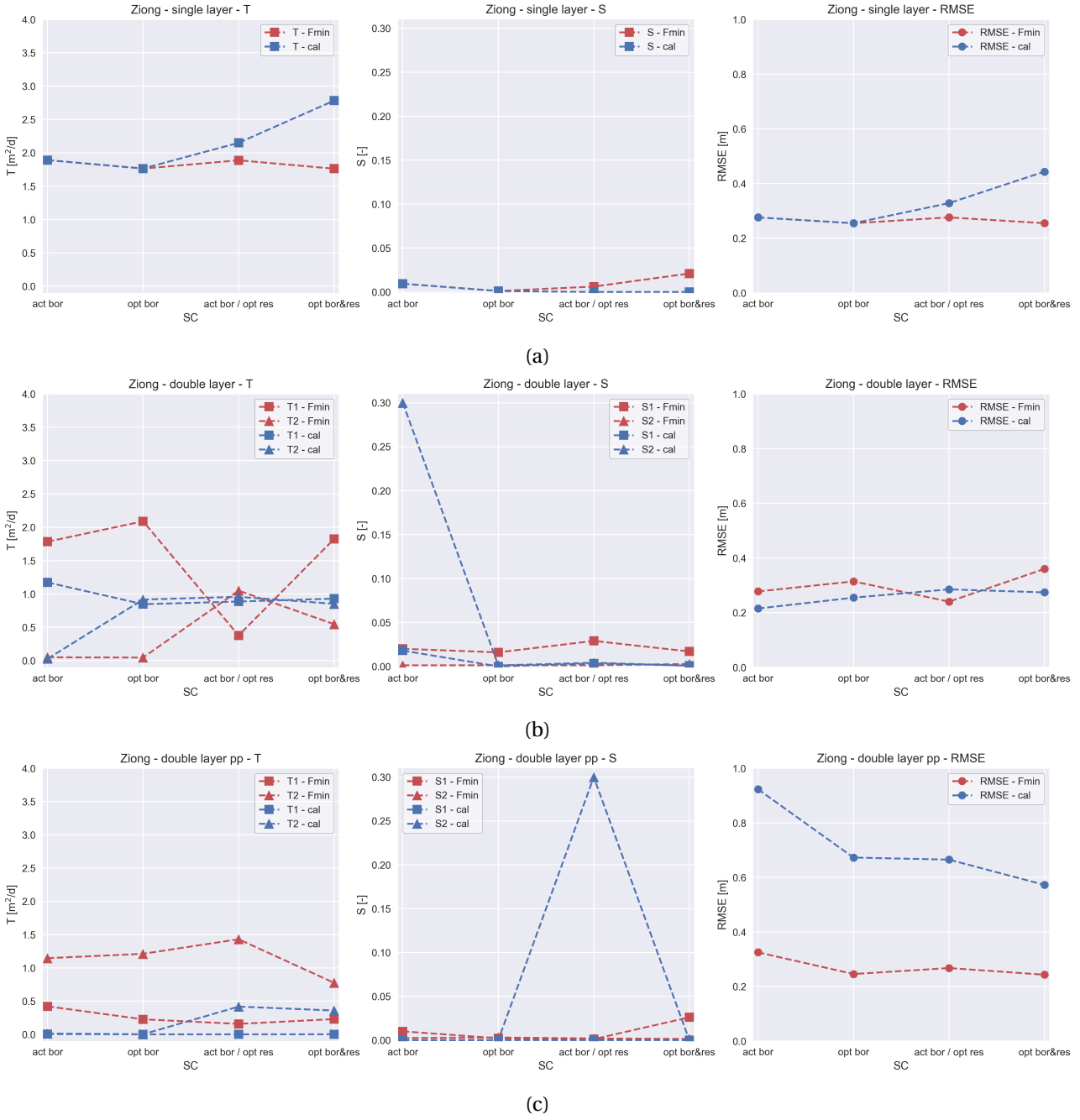
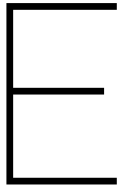


Figure D.20: Ziong - overview determined (Fmin and Cal) optimal parameter values of (a) a single layer system, (b) a double layer system, and (c) a system with two layers and partial penetration of the well



MODFLOW - Model definition

E.1. Model design

For the ASR-system simulation MODFLOW is used. A finite difference model, written by US Geological Survey (USGS). It is stated to be the worldwide most convenient (open source) computer program for the simulation of groundwater flow. MODFLOW has a modular structure. A variety of aquifer features can be simulated by the introduction of (free available) packages. In this research, input files (needed by MODFLOW) are created by the use of Python and the FloPy package ((Harbaugh, 2005; Niswonger et al., 2011)).

Unmodified versions of MODFLOW uses Cartesian geometry. Simulations are standard performed in a (single or multi layer) rectangular grid model. These models can simulate the three-dimensional ASR-system performance accurately. However, it requires disadvantageous large computational power. In this particular case the single well simulation is approached axially symmetric. As prescribed by Langevin (2008), the rectangular model structure is radially scaled by the adjustment of several input parameter. Results are advantageous on model precision and run times. A detailed description of this radial scaled MODFLOW model can be found in Appendix F.

Due to the applied MODFLOW radial scaling the defined grid consist of a single row (1 m width) and multiple columns. The well is located in the first cell (column 0, row 0). Column width increases (grouped) stepwise, based on the (radial) distance between the specific column and the well. By the use of the cell sizes 0.0635 m (40x), 0.1 m (25x), 0.5 m (20x), 1.0 m (25x), 2.0 m (30x) and 5.0 m (10x) a total (radial) length of 150 m is simulated. An extent assumed to be sufficient for the purposes of this research (Appendix E.2). The vertical (third) dimension is added to the model by a total of 50 layers (thickness of 1.0 m each).

Model timespan (one year) is devised into an abundance of logarithmic time frames. Higher temporal resolutions is added to the moments at which fluctuation in head are expected. The design of four months infiltration contains a single logarithmic time frame of 200 steps. Every single day in dry season (243 days) contains a 4 hour logarithmic time frame for pumping (8 steps) and a subsequent 20 hour logarithmic time frame for recovery (10 steps). This puts the year-round total number of time steps on 4574.

E.1.1. MODFLOW-NWT

Due to initial conditions and expected strong temporal variations in GWT cells may fall dry and become wet again over time. Model simulation is therefore performed through the use of MODFLOW-NWT: The Newton-Raphson formulation for the (more convenient) MODFLOW-2005 program. As stated by Niswonger et al. (2011), MODFLOW-NWT is intended for solving problems involving drying and re-wetting non-linearities of the unconfined groundwater-flow equation. MODFLOW-NWT requirs a combined use with the Upstream Weighting (UPW) package for calculation conductances between cells (instead of the BCF, LPF or HUF package applicable with MODFLOW-2005). The UPW package keeps dry cells active, while water outflow of the cell is not allowed. Moreover, if applicable inflow to a dry cell automatically flows further down to the adjacent (non-dry) cell in the layer below (Niswonger et al., 2011). In correspondence with the use of MODFLOW-NWT the (own) NWT solver is used for model simulation (instead of the convenient PCG solver).

E.1.2. MODFLOW - GHB

Wet season infiltration is included by the use of the General Head Boundary (GHB) package. For as long as the wet season (stress periods), GHB cells are specified through stress period data. General Head Boundaries are added to the well cells (row 0, column 0) in the predefined layers of penetration (layer 20-46). The GHB stress period data requires an additional definition of stage and cond (conductance) (Harbaugh et al., 2000). The stage equals the constant flood inundation level ($h^* = 2 \text{ m}$). For the purposes of this research conductances are aligned with the CWC (Cell-to-Well hydraulic conductance). More information on the CWC can be found in Section E.1.3.

E.1.3. MODFLOW - MNW2

The ASR-system of interest contains a well which is partially penetrating the aquifer. In simulation, the aquifer consists of multiple model layers. A set-up causing the convenient Well package to be insufficient. For a solid simulation the more extended Multi-Node-Well2 (MNW2) package is used. MNW2 houses several additional well options (e.g. bounded drawdown, addition of well skin resistances and pump related adjustments in discharge). Thence, definition of an abundant list of parameters is required (within the node data and the stress period data) (Konikow et al., 2009).

Many parameters are by default correct, some however need specification. The well penetration interval (screen) is recorded by the definition of ztop and zbotm. MNW2 assigns the well screen to model nodes (well cells in the corresponding layers). In-well GWT preferable does not drop below the elevation of -20 m. Hlim definition guarantees this desire. The flag of qlimit is 1 activates the definition of Hlim. Moments (stress-periods) of pump operation are set by ITMP is 1, all other moments (stress-periods) ITMP is set 0. Furthermore, MNW2 requires the input of a desired discharge (qdes and specification of Cell-to-Well hydraulic conductance (CWC), topics highlighted below.

Desired discharge (qdes)

Based on a predefined desired discharge the MNW2 determines a (model) layer dependent discharge iteratively. As long as the head bound (Hlim) is not restrictive, summed layer discharges equal (approximately) the desired discharge. The predefined desired discharges are based on the predefined criteria of sustainable system use. The dry season (total) discharge volume should not exceed the wet season (total) recharge volume. The desired discharge (qdes) is predefined in such a way, this condition is always met.

FloPy is used for reading MODFLOW binary output files. In other words, the actual simulated recharges and discharges are obtained by reading the `binaryfile.CellBudgetFile`.

MODFLOW standard - Cell-to-Well hydraulic conductance (CWC)

Due to MNW2 application, the occurrence of a difference between the head in the well and the head in the model (well)cell is inevitable. Multiple model elements contribute to the head difference. Total head difference is dependent on the expression of Cell-to-Well hydraulic conductance (CWC), depicted in Equation E.1 (Konikow et al., 2009).

$$CWC_n = [A + B + CQ_n^{(P-1)}]^{-1} \quad (\text{E.1})$$

Where CWC_n (m^2/d) is the n^{th} Cell-to-Well hydraulic conductance, A is the linear aquifer-loss coefficient resulting from the well having a smaller radius than the horizontal dimensions of the cell in which it is located, B is the linear well-loss coefficient accounting for head losses that occur adjacent to and within the borehole and well screen (skin effects) and $CQ_n^{(P)}$ accounts for non-linear head losses due to turbulent flow near the well (Konikow et al., 2009).

$$A = \frac{\ln(r_o/r_w)}{2\pi b \sqrt{K_x K_y}} \quad (\text{E.2})$$

$$r_o = 0.14 \sqrt{\Delta x^2 + \Delta y^2} \quad (\text{E.3})$$

$$B = \frac{SKIN}{2\pi b \sqrt{K_x K_y}} \quad (E.4)$$

$$SKIN = \left(\frac{b K_h}{b_w K_{SKIN}} - 1 \right) \ln \left(\frac{r_{skin}}{r_w} \right) \quad (E.5)$$

Where r_o (m) is the effective external radius of a rectangular finite-difference cell for isotropic porous media, r_w (m) is the well radius, r_{skin} (m) is the well radius plus the thickness of improved soil around the well, b (m) is the saturated thickness of the cell(layer), b_w (m) is the saturated (active) length of the borehole in the cell(layer) (in the purposes of this research equal to b (1m)), K_h (m/d) is the horizontal (non-radial scaled) hydraulic conductivity (equals K_x and K_y due to the assumption of horizontal anisotropy), Δx (m) is the grid spacing in the x-(column-)direction and Δy (m) is the grid spacing in the y-(row-)direction (Konikow et al., 2009).

As stated, the aquifer-loss coefficient (A) accounts for the difference in dimensions between the well (cross-section) and the (well)cell. Perfectly understandable in the case of an unmodified (Cartesian geometry) rectangular grid MODFLOW model. However, simulation is performed in a radial scaled model, according to the principles as stated by Langevin (2008). Well cell width perfectly aligns the radius of the well. It is therefore no longer known how to interpret the A term. The same applied for the implementation of the $CQ_n^{(P)}$ term. Further research should be done on the implementation of the MNW2 Cell-to-Well hydraulic conductance in combination with a radial scaled MODFLOW model. In this research the CWC values are specified manually. The applied conductances are calculated by the Equations 3.1 - 3.4 (Section 3.1.2).

E.2. Leakage factor λ

MODFLOW model extent is based on the double layer leakage factor. The analytical solution for the leakage factor (λ) is depicted in equation E.6 (bron geo1 lecture notes week3).

$$\lambda = \sqrt{\frac{c * T_0 * T_1}{T_0 + T_1}} \quad (E.6)$$

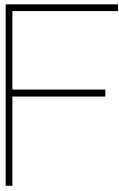
where λ is the leakage factor (m), c (d) is the resistance of the leaky layer between aquifer one and two and T_0 and T_1 are the transmissivities of respectively aquifer one and two.

As a source of input the optimal values (T_0 and T_1) determined by fieldwork analysis TTIm (Fmin); double layer system and the system with a double layer and partial penetration of the well are used. In TTIm Model3D soil stratification is not characterized by a regular sequence of alternately aquifers and leaky layers. TTIm Model3D houses an accumulation of aquifers. Resistance of the fictive leaky layer is computed from the middle of first layer to the middle of the second layer (Bakker, 2013a,b). For the determination of the leakage factor an vertical anisotropy of 0.25 (-) is assumed. An overview of all generate leakage factors can be found in Table E.1.

Table E.1: Lambda (m) overview per location

SC	Bingo 2lay	Bingo 2lay pp	Nyong Nayili 2lay	Nyong Nayili 2lay pp	Janga (1/2) 2lay	Janga (1/2) 2lay pp	Janga (2/2) 2lay	Janga (2/2) 2lay pp	Ziong 2lay	Ziong 2lay pp
a	31.11	31.11	33.94	33.94	51.51	17.01	51.95	20.10	35.25	32.31
b	31.27	31.11	36.77	33.96	52.33	34.56	52.33	17.01	35.27	31.82
c	31.38	31.25	35.32	36.77	52.33	51.15	52.33	38.37	32.29	31.56
d	31.21	31.20	33.94	36.77	52.33	52.33	27.97	49.54	34.42	32.13

A model extent of 3 to 4 times the leakage factor (characteristic length) is desirable. By meeting this requirement it can be expected that 95-99% of the actual water flow is taken into account by the model. Moreover, the head at the model tail is by approximation no longer affected by the (centrally positioned) well behaviour. The assumption of a constant head at model tail becomes valid (bron geo1 lecture notes week3). The majority of the leakage factors are in close range of the 36.74 m average leakage factor of obtained. To comply the above mentioned requirement a total model extent (radius) of 150 m is implemented.



MODFLOW - Radial conversion

Introduction

The general thesis topic is pointed at the groundwater flow around a well. Due to seasonal circumstances the same well acts both as extraction and injection well. Direction of groundwater flow is alternately pointed towards and away from the well. This phenomenon can be simulated straightforward by the use of the USGS's modular hydrologic model MODFLOW. To generate adequate results in groundwater fluctuations high model accuracies are desirable, especially close to the well. The model preferably accommodates a fine-meshed grid by the implementation of a multitude of rows and columns. As a consequence model run times will last long.

However, groundwater flow around a well can (under specific conditions) be approached as a phenomenon of radial symmetry. Minor radial parameter conversions can reduce the number of dimensions in the MODFLOW model. A modification that reduces model run times substantially (Langevin, 2008). The section below contains a detailed description of the required radial scaling of parameters, as applied in this thesis. In addition, three examples are included to test and compare the radial scaled model performance.

Theoretical method

MODFLOW is naturally based on rectangular geometry. Without the inclusion of specific adjustments this results in (multi layered) rectangular models. Model shapes not by definition necessary in the case of a well simulation. Under the assumption of subsurface conditions to be homogeneous and the absence of elements disturbing the regional hydraulic gradient it is possible to interpret the groundwater flow around a well as a phenomenon strictly cylindrical. Assumptions on which one would approach well flow model simulation as being axially symmetric (Figure F.1).

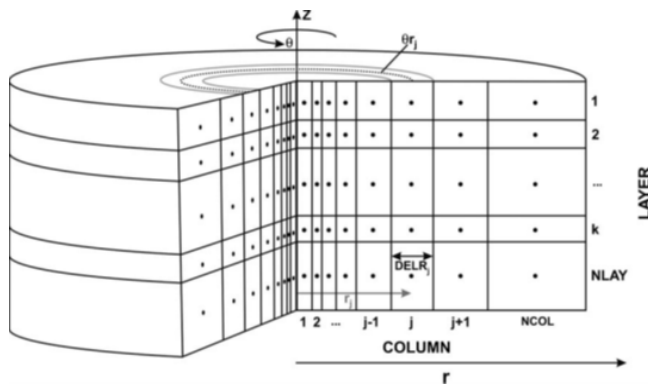


Figure F.1: Schematic of an axially symmetric model (Langevin, 2008)

The in figure F.1 displayed cylindrical approach of a well model can be simulated by an MODFLOW model (rectangular geometry) which accommodates one or more layer(s), one row only and multiple columns. In this single row model it is assumed the well is included in the first column. Moreover, the single row should

act as the representation of a subsurface slice. This is achieved by the radial modification of multiple parameters. Radial parameter scaling guarantees the conversion of a rectangular (single row) MODFLOW model into a fictive radial model. Elaborating on the explanation of Langevin (2008) the following parameters become radial dependent:

$$K_h \rightarrow K_{h,j}^* = K_{h,j} \theta r_j \quad (\text{F.1})$$

$$K_v \rightarrow K_{v,j}^* = K_{v,j} \theta r_j \quad (\text{F.2})$$

$$S_s \rightarrow Ss_j^* = Ss_j \theta r_j \quad (\text{F.3})$$

$$S_y \rightarrow Sy_j^* = Sy_j \theta r_j \quad (\text{F.4})$$

$$n \rightarrow n_j^* = n_j \theta r_j \quad (\text{F.5})$$

Where K_h and K_v represent the horizontal and vertical hydraulic conductivity, S_s is the specific storage, S_y is the specific yield (phreatic storage) and n is the porosity. Scaled parameters modification is highlighted by the introduction of the superscript *. As visible by the subscript j the parameters hereby become column (radial) dependent. r_j is the radial distance between column j and the well (column 1) and θ is the angle of the representing slice. For the purpose of radial scaling θ covers a complete ring; $\theta == 2\pi$.

Main advantage of the implementation of the radial parameter conversion is the reduction in model dimensions. At local scale (close to well) the model can contain a detailed meshed-grid without the emergence of excessive model run times. Moreover the parameter is applied within the common modelling program MODFLOW itself, no specialized programs are required. However, it has to be mentioned the circular model approach can only be applied under the specific assumptions of radial symmetry (Langevin, 2008).

Test application

To validate the radial scaled model performance, a total of three fictive test exercises are applied. In these exercises a comparison is made between the radial scaled model (Figure F2c) and two natural rectangular based MODFLOW models (Figure F2a and Figure F2b). The rectangular MODFLOW model is the most straightforward. Due to the squared shape deviations in model outcome are expected. Whereas the rectangular round MODFLOW model is manually circularized. This model accommodates the gradual increase in flow area in the radial direction. Based on Langevin (2008) it is expected the rectangular round model should approximate radial model outcomes.

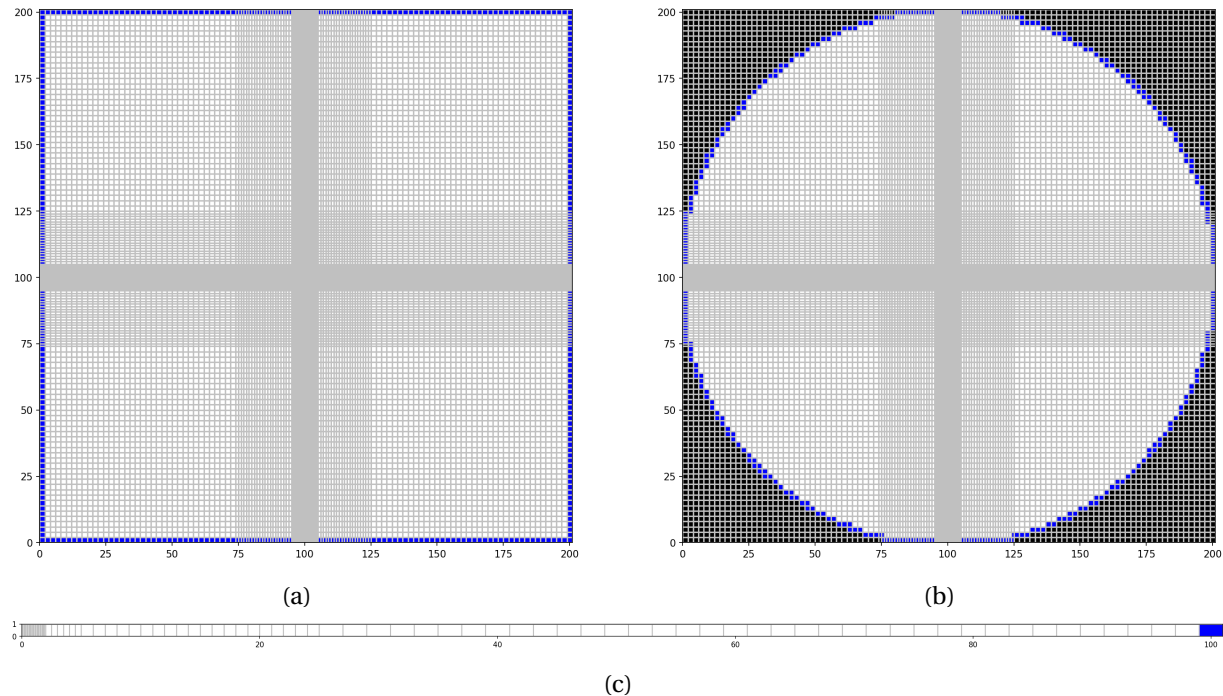


Figure F.2: MODFLOW topview schematisation of a: (a) Rectangular model, (b) Rectangular round model and (c) Single row model
(grey = cell boundary, red = well position, blue = boundary condition, black = inactive cell)

The exercises applied deliberately show strong similarities with the first two test problem cases described by Langevin (2008). In terms of content the exercises are designed with the same set of parameters, making it possible to validate the results in general. As an exception a small deviation is applied in terms of grid definition. In these exercises the cell sizes increase (grouped) stepwise based on an increasing (radial) distance from the well. By the use of the cell sizes 0.1 (20x), 0.5 (6x), 1.0 (20x) and 2.0 m (38x) a total model length (radial length) of 101 m is simulated. This grid structure is applicable on the single row (radial) model. The rectangular and rectangular round model accommodate a same and corresponding grid structure, as visible in the model top views of figure F.2.

F.1. Test 1: Steady flow to a fully penetrating well in confined aquifer

The steady state solution of a confined aquifer fully penetrated by a well is applied as a first MODFLOW model performance test. The exercise schematic configuration is depicted in the overview of figure F.3. The case is characterized by its simplicity, making it an exercise ideally suitable for the comparison against the analytical solution. Thiem's method (Equation F.6) is applied as the analytical drawdown solution for radial well flow in a confined aquifer (Kruseman and de Ridder, 2000):

$$S_j = \frac{Q \ln(\frac{r_2}{r_j})}{2\pi K_{(h)} H} \quad (\text{F.6})$$

Where S_j is the drawdown in column j , Q is the discharge, $r_2 = 100$ m (constant head at a distance of in this case 100 m from the well), r_j is the radial distance between column j and the well (column 1), $K_{(h)}$ is the horizontal hydraulic conductivity and H is the aquifer thickness.

Decline in groundwater head due to well behaviour can also be expressed directly by the use of the analytical discharge potential (ϕ), as depicted in (Equation F.7). Applied on confined conditions it is assumed: $H = h_0$ (Bakker and Anderson, 2011; Strack, 1989). As a result confined heads can be determined by the application of equation F.9. Head values determined are in complete correspondence with the drawdown calculated by Thiem's method.

$$\phi_j = \frac{Q}{2\pi} \ln\left(\frac{r_j}{R}\right) + \phi_0 \quad (\text{F.7})$$

$$h_j = \frac{\phi_j}{k_h H} \quad (\text{F.8})$$

$$h_j = \frac{\phi_j}{k_h H} \quad (\text{F.9})$$

Where ϕ_j is the discharge potential at column j , Q is the discharge, $R = 100$ m (constant head (h_0) at a distance of in this case 100 m from the well), r_j is the radial distance between column j and the well (column 1), $K_{(h)}$ is the horizontal hydraulic conductivity and H is the aquifer thickness.

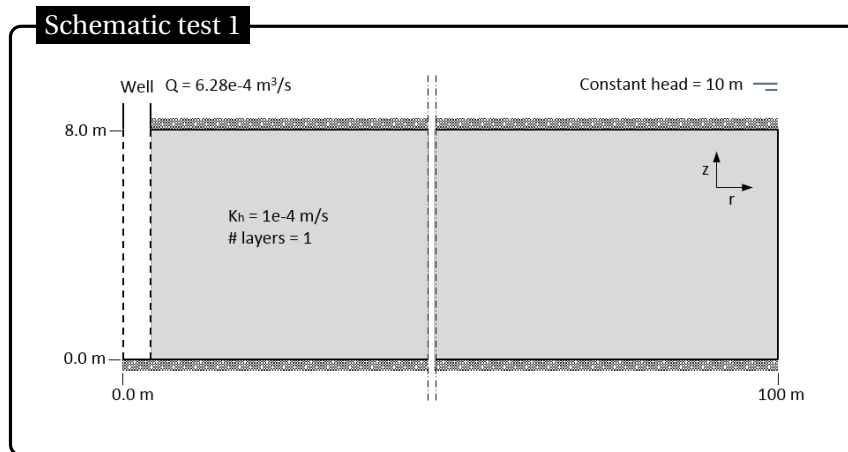


Figure F.3: Schematic test 1

The rectangular MODFLOW model overestimates drawdown (modelled heads are slightly lower) compared to the analytical solution. This difference can be explained by the rectangular shape of the model; imposed boundary condition along the model edge (especially the corners) are positioned 'outside' the defined radial boundary of 100 m from the well. The rectangular model works around this inconvenience, and already shows more similarities with the analytical solution. Some deviation in the first meter(s) around the well still exist, which can potentially be attributed to the cell structure. These minor deviations are no longer present by the application of the radial scaled (single row) model. Regardless the (radial) position,

modelled heads and drawdown are identical to the analytical solution. A first indication the radial scaled MODFLOW model is preferential applicable on this thesis purposes.

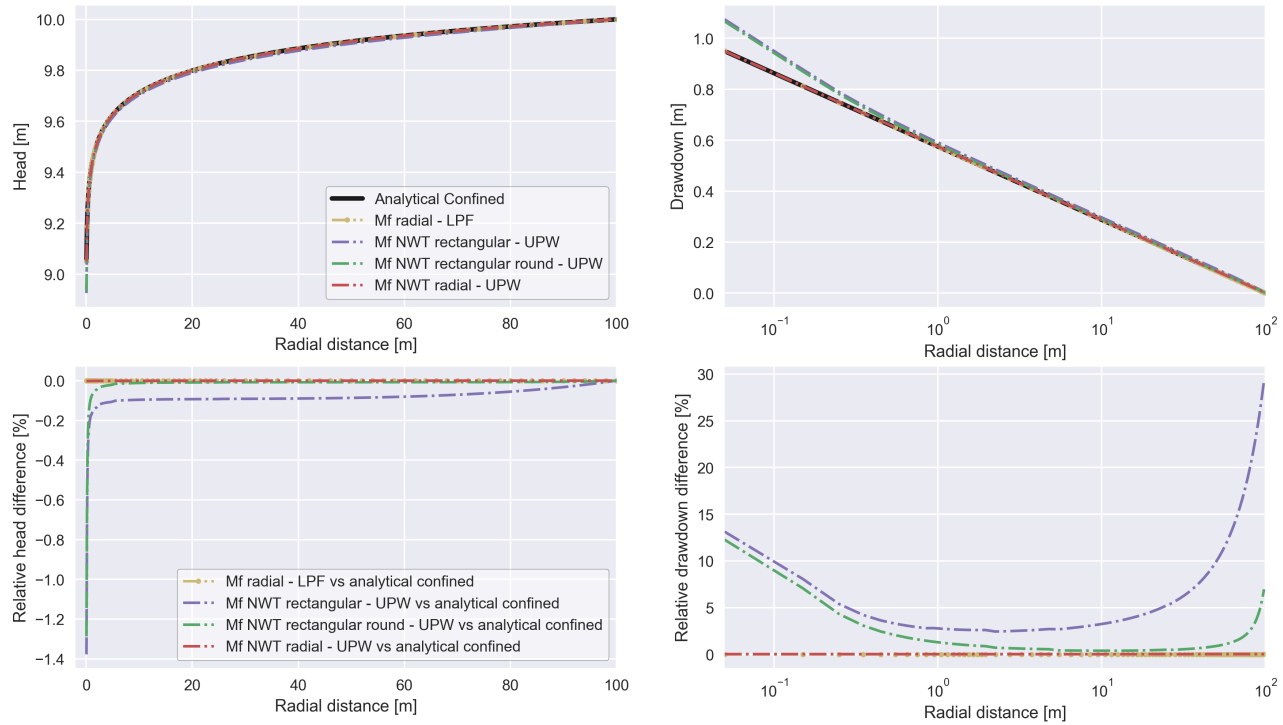


Figure E4: Results test 1

F.2. Test 2: Steady flow to a fully penetrating well in unconfined aquifer

Example exercise two (Figure F.5) accommodates the same test problem as depicted in test 1, only exception is the transition towards unconfined aquifer conditions. In this example the analytical drawdown solution presented by the Thiem-Dupuit's method for steady-state flow to a fully penetrating well in an unconfined aquifer is used as a reference(Kruseman and de Ridder, 2000):

$$S'_j = \frac{Q \ln(\frac{r_2}{r_j})}{2\pi K_{(h)} D} \quad (\text{F10})$$

$$S'_j = S_j - \frac{S_j}{2D} \quad (\text{F11})$$

Where S'_j is the uncorrected drawdown in column j, S_j is the iteratively corrected drawdown in column j, Q is the discharge, $r_2 = 100$ m (constant head at a distance of 100 m from the well), r_j is the radial distance between column j and the well (column 0), $K_{(h)}$ is the horizontal hydraulic conductivity and D is the thickness between aquifer bottom and constant head. For the purposes of this exercise the analytical drawdowns are iteratively determined with a precision of 1e-6.

Also under unconfined conditions the analytical discharge potential (Equation F12) can be applied (Bakker and Anderson, 2011; Strack, 1989). Only exception, compared to the confined conditions, is the minor change in head derivation, visualised in F.14. Major advantage, with respect to the analytical Thiem-Dupuit's method, is the absence of the iterative head derivation process. Result is a fast and accurate analytical calculation of heads by the application of the discharge potential.

$$\phi_j = \frac{Q}{2\pi} \ln\left(\frac{r_j}{R}\right) + \phi_0 \quad (\text{F12})$$

$$\phi_0 = \frac{1}{2} k_h h_0^2 \quad (\text{F13})$$

$$h_j = \sqrt{\frac{2\phi_j}{k_h}} \quad (\text{F14})$$

Where ϕ_j is the discharge potential at column j, Q is the discharge, $R = 100$ m (constant head (h_0) at a distance of in this case 100 m from the well), r_j is the radial distance between column j and the well (column 1), $K_{(h)}$ is the horizontal hydraulic conductivity and H is the aquifer thickness.

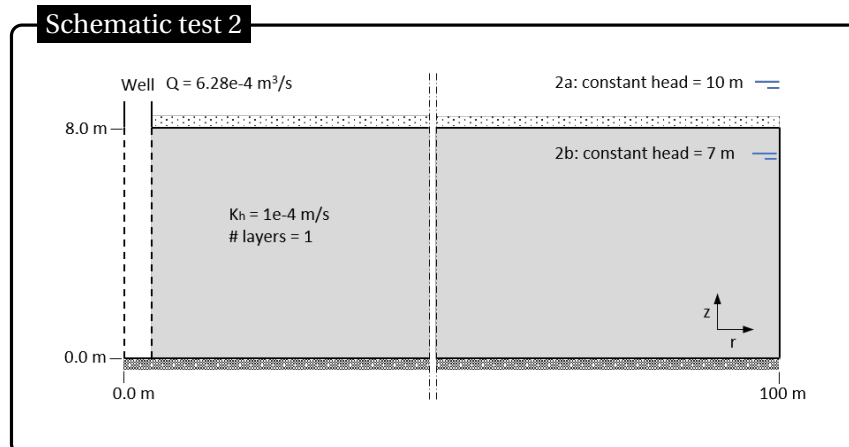


Figure F.5: Schematic test 2

F2.1. Constant head is 10 m

Due to a 10 m constant head boundary the aquifer area of flow is fictive enlarged in the unconfined case (compared to the 8 m aquifer height under confined conditions). In accordance with the solutions in Langevin (2008), overall drawdowns in the unconfined conditions are slightly lower with respect to the confined situation. Model performances of the unconfined example exercise show similar behaviour as the

confined example exercise. Differences in modelled and analytical determined heads and drawdowns are minuscule in general. As expected largest deviations from the analytical solution are present in the MODFLOW rectangular model. The differences in outcome of this model do persist over almost the entire radial distance from the well, regardless the use of the BCF or LPF package. Although it is only slightly, the use of the LPF package shows slightly better performance. For the purposes of this thesis the LPF package is assumed to be preferential in setting the aquifer properties. Application of this package in the MODFLOW round rectangular model results in improved model results, however deviations do continue to exist. In contrast with the confined exercise (F1) application of the radial scaled MODFLOW model under unconfined aquifer conditions deviations from the analytical solution are still present. Modelled drawdowns show strong similarities with the uncorrected analytical solution. Moreover, relative to the analytical solution the absolute radial scaled MODFLOW model outcomes performs most accurately. Making the radial scaled (single row) MODFLOW model suitable for the unconfined aquifer conditions of this thesis.

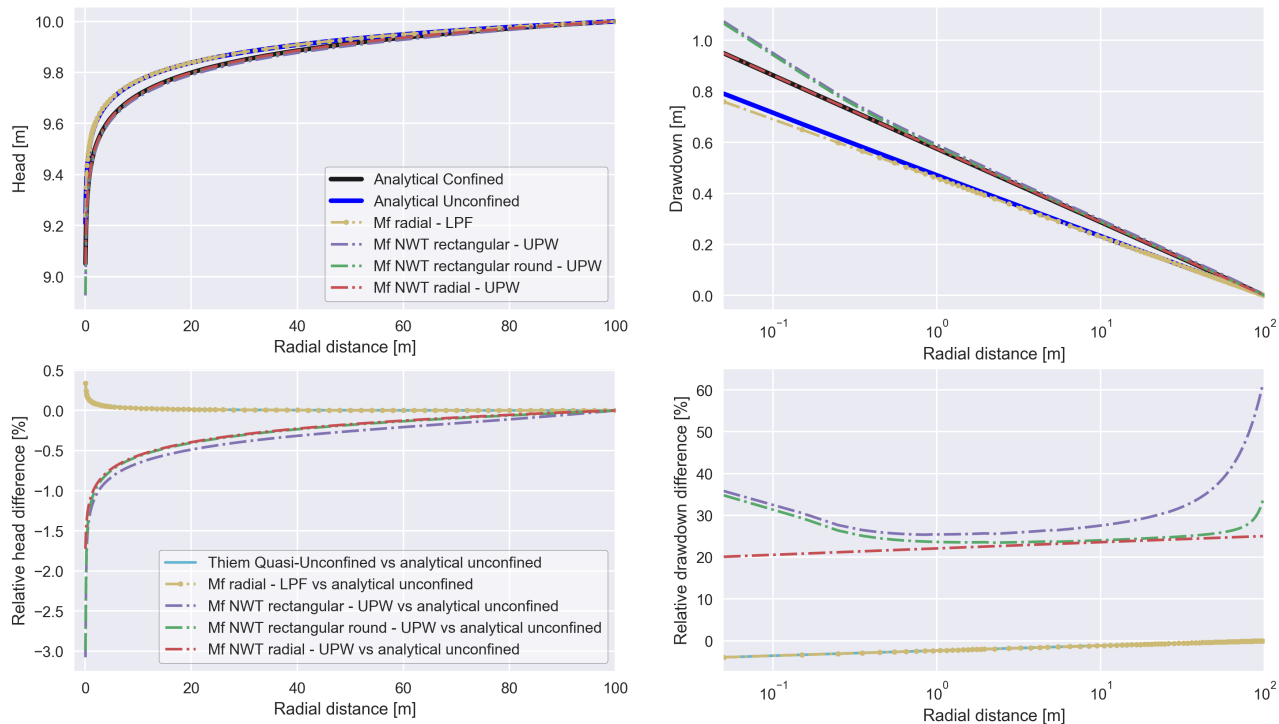


Figure E6: Results test 2a

F2.2. Constant head is 7 m

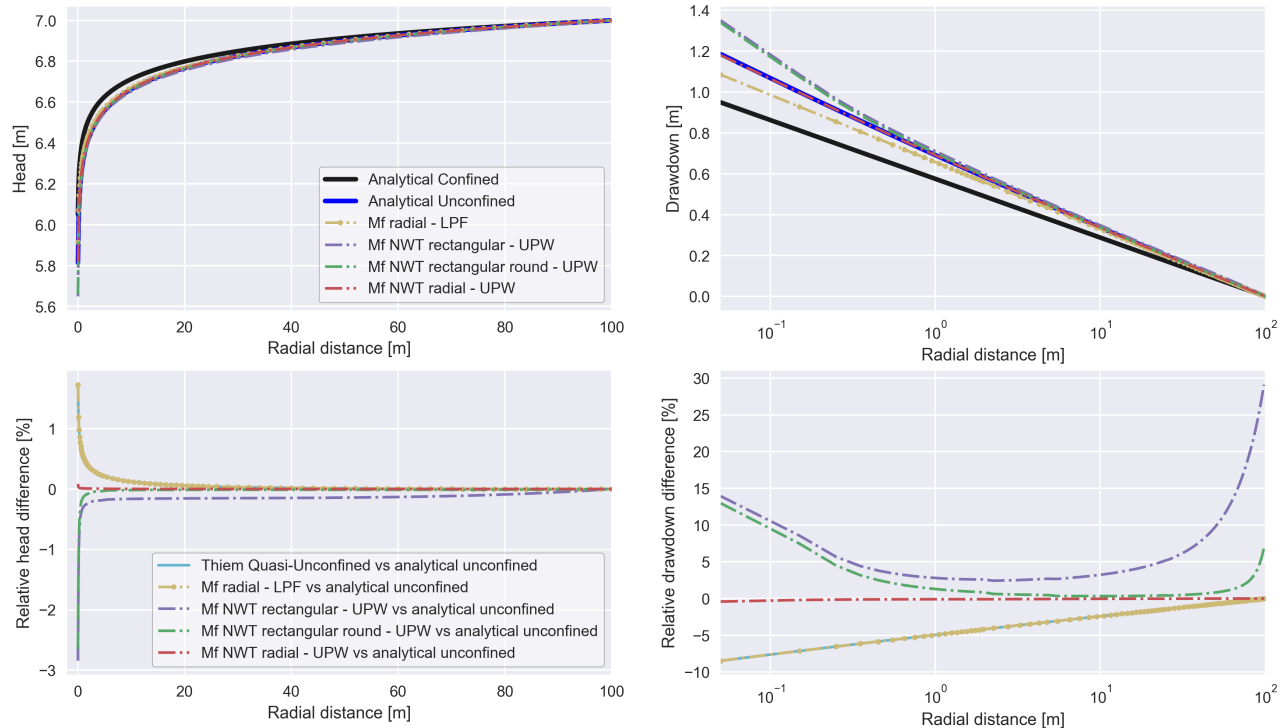


Figure F7: Results test 2b

F3. Test 3: Unsteady flow to a partially penetrating well in unconfined aquifer

As a final exercise the different MODFLOW models are subjected to a more complicated case (Figure F8). This specific exercise includes all model parameters dependent on radial scaling to test the overall radial model performance. This case accommodates a well which is partially penetrating the aquifer, making it a multi-layered problem. Sum up of the fractional discharges of the penetrating layers (48-72) results in the total well discharge. Moreover the exercise is time dependent. In this case all results are obtained after one day of groundwater withdrawal.

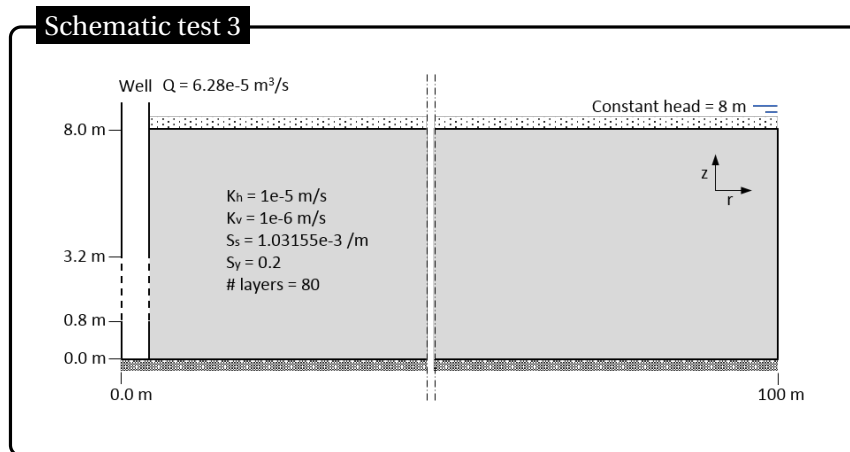


Figure F8: Schematic test 3

Performance of the radial scaled (single row) MODFLOW model is visualized by the head contour plot in figure F9. From the perspective of proper comparison results of the different models are in this case shown at an height of 2.0 m (relative to aquifer bottom) along the entire aquifer (Figure F10). Outcome of the comparative study is a scaled (single row) radial model which performs as expected. With the exception of the first meter(s) around the well differences between the rectangular round and the radial MODFLOW models are negligible small. Deviations at close range to the well can be attributed to the chosen grid structure. Based on the test exercises 1 and 2 it can be assumed the results of the radial model simulates the natural well behaviour properly. Application of the radial scaled (single row) MODFLOW model with the use of the LPF package is a relative fast and suitable model for this thesis purposes.

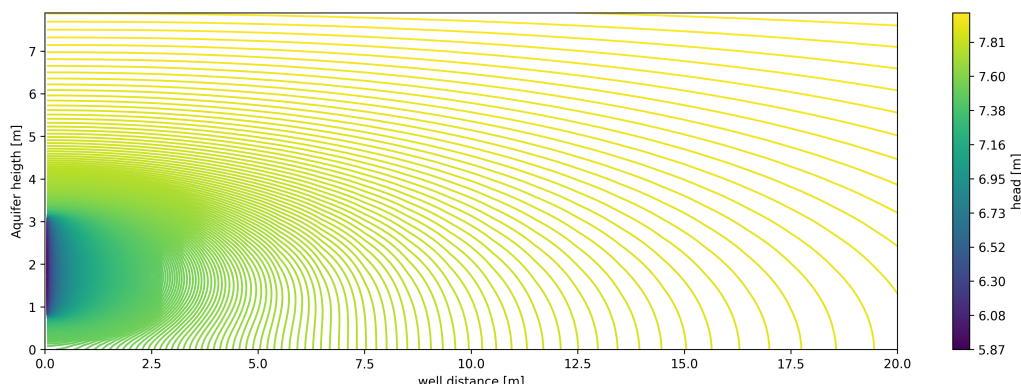


Figure F9: Results test 3: Cross-section head contour after 1 day of pumping

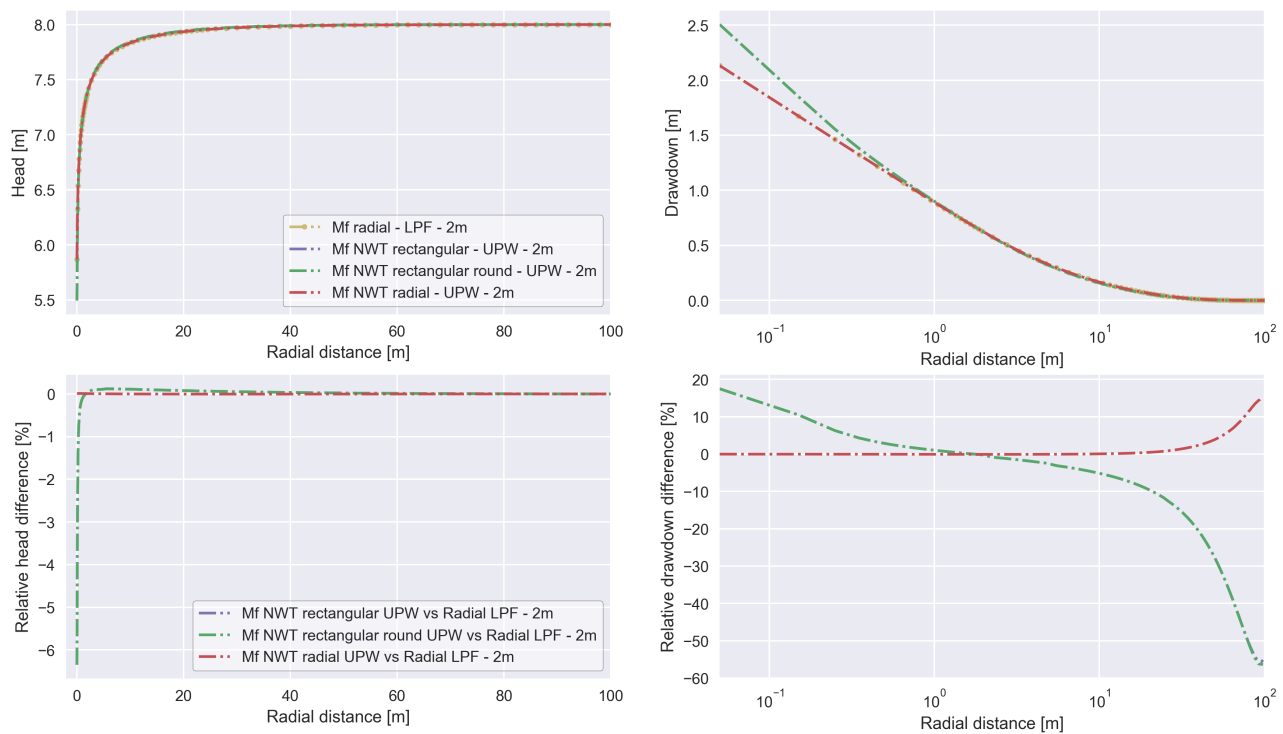


Figure F10: Results test 3: Head after 1 day of pumping at 2.0m (relative to aquifer bottom)

G

MODFLOW - Additional model results

G.1. ASR system base model performance

Figure G.1 illustrates the precise impact of flood based ASR-system infiltration on soil scenario 3 groundwater heads in several representative (model) layers. Worth mentioning, groundwater level increase is already limited at relative short radial distance (steep groundwater cone).

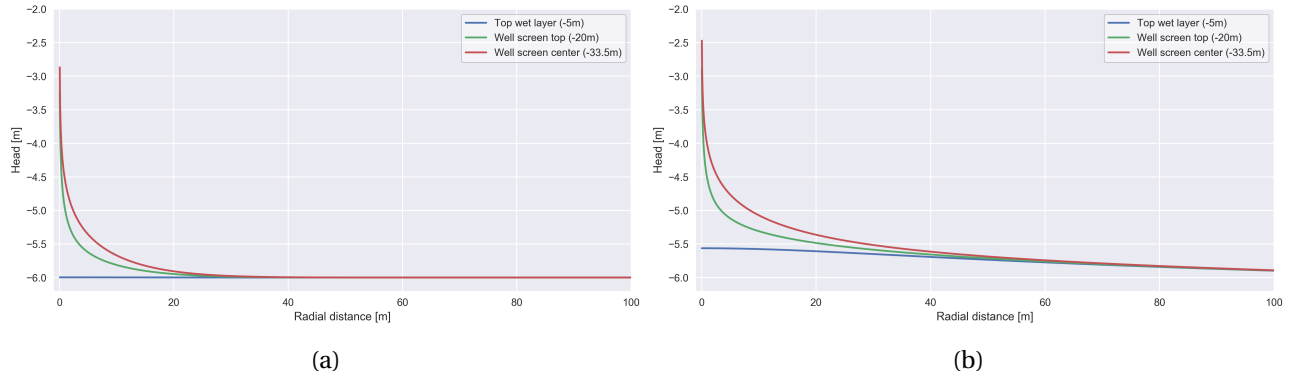


Figure G.1: Base model soil scenario 3 - Head in representative layers after (a) five days and (b) 122 days of infiltration

Figure G.2 presents the precise impact of discharge on soil scenario 3 groundwater heads in several representative (model) layers. After the first day of pumping the transition from wet (recharge) to dry season (discharge) is still of influence. Most definitely in the higher model layers (close to surface) the increased heads (due to wet season recharge) remain active for some time. Towards the end of dry season this impact is no longer present.

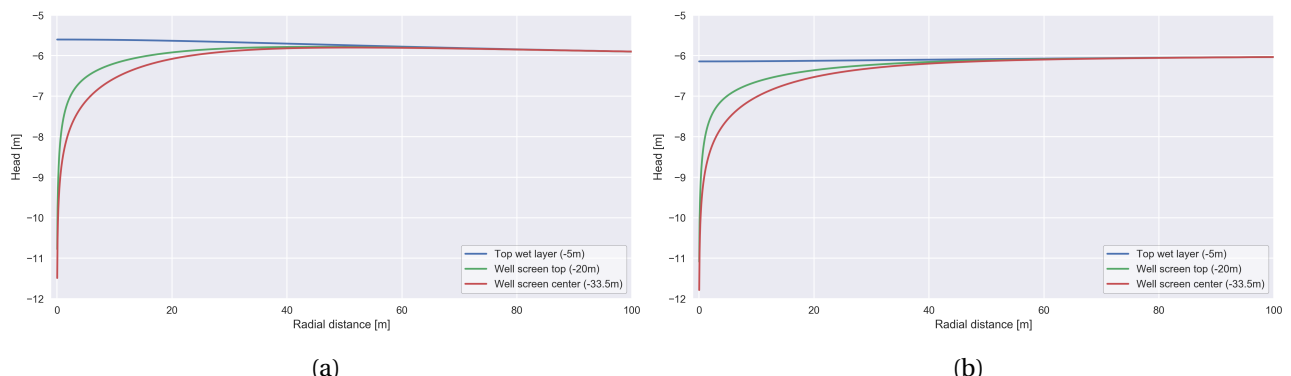


Figure G.2: Base model soil scenario 3 - Head in representative layers after four hours of pumping on (a) the first day (day 123) and (b) the last day (day 365) of dry season

G.2. ASR system sensitivity

Table G.1: Degradation of well depth - soil scenario 3 - Screen average specific recharge and discharge volumes (m^3/m)

Screen length (m)	30	25	20	15	10
Average specific recharge volume (m^3/m)	195.23	199.98	203.57	207.58	212.96
Average specific discharge volume (m^3/m)	121.03	122.67	123.65	124.89	126.85

Table G.2: Degradation of well depth - soil scenario 3 - Total recharge and discharge volumes specific reduction (m^3/m)

Reduction screen length (m)	5	10	15	20
Total recharge volume specific reduction (m^3/m)	171.47	178.54	182.87	186.36
Total discharge volume specific reduction (m^3/m)	112.84	115.78	117.17	118.12

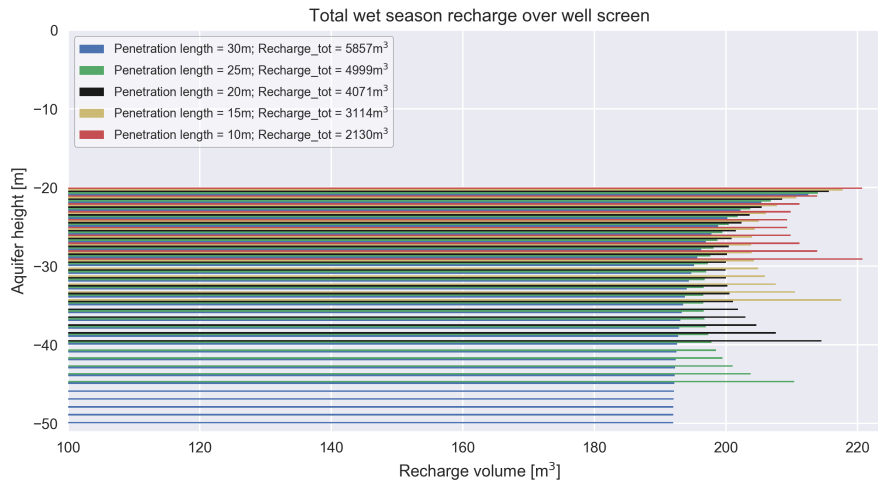


Figure G.3: Degradation of well depth - Total recharge volume by layer - soil scenario 3

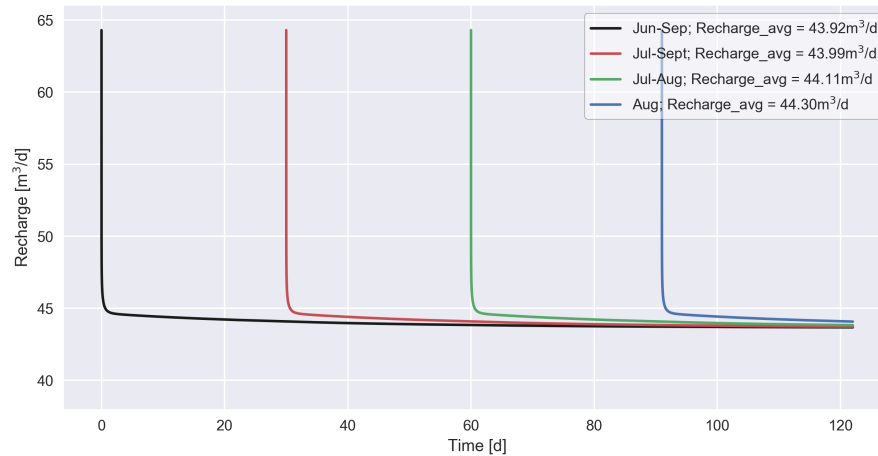


Figure G.4: Shortening wet season inundation time-span - Recharge over time - soil scenario 3

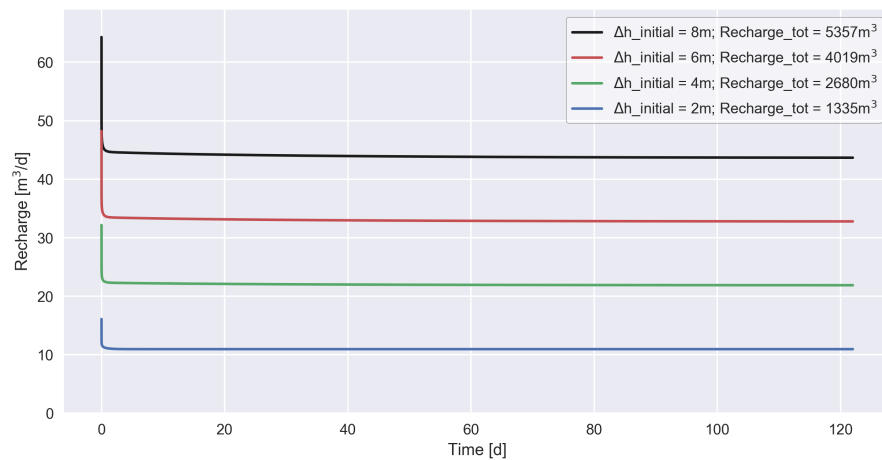
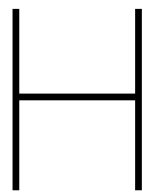


Figure G.5: Reduction wet season inundation levels - Recharge over time - soil scenario 3



Product specifications - Pedrollo 4" submersible pump

Available pump: Type 4SR4/18

4SR

4" submersible pumps



- Clean water
(Maximum sand content 150 g/m³)
- Domestic use
- Civil use
- Industrial use

PERFORMANCE RANGE

- Flow rate up to **340 l/min** (20.4 m³/h)
- Head up to **405 m**

APPLICATION LIMITS

- Maximum liquid temperature +35 °C
- Maximum sand content **150 g/m³**
- **100 m** immersion limit
- Installation:
 - vertical
 - horizontal, with the following limits:
 - 4SR1 - 4SR1.5 - 4SR2 - 4SR4 up to **27 stages**
 - 4SR6 - 4SR8 up to **17 stages**
 - 4SR10 - 4SR12 - 4SR15 up to **12 stages**
- Starts/hour: **20** at regular intervals
- Minimum flow rate for motor cooling **8 cm/s**
- Continuous service **S1**

CONSTRUCTION AND SAFETY STANDARDS

ELECTRIC MOTOR

- Single-phase 230 V - 50 Hz
- Three-phase 400 V - 50 Hz

Length of power cable:

- for P2 from 0.37 to 3 kW: **1.7 m** 4SR-PD, **2.0 m** 4SR-PS
- for P2 from 4 to 7.5 kW: **2.7 m** 4SR-PD, **3.0 m** 4SR-PS
- ⇒ The **4SR-PD** and **4SR-PS** single-phase versions supplied with a capacitor included in the packaging.

EN 60335-1
IEC 60335-1
CEI 61-150

EN 60034-1
IEC 60034-1
CEI 2-3



EU REGULATION N. 547/2012

CERTIFICATIONS

Company with management system certified DNV
ISO 9001: QUALITY
ISO 14001: ENVIRONMENT



INSTALLATION AND USE

Suitable for use with clean water with a sand content of no more than **150 g/m³**. Because of their high efficiency and reliability, they are suitable for use in domestic, civil and industrial applications such as for the distribution of water in combination with pressure tanks, for irrigation, for washing plants and for pressure boosting in fire-fighting sets, etc.

PATENTS - TRADE MARKS - MODELS

- Patent n. EP2419642

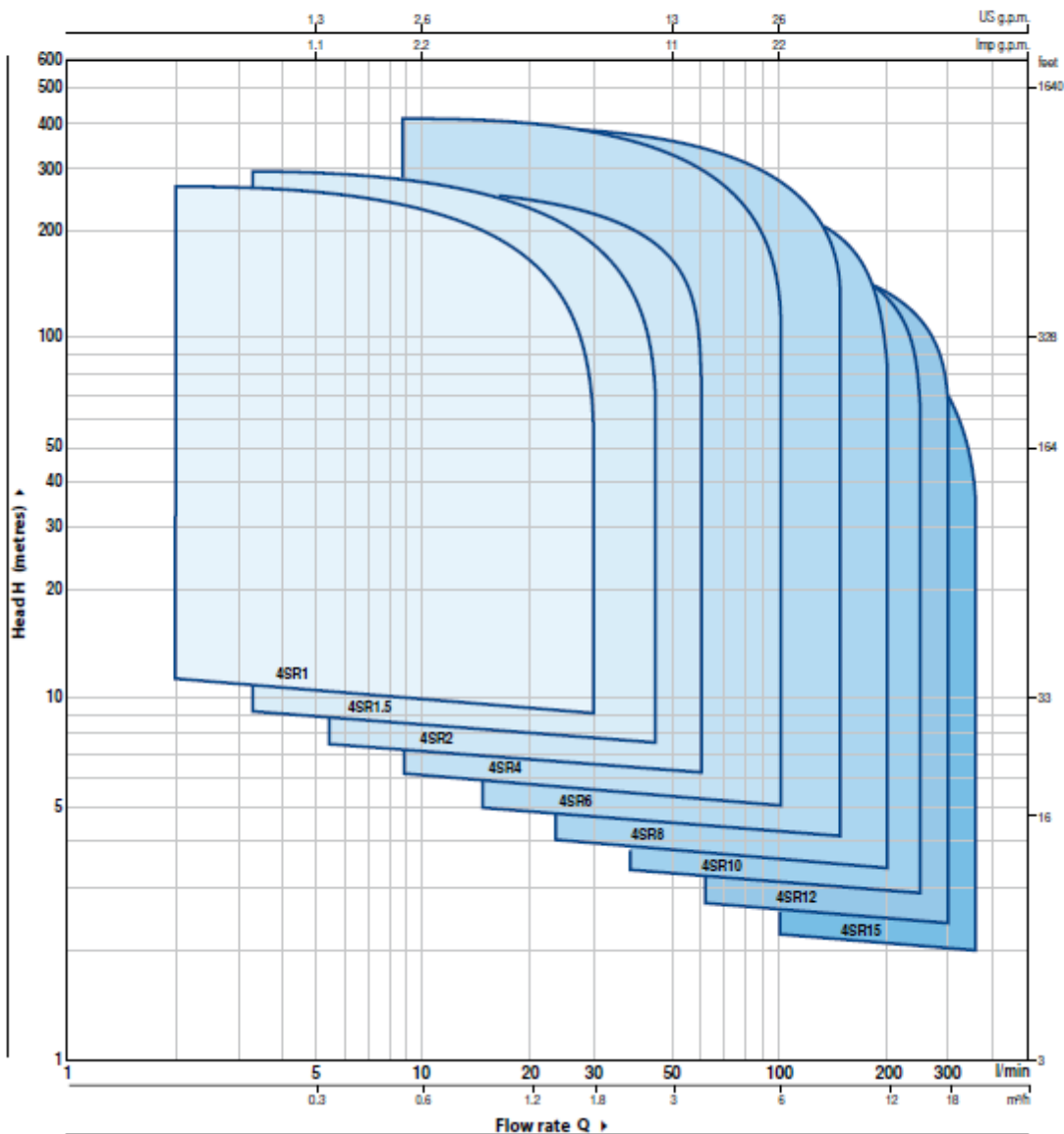
OPTIONS AVAILABLE ON REQUEST

- Other voltages or 60 Hz frequency
- Kit of cooling jacket complete with filter and supports



PERFORMANCE RANGE

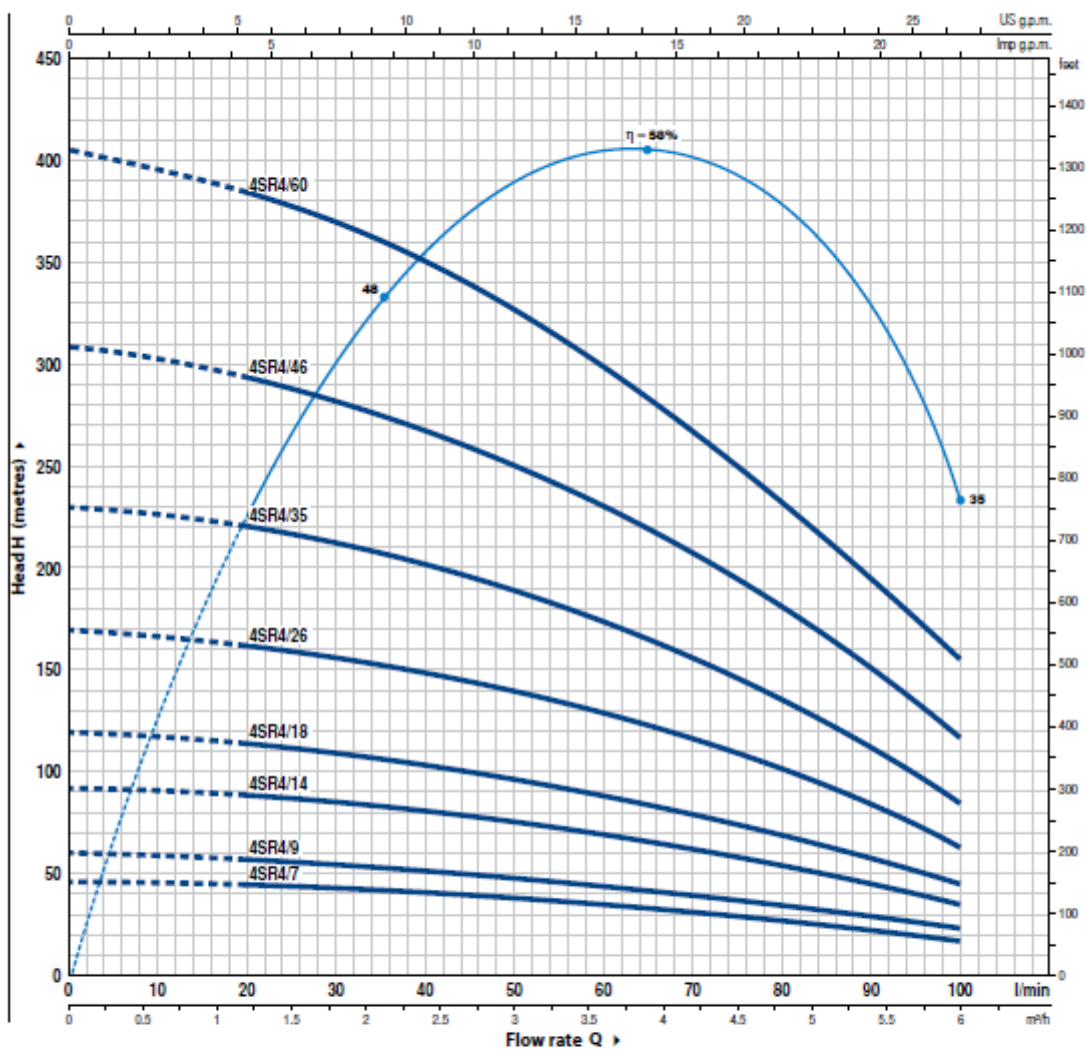
50 Hz n = 2900 rpm


NOMENCLATURE
4 SR 1 m / 13 - PD or PS or HYD

- Borehole diameter in inches _____
- Series _____
- Flow rate in m³/h at the point of highest efficiency _____
- Single-phase motor _____
- Number of stages _____
- PD: pump with "4PD PEDROLLO" motor _____
- PS: pump with "4PS PEDROLLO" motor _____
- HYD: pump without motor _____

CHARACTERISTIC CURVES AND PERFORMANCE DATA

50 Hz n = 2900 rpm



MODEL		POWER (P ₂)		Q l/min	H metres	0	1.2	1.8	2.4	3.0	3.6	4.2	4.8	5.4	6.0
Single-phase	Three-phase	kW	HP			0	20	30	40	50	60	70	80	90	100
4SR4m/7	4SR4/7	0.55	0.75	46	44	42	40	38	35	32	28	23	17		
4SR4m/9	4SR4/9	0.75	1	60	56	55	52	49	45	40	35	29	23		
4SR4m/14	4SR4/14	1.1	1.5	92	88	85	81	76	70	63	55	45	35		
4SR4m/18	4SR4/18	1.5	2	120	112	109	104	98	90	81	70	58	45		
4SR4m/26	4SR4/26	2.2	3	170	162	157	150	141	130	116	101	84	63		
-	4SR4/35	3	4	230	220	211	202	190	175	157	137	113	85		
-	4SR4/46	4	5.5	308	293	280	269	249	230	205	181	151	117		
-	4SR4/60	5.5	7.5	405	385	370	350	325	300	270	235	195	155		

Q = Flow rate H = Total manometric head

Tolerance of characteristic curves in compliance with EN ISO 9906 Grade 3B.